

30853

NATIONAL LIBRARY  
OTTAWA



BIBLIOTHÈQUE NATIONALE  
OTTAWA

NAME OF AUTHOR.....MARY...COREEN...TOURANGEAU  
 TITLE OF THESIS..Nuclear...Magnetic...Resonance...Studies of the  
 ..Solution...Chemistry...of...Methylmercury Complexes  
 ..and...of...Aqueous...Lanthanide...Shift Reagents  
 UNIVERSITY...U...of...Alberta.....  
 DEGREE FOR WHICH THESIS WAS PRESENTED.....Ph.D.....  
 YEAR THIS DEGREE GRANTED.....1976.....

Permission is hereby granted to THE NATIONAL LIBRARY  
 OF CANADA to microfilm this thesis and to lend or sell copies  
 of the film.

The author reserves other publication rights, and  
 neither the thesis nor extensive extracts from it may be  
 printed or otherwise reproduced without the author's  
 written permission.

(Signed)...*Mary Coreen Tourangeau*

PERMANENT ADDRESS:

.....609.....N.W. HT. CRESCENT  
 .....DORVAL, QUEBEC  
 .....H9P 2C3.....

DATED...*July 30*.....1976.

**INFORMATION TO USERS**

**THIS DISSERTATION HAS BEEN  
MICROFILMED EXACTLY AS RECEIVED**

This copy was produced from a microfiche copy of the original document. The quality of the copy is heavily dependent upon the quality of the original thesis submitted for microfilming. Every effort has been made to ensure the highest quality of reproduction possible.

**PLEASE NOTE:** Some pages may have indistinct print. Filmed as received.

Canadian Theses Division  
Cataloguing Branch  
National Library of Canada  
Ottawa, Canada K1A 0N4

**AVIS AUX USAGERS**

**LA THESE A ETE MICROFILMEE  
TELLE QUE NOUS L'AVONS RECUE**

Cette copie a été faite à partir d'une microfiche du document original. La qualité de la copie dépend grandement de la qualité de la thèse soumise pour le microfilmage. Nous avons tout fait pour assurer une qualité supérieure de reproduction.

**NOTA BENE:** La qualité d'impression de certaines pages peut laisser à désirer. Microfilmée telle que nous l'avons reçue.

Division des thèses canadiennes  
Direction du catalogage  
Bibliothèque nationale du Canada  
Ottawa, Canada K1A 0N4

THE UNIVERSITY OF ALBERTA

NUCLEAR MAGNETIC RESONANCE STUDIES OF THE SOLUTION  
CHEMISTRY OF METHYLMERCURY COMPLEXES AND OF  
AQUEOUS LANTHANIDE SHIFT REAGENTS

by



MARY COREEN TOURANGEAU

A THESIS

SUBMITTED TO THE FACULTY OF GRADUATE STUDIES AND RESEARCH  
IN PARTIAL FULFILMENT OF THE REQUIREMENTS FOR THE DEGREE  
OF DOCTOR OF PHILOSOPHY

DEPARTMENT OF CHEMISTRY

EDMONTON, ALBERTA

FALL, 1976

THE UNIVERSITY OF ALBERTA  
FACULTY OF GRADUATE STUDIES AND RESEARCH

The undersigned certify that they have read,  
and recommend to the Faculty of Graduate Studies and  
Research, for acceptance, a thesis entitled NUCLEAR.....  
MAGNETIC RESONANCE STUDIES OF THE SOLUTION CHEMISTRY.....  
OF METHYLMERCURY COMPLEXES AND OF AQUEOUS LANTHANIDE.....  
SHIFT REAGENTS.....  
submitted by MARY COREEN TOURANGEAU.....  
in partial fulfilment of the requirements for the degree  
of DOCTOR OF PHILOSOPHY.

*Dallas Rabenstein*.....  
D.L. Rabenstein (Supervisor)

*Gunn Horlick*.....  
G. Horlick.

*Byron Kratochvil*.....  
B. Kratochvil.

*Georg Kotowycz*.....  
G. Kotowycz.

*Fred Wolfe*.....  
F. Wolfe.

*Donald E. Leyden*.....  
D. Leyden,  
(External Examiner).

Date: ..... *July 28* ....., 1976.

## ABSTRACT

### Part I

The aqueous solution chemistry of the methylmercury complexes of selected inorganic anions has been investigated by proton magnetic resonance spectroscopy. Formation constants were determined for the sulfate, selenate, sulfite, selenite, hydrogen selenite, thiocyanate, and selenocyanate complexes from the pH dependence of the chemical shift and the  $^{199}\text{Hg}$ - $^1\text{H}$  spin-spin coupling constant of the methyl group of methylmercury in solutions containing both methylmercury and the ligand. The chemical shift and the  $^{199}\text{Hg}$ - $^1\text{H}$  spin-spin coupling constant of the methylmercury in each of the complexes were also obtained from the same measurements. NMR parameters were measured for several complexes with sulfide and selenide. The ligand donor atom in each of the complexes was identified using the formation constants, the  $^{199}\text{Hg}$ - $^1\text{H}$  spin-spin coupling constant of the complexed methylmercury, and in some cases, Raman spectral data. It is of particular interest that selenite, which can act as a protecting agent against methylmercury poisoning in animals, does not form a particularly strong complex with methylmercury.

## Part II

The hydrated Pr(III) and Eu(III) cations and the ethylenediaminetetraacetic acid, the N-(2-hydroxyethyl)-ethylenediaminetriacetic acid, and the cyclohexanediaminetetraacetic acid chelates of Pr(III) have been investigated as potential NMR shift reagents for general use in aqueous solution. Pr(III) and Eu(III) were useful only at low pH values, because of their precipitation as hydroxides at pH greater than *ca.* 6.5. Pr(III) induced shifts were more suitable than Eu(III) induced shifts in aqueous solution, and the effect of the counterion of the Pr(III) salt on the induced shifts was studied. The interaction of the various shift reagents with monofunctional molecules containing carboxylic acid, amino, imidazole, sulfhydryl, and sulfonic acid functional groups was studied. Pr(III) complexes only the carboxylate and sulfonate groups. The Pr(III) chelates of the aminopolycarboxylic acids were found to function as shift reagents over the entire pH range 1 to 12. They interact with the carboxylate, amino, imidazole, and sulfonate functional groups. The pH dependence of the induced shifts indicates that these shift reagents complex the deprotonated carboxylate and sulfonate groups, and form ion pairs with the protonated amino and imidazole groups.

## ACKNOWLEDGEMENTS

I would like to express my thanks to my supervisor, Dr. D.L. Rabenstein, for his guidance throughout the course of this research.

I am also grateful to my family, to other members of our research group, and to my friends for their encouragement and advice on many occasions.

I also want to thank Dr. G. Kotowycz for reading and commenting on the rough draft of this thesis, and Miss Vi Melnychuk for her secretarial assistance.

Financial support from the National Research Council of Canada and the University of Alberta is gratefully acknowledged.

TABLE OF CONTENTS

CHAPTER	PAGE
LIST OF TABLES . . . . .	xi
LIST OF FIGURES . . . . .	xiv

Part I

METHYLMERCURY COMPLEXES OF SELECTED INORGANIC ANIONS

I. INTRODUCTION . . . . .	2
A. The Aqueous Solution Chemistry of Methylmercury . . . . .	4
B. The Coordination Chemistry of Methylmercury . . . . .	6
C. Overview of Part I . . . . .	17
II. EXPERIMENTAL . . . . .	22
A. Chemicals . . . . .	22
B. Preparation and Standardization of Methylmercuric Hydroxide Solutions . . . . .	22
C. Preparation and Standardization of Ligand Solutions . . . . .	25
D. pH Measurement . . . . .	28
E. Solutions for Nuclear Magnetic Resonance and Raman Spectroscopic Measurements . . . . .	28
1. NMR Experiments . . . . .	28
2. Raman Experiments . . . . .	30
F. Proton Magnetic Resonance Measurements . . . . .	31
G. Raman Spectroscopic Measurements . . . . .	32
H. Determination of Formation Constants by NMR Spectroscopy . . . . .	33



CHAPTER	PAGE
III. METHYLMERCURY SPECIES AND EQUILIBRIA IN	
AQUEOUS SOLUTION . . . . .	37
A. Introduction . . . . .	37
B. Results and Discussion . . . . .	40
IV. METHYLMERCURY COMPLEXES OF SELECTED	
INORGANIC ANIONS . . . . .	57
A. Introduction . . . . .	57
B. Results . . . . .	57
1. The Sulfate and Selenate Complexes of Methylmercury . . . . .	57
2. The Sulfite Complex of Methylmercury	74
3. The Selenite Complexes of Methyl- mercury . . . . .	83
4. The Thiocyanate and Selenocyanate Complexes of Methylmercury . . . . .	94
5. The Sulfide and Selenide Complexes of Methylmercury . . . . .	101
6. The Interaction of Phosphite with Methylmercury . . . . .	114
C. Discussion . . . . .	115
1. The Complexation of Methylmercury by Inorganic Anions . . . . .	115
2. Significance of the Mercury Proton Coupling Constant of Methylmercury Compounds . . . . .	118
BIBLIOGRAPHY . . . . .	120

CHAPTER	Part II	PAGE
AQUEOUS LANTHANIDE SHIFT REAGENTS		
V.	INTRODUCTION . . . . .	127
	A. Theory of Paramagnetic Shift Reagents . . . . .	129
	B. Lanthanide Shift Reagents . . . . .	137
	C. Overview of Part II . . . . .	142
VI.	EXPERIMENTAL . . . . .	144
	A. Chemicals . . . . .	144
	B. Preparation of Solutions . . . . .	144
	C. Preparation and Standardization of Lanthanide Salt and Ligand Solutions . . . . .	144
	D. pH Measurements . . . . .	145
	E. NMR Measurements and Reference Compounds . . . . .	146
VII.	THE HYDRATED Pr(III) AND Eu(III) CATIONS AS AQUEOUS SHIFT REAGENTS . . . . .	148
	A. Introduction . . . . .	148
	B. Results . . . . .	149
	1. A Comparison of the Shift Reagent Properties of $\text{Eu}(\text{NO}_3)_3$ and $\text{Pr}(\text{NO}_3)_3$ . . . . .	149
	2. The Counterion Dependence of Pr(III) Induced Chemical Shifts in Aqueous Solution . . . . .	162
	3. The Interaction of Praseodymium(III) with the Potential Donor Groups of Organic Molecules . . . . .	168
	i) The Carboxylate Group . . . . .	168
	ii) The Amino Group . . . . .	168
	iii) The Sulfonate Group . . . . .	170

CHAPTER	PAGE
iv) The Sulfhydryl Group . . . . .	171
v) The Imidazole Group . . . . .	173
C. Discussion . . . . .	173
VIII. AMINOPOLYCARBOXYLIC ACID CHELATES OF Pr(III) AS AQUEOUS SHIFT REAGENTS . . . . .	177
A. Introduction . . . . .	177
B. Results . . . . .	178
1. The Pr(III) Complex of EDTA as an Aqueous Shift Reagent . . . . .	178
2. The Pr(III) Complex of HEDTA as an Aqueous Shift Reagent . . . . .	179
i) The Carboxylate Group . . . . .	180
ii) The Amino Group . . . . .	185
iii) The Imidazole Group . . . . .	187
iv) The Sulfhydryl Group . . . . .	188
3. The Pr(III) Complex of CDTA as an Aqueous Shift Reagent . . . . .	190
i) The Carboxylate Group . . . . .	190
ii) The Amino Group . . . . .	191
C. Discussion . . . . .	194
BIBLIOGRAPHY . . . . .	199

LIST OF TABLES

Table	Description	Page
1	Formation Constants of Methylmercury Complexes of Selected Ligands	16
2	The Mercury-Proton Coupling Constant of Methylmercury in Selected Methylmercury Complexes	20
3	Chemical Shift of the Methyl Protons and the Mercury-Proton Coupling Constant of Methylmercury in Aqueous Methylmercury Species	52
4	Mercury-Proton Coupling Constant as a Function of pH for the Methylmercury in an Aqueous Solution Containing 0.106 M Methylmercury and 0.211 M Sodium Sulfate	60
5	The Formation Constant of Methylmercuric Sulfate Calculated from Methylmercury Chemical Shift Data	65
6	Formation Constants and NMR Parameters of Methylmercuric Sulfate and Methylmercuric Selenate	71
7	Some Raman Bands of Methylmercuric Complexes, $\text{CH}_3\text{HgX}$	73
8	NMR Data for the Methylmercury-Sulfite System at pH = 5.0	76
9	NMR Data for the Methylmercury-Sulfite System at pH = 10.51	78
10	NMR Data for the Methylmercury-Sulfite System at pH = 12.00	79
11	Raman Spectrum of $[\text{CH}_3\text{HgSO}_3]^-$	82
12	Calculated Values of $K_F$ for Methylmercuric Selenite from the Chemical Shift of the Methylmercury Protons in the High pH Region	87

Table	Description	Page
13	Formation Constants and NMR Parameters for Selenite Complexes of Methylmercury	91
14	NMR Data for the Methylmercury-Selenocyanate System	100
15	NMR Data for the Methylmercury-Sulfide System at pH = 13.2	103
16	Calculated Mercury-Proton Coupling Constants for the Trimethylmercurisulphonium Ion	108
17	NMR Data for the Methylmercury-Sulfide System at pH = 1.0	110
18	NMR Data for the Methylmercury-Selenide System at pH = 13.51	113
19	Summary of Formation Constants and Coupling Constants of Methylmercury Complexes with Selected Inorganic Ligands	116
20	The Chemical Shift of the Methyl Protons of Acetic Acid as a Function of pH in $\text{Eu}(\text{NO}_3)_3$ -Acetic Acid Solutions	151
21	The Chemical Shift of the Methyl Protons of Acetic Acid as a Function of pH in $\text{Pr}(\text{NO}_3)_3$ -Acetic Acid Solutions	152
22	Formation Constants and Complex Chemical Shifts for $\text{Pr}(\text{III})$ -Acetate and $\text{Eu}(\text{III})$ -Acetate Complexes	161
23	The Chemical Shift of the Methyl Protons of Acetic Acid as a Function of pH in $\text{PrCl}_3$ -Acetic Acid Solutions	164
24	The Chemical Shift of the Methyl Protons of Acetic Acid as a Function of pH in $\text{Pr}(\text{ClO}_4)_3$ -Acetic Acid Solutions	165

Table	Description	Page
25	Formation Constants and Complex Chemical Shifts for Pr(III)-Acetate Complexes in the Presence of the Nitrate, Chloride, and Perchlorate Counterions	167
26	The Chemical Shift of the Methyl Protons of Methanesulfonic Acid in Solutions of Pr(ClO <sub>4</sub> ) <sub>3</sub> and Methanesulfonic Acid at pH 4.0	172
27	The Chemical Shift of the Methyl Protons of Methylamine as a Function of pH in a Solution Containing 0.101 <u>M</u> PrCDTA <sup>-</sup> and 0.117 <u>M</u> Methylamine	193

## LIST OF FIGURES

Figure		Page
1	Proton NMR spectrum of methylmercury in a 0.190 <u>M</u> aqueous solution.	41
2	pH dependence of the chemical shift of the methyl protons of methylmercury in an aqueous solution containing 0.190 <u>M</u> methylmercury.	42
3	pH dependence of the mercury-proton spin-spin coupling constant of methylmercury in an aqueous solution containing 0.190 <u>M</u> methylmercury.	43
4	pH dependence of the chemical shift of the methyl protons of methylmercury in aqueous solutions containing 0.0451 <u>M</u> methylmercury, 0.0901 <u>M</u> methylmercury, and 0.213 <u>M</u> methylmercury.	45
5	NMR chemical shift titration curves for the titration of $[(\text{CH}_3\text{Hg})_3\text{O}]\text{ClO}_4$ with KOH in aqueous and in methanolic media.	48
6	Raman spectra of a solution supersaturated with respect to $[(\text{CH}_3\text{Hg})_3\text{O}]\text{ClO}_4$ and of the crystals which separated from the solution.	54
7	pH dependence of the fractional concentrations of the methylmercury-containing species in an aqueous solution containing 0.200 <u>M</u> methylmercury.	56
8	pH dependence of the chemical shift of the methyl protons of methylmercury in an aqueous solution containing 0.100 <u>M</u> methylmercury and in an aqueous solution containing 0.0532 <u>M</u> methylmercury and 0.213 <u>M</u> sodium sulfate.	59
9	pH dependence of the chemical shift of the methyl protons of methylmercury in an aqueous solution containing 0.100 <u>M</u> methylmercury and in an aqueous solution containing 0.0521 <u>M</u> methylmercury and 0.208 <u>M</u> sodium selenate.	68

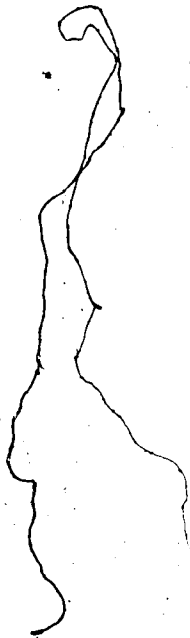
Figure		Page
10	pH dependence of the mercury-proton spin-spin coupling constant of methylmercury in an aqueous solution containing 0.100 M methylmercury and in an aqueous solution containing 0.0521 M methylmercury and 0.208 M sodium selenate.	69
11	pH dependence of the chemical shift of the methyl protons of methylmercury in an aqueous solution containing 0.100 M methylmercury and in an aqueous solution containing 0.112 M methylmercury and 0.224 M sodium selenite.	84
12	pH dependence of the mercury-proton spin-spin coupling constant of methylmercury in an aqueous solution containing 0.100 M methylmercury and in an aqueous solution containing 0.112 M methylmercury and 0.224 M sodium selenite.	85
13	Observed and calculated pH dependence of the chemical shift of the methyl protons of methylmercury in an aqueous solution containing 0.112 M methylmercury and 0.224 M sodium selenite.	88
14	pH dependence of the chemical shift of the methyl protons of methylmercury in an aqueous solution containing 0.100 M methylmercury and in an aqueous solution containing 0.0563 M methylmercury and 0.0132 M potassium thiocyanate.	96
15	pH dependence of the mercury-proton spin-spin coupling constant of methylmercury in an aqueous solution containing 0.100 M methylmercury and in an aqueous solution containing 0.0563 M methylmercury and 0.0132 M potassium thiocyanate.	97
16	pH dependence of the mercury-proton spin-spin coupling constant in an aqueous solution containing 0.100 M methylmercury and in an aqueous solution containing 0.108 M methylmercury and 0.215 M sodium sulfide.	106



Figure		Page
17	Plot of $(\delta_{\text{obs}} - \delta_f) / \alpha[\text{Pr}^{+3}]$ versus the observed chemical shift of the methyl protons of acetic acid in an aqueous solution containing 0.0980 M acetic acid and 0.0800 M $\text{Pr}(\text{NO}_3)_3$ at pH values ranging from 3.01 to 4.33.	158
18	pH dependence of the chemical shift of the methyl protons of acetic acid in an aqueous solution containing 0.0305 M acetic acid and in an aqueous solution 0.100 M acetic acid, 0.111 M $\text{Pr}(\text{ClO}_4)_3$ and 0.111 M HEDTA.	181
19	Potentiometric titration curves for the titration of 250 ml of an aqueous solution containing $1.27 \times 10^{-3}$ M HEDTA with 0.05356 M NaOH and for the titration of 250 ml of an aqueous solution containing $1.27 \times 10^{-3}$ M $\text{Pr}(\text{ClO}_4)_3$ and $1.27 \times 10^{-3}$ M HEDTA with 0.05356 M NaOH.	183
20	pH dependence of the chemical shift of the methyl protons of methylamine in an aqueous solution containing 0.10 M methylamine and in an aqueous solution containing 0.118 M methylamine, 0.102 M $\text{Pr}(\text{ClO}_4)_3$ , and 0.102 M HEDTA.	186
21	pH dependence of the chemical shift of the methyl protons of N-methyl imidazole in an aqueous solution containing 0.140 M N-methyl imidazole and in an aqueous solution containing 0.0900 M N-methyl imidazole, 0.110 M $\text{Pr}(\text{ClO}_4)_3$ , and 0.110 M HEDTA.	189
22	pH dependence of the chemical shift of the methyl protons of acetic acid in an aqueous solution containing 0.0305 M acetic acid and in an aqueous solution containing 0.0912 M acetic acid, 0.100 M $\text{Pr}(\text{ClO}_4)_3$ , and 0.100 M CDTA.	192

Part I

METHYLMERCURY COMPLEXES OF SELECTED INORGANIC ANIONS



## CHAPTER I

### INTRODUCTION

The coordination chemistry of the methylmercury cation,  $\text{CH}_3\text{Hg}^+$ , has been the subject of much research. It is an essentially unifunctional metallic species (1) and the simplest soft acid known (2). The apparent absence from chelating effects with methylmercury renders this cation an excellent probe for studies of heavy metal binding (3).

Methylmercury has a strong affinity for sulfur and it has been used as a highly selective reagent for protein sulfhydryl groups for some time (4). The formation constants of methylmercury complexes of amino acids (5), nucleosides (6), and inorganic anions (1) have been measured potentiometrically. Formation constants (7,8,10), sites of binding (8-10) and ligand exchange kinetics (10) have been studied for a variety of methylmercury complexes of amino acids by nuclear magnetic resonance techniques.

Part I of this thesis reports nuclear magnetic resonance and Raman spectroscopic studies of the aqueous solution chemistry of methylmercury complexes of a variety of inorganic anions, including some which have oxygen, sulfur, or selenium as potential donor atoms. These studies are of particular interest in view of the role of

methylmercury in environmental pollution by mercury compounds. Methylmercury has been shown to be the species involved in several mercury poisoning incidents (11) in which there was irreversible damage to the central nervous systems of the victims.

The present widespread concern over mercury in the environment is a consequence of the discovery that metallic and inorganic mercury, both of which are highly insoluble and therefore reasonably harmless to the environment, can be methylated by microorganisms present in nature to form methylmercury (12-14). This methylation can take place anaerobically via enzymatic and non-enzymatic pathways. The highly toxic methylmercury is water-soluble and biologically mobile. It is capable of leaving the bottom sediments of rivers and lakes, entering the aquatic system, and concentrating in the food chain. Thus, a detailed knowledge of the coordination chemistry of methylmercury with inorganic anions is of interest to our understanding of the behavior of methylmercury in natural water systems.

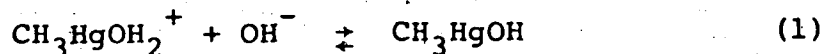
The complexation of methylmercury by inorganic anions is also of interest in view of recent studies on antidotes for methylmercury poisoning. The usual heavy metal poisoning antidotes such as British Anti Lewisite (BAL), sodium ethylenediaminetetraacetate, and penicillimine are ineffective for methylmercury poisoning (15).

4

However, it has been reported recently that sodium selenite decreased the toxicity of methylmercury added to the diet of rats (16,17). Related to this are the findings that selenium and mercury tend to accumulate together in fish (12), and that dietary tuna fish decreased the toxicity of methylmercury administered to quail (16).

A. The Aqueous Solution Chemistry of Methylmercury

The first investigation of the aqueous solution chemistry of methylmercury was reported in 1955 by Waugh, Walton, and Laswick (18). By the potentiometric titration of methylmercuric hydroxide with nitric and perchloric acids, they determined the formation constant of methylmercuric hydroxide, as described by Equations 1 and 2, to be  $3.1 \times 10^9$ . This method is based on the

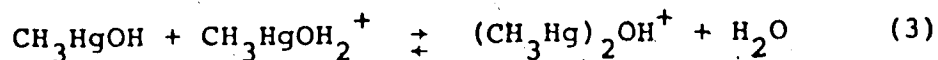


$$K_1 = \frac{[\text{CH}_3\text{HgOH}]}{[\text{CH}_3\text{HgOH}_2^+][\text{OH}^-]} \quad (2)$$

assumptions that the only methylmercury species are the hydrated cation  $\text{CH}_3\text{HgOH}_2^+$  and methylmercuric hydroxide  $\text{CH}_3\text{HgOH}$ , and that there is no association between methylmercury and the nitrate or perchlorate anions.

In 1965, Schwarzenbach and Schellenberg (1)

developed a model for the aqueous solution chemistry of methylmercury which included a third methylmercury species, a dinuclear complex with two methylmercury cations coordinated to the same hydroxide ion,  $(\text{CH}_3\text{Hg})_2\text{OH}^+$ . This more complete model is described by Equations 1-4. By



$$K_2 = \frac{[(\text{CH}_3\text{Hg})_2\text{OH}^+]}{[\text{CH}_3\text{HgOH}][\text{CH}_3\text{HgOH}_2^+]} \quad (4)$$

potentiometric titration, the values  $2.34 \times 10^9$  and  $2.34 \times 10^2$  were obtained for  $K_1$  and  $K_2$  (1).

In a study of the solution chemistry of methylmercury not referenced by Schwarzenbach and Schellenberg, Grdenic and Zado (19) reported that trimethylmercurioxonium perchlorate,  $[(\text{CH}_3\text{Hg})_3\text{O}]\text{ClO}_4$ , precipitates from concentrated methylmercuric hydroxide solutions titrated with perchloric acid. On the basis of these results, the completeness of the model proposed by Schwarzenbach and Schellenberg has been questioned by Green (20) and by Tobias and coworkers (21), who suggest that  $(\text{CH}_3\text{Hg})_3\text{O}^+$  should be included in the aqueous solution model of methylmercury. It should be mentioned, however, that a number of the conclusions drawn by Grdenic and Zado are not in accord with current knowledge of the solution

chemistry of methylmercury. For example, Grdenic and Zado concluded that methylmercuric hydroxide does not exist except in dilute aqueous solution as the dissociation product of  $[(\text{CH}_3\text{Hg})_3\text{O}]\text{OH}$ . Furthermore, they claimed to have prepared  $[(\text{CH}_3\text{Hg})_3\text{O}]\text{OH}$  by a reaction between  $[(\text{CH}_3\text{Hg})_3\text{O}]\text{ClO}_4$  and KOH in methanol. They also concluded from conductance data, that  $(\text{CH}_3\text{Hg})_3\text{O}^+$  is stable in alkaline methanol solution and that the compound previously thought to be  $\text{CH}_3\text{HgOH}$  is actually  $[(\text{CH}_3\text{Hg})_3\text{O}]\text{OH}$  or its dehydration product.

In Chapter III of this thesis, the aqueous solution models of methylmercury are considered further and the Schwarzenbach and Schellenberg model is modified to include the trimethylmercurioxonium ion.

#### B. The Coordination Chemistry of Methylmercury

The coordination chemistry of the methylmercury cation is characterized by its unifunctional nature (1), the tendency to linear two-coordination typical of divalent mercury being greatly accentuated when one ligand is an organic radical. The non-lability of the mercury-carbon bond of methylmercury is proven by the presence of satellite resonances in the NMR spectra of methylmercury complexes (22). These satellites arise from spin-spin coupling between the 16.9% of mercury atoms having nuclear spin one-half ( $^{199}\text{Hg}$ ) and the protons of the methyl groups attached to these mercury atoms. The

satellite resonances would be very broad or undetectable in methylmercury spectra if there were dissociation of the mercury-carbon bond on the NMR time scale.

In early NMR studies of methylmercury compounds some confusion existed as to the lability of the mercury-carbon bond because the satellite resonances are broadened in the iodo- and bromo- methylmercury complexes (23). In 1967 it was shown that this broadening is not a result of exchange of labile methyl groups, but rather is due to quadrupole interactions between the  $^{199}\text{Hg}$  and the bromine or the iodine (24).

The uncomplexed methylmercury cation,  $\text{CH}_3\text{Hg}^+$ , is never observed in aqueous solution (25). Stoichiometrically, it resembles the proton in complex formation (1). In aqueous solution containing only methylmercury it exists as  $\text{CH}_3\text{HgOH}_2^+$  at  $\text{pH} < 2$ , analogous to the hydronium ion. At higher  $\text{pH}$ , methylmercury complexes to hydroxide, existing entirely as  $\text{CH}_3\text{HgOH}$  at  $\text{pH} > 9$  (26). Methylmercury shows a strong tendency for higher complex formation and many polynuclear complexes are known. Series of the type  $\text{L}^{n-} \rightarrow \text{CH}_3\text{HgL}^{1-n} \rightarrow (\text{CH}_3\text{Hg})_2\text{L}^{2-n} \rightarrow (\text{CH}_3\text{Hg})_3\text{L}^{3-n}$  have been studied for a variety of ligands, similar to the series  $\text{L} \rightarrow \text{HL} \rightarrow \text{H}_2\text{L} \rightarrow \text{H}_3\text{L}$ . For example, methylmercury forms the oxide complexes  $(\text{CH}_3\text{HgOH}, (\text{CH}_3\text{Hg})_2\text{OH}^+, (\text{CH}_3\text{Hg})_3\text{O}^+)$  in water. This series is discussed in detail in Chapter III. Analogous methylmercury complexes of



sulfur (1,27), nitrogen (28), phosphorous (29), selenium (30), and arsenic (31) have also been reported although they exist in slightly different forms due to the weaker acidity of oxygen-bound protons. For example, Schwarzenbach and Schellenberg (1) reported the complexes  $\text{CH}_3\text{HgS}^-$ ,  $(\text{CH}_3\text{Hg})_2\text{S}$ ,  $(\text{CH}_3\text{Hg})_3\text{S}^+$  to be present in the aqueous methylmercury-sulfide system.

Although the methylmercury cation most frequently adds just one ligand, a coordination number of four is often characteristic of  $\text{Hg}^{2+}$  (32). Therefore, the possibility of further complexation to methylmercury must be considered. Complexes of the type  $\text{CH}_3\text{HgL}_2^{1-2n}$  and  $\text{CH}_3\text{HgL}_3^{1-3n}$  rarely have been detected in aqueous solution studies, but they have been found in non-aqueous solution and in the solid state (33-34). Plazzogna and coworkers (33) reported a formation constant of  $1.00 \times 10^3$  for  $\text{CH}_3\text{HgCl}_2^-$  in acetonitrile solution. This constant was determined by a spectrophotometric method which measured the free chloride concentration by its effect on the ionization of  $(\text{C}_6\text{H}_5)_3\text{CCl}$ . Canty and Marker (34) reported the formation of three-coordinate methylmercury in complexes of neutral donor ligands (pyridine and pyridine derivatives) in the solid state and in methanol solution. The solid state complexes were studied by infrared spectroscopy and x-ray crystallography while the solution complexes were studied by NMR spectroscopy.

Schwarzenbach and Schellenberg (1) measured the tendency of  $\text{CH}_3\text{Hg}^+$  toward higher complexation in aqueous solution by a solubility study of methylmercuric iodide in potassium nitrate and in potassium iodide. They observed solubilities of  $1.67 \times 10^{-3}$  moles/l. in 0.1 M KI and  $1.41 \times 10^{-3}$  moles/l. in 0.1 M  $\text{KNO}_3$ . This difference was attributed to the formation of  $\text{CH}_3\text{HgI}_2^-$  in excess iodide solution. They calculated the formation constant of  $\text{CH}_3\text{HgI}_2^-$  to be  $\sim 2$  compared to  $4 \times 10^8$  for the  $\text{CH}_3\text{HgI}$  complex. Similar results were obtained in the study of  $\text{CH}_3\text{Hg}(\text{CN})_2^-$  and  $\text{CH}_3\text{Hg}(\text{SCH}_2\text{CH}_2\text{OH})_2^-$ , suggesting that methylmercury has little tendency for complexing more than one ligand.

The same conclusion was reached by Simpson (5) from his studies of the methylmercuric cyanide complex by solute distribution experiments in toluene and water, and by Goggin and Woodward (35) who were unable to detect  $\text{CH}_3\text{Hg}(\text{CN})_n^{1-n}$  type complexes by Raman spectroscopy.

Sytsma and Kline (36) reported an NMR study of methylmercury complexes of some potentially chelating thiophenols. They observed mercury-proton coupling constants typical of methylmercury coordinated to one ligand and not of methylmercury bound to two or three ligands, and concluded that thiophenol binds as a monodentate ligand to methylmercury.

Barbieri and Bjerrum (37), however, found evidence

for three and four-coordinate mercury in the ethylmercury-thiocyanate and -iodate systems which they studied by polarography. They determined the formation constants of  $C_2H_5Hg(SCN)_2^-$  and  $C_2H_5Hg(SCN)_3^{2-}$  to be 0.80 and 1.6 respectively and the formation constants of the corresponding iodate complexes to be 0.22 and 5.6. These results are consistent with the conclusion of Schwarzenbach (1) that only one-coordinate methylmercury complexes are important in aqueous solution.

Relf, Cooney and Hennicke (38) studied the methylmercury-thiocyanate system by NMR and vibrational spectroscopy. They monitored the mercury-proton coupling constant in the NMR spectrum and the Hg-S stretching frequency in the Raman spectrum as a function of the thiocyanate to methylmercury ratio. Neither the coupling constant nor the Hg-S stretching frequency changed appreciably from an equimolar methylmercury-thiocyanate solution to a solution containing a sixteen fold excess of ligand. These results were taken to indicate that no appreciable change in the hybridization of the mercury occurred and, therefore, that only one thiocyanate ligand binds covalently to the methylmercury. The formation of an ion-dipole complex,  $CH_3Hg(SCN)_2^-$ , was not eliminated by these studies.

Ionic interactions resulting in effective mercury coordination numbers of three and four have been observed

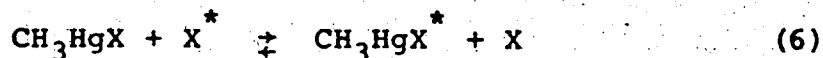
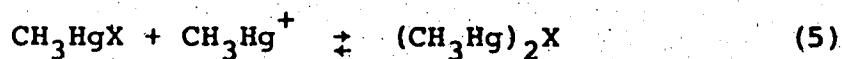
in solid state studies of methylmercury complexes of amino acids (39-40). In the x-ray study of the 2:1 methylmercury-penicillamine complex (39), Carty and coworkers report the formation of a zwitterion complex with the dianion of penicillamine. In this complex, one methylmercury is bound to the deprotonated sulfhydryl group and the second methylmercury to the amino and carboxylate groups, with a positive charge localized on the amino group and a negative charge on the carboxyl group. In a separate x-ray study (40), Carty investigated the methylmercury complexes of L-cysteine and methionine. In each case, strong covalent interaction between the methylmercury and one functional group (the deprotonated sulfhydryl of cysteine and the amino of methionine) was evident. But in both cases, additional weak ionic interaction with the carboxyl group was indicated by a Hg-O distance shorter than the sum of the Van der Waals radii.

These methylmercury complexes of penicillamine, cysteine, and methionine have been studied in aqueous solution by nuclear magnetic resonance spectroscopy (8,10). In all cases, there was no evidence of methylmercury being more than one-coordinate in aqueous solution. These results are consistent with a predominant coordination number of one for  $\text{CH}_3\text{Hg}^+$  and indicate that complexes of higher coordination number cannot form without the advantages that the solid state or non-aqueous solvents offer.

In methylmercury complexes, the mercury-ligand bond is quite labile resulting in exchange of the ligand among the methylmercury ions. This exchange is usually fast on the NMR time scale, however, in some instances the rate of exchange is slow enough to be measurable by NMR line broadening techniques. In 1967, Simpson (22) studied the displacement of hydroxide ion from methylmercuric hydroxide by the cyanide ion. This reaction appears to proceed via an associative mechanism rather than the dissociative mechanism characteristic of most other metal complexation reactions (41). Simpson, Hopkins, and Hague (9) have reported kinetic data for the binding of methylmercuric chloride by N-acetyl-L-cysteine. They concluded that the exchange of peptide between the free and complexed forms is by a first order dissociative mechanism. Their study is suspect, however, because the rate constant predicted for the reaction of methylmercury and N-acetyl-L-cysteine from their results and the formation constant of methylmercuric cysteine (5) is several orders of magnitude larger than that for a diffusion-controlled bimolecular reaction. Recently, NMR studies of the kinetics of the methylmercury-methylamine (42) and the methylmercury-glutathione (10) systems have been reported. In the methylamine system, first order dissociation of the complex was found to be the significant contributor to the methylamine exchange. For the glutathione system,

the major pathway for ligand exchange was found to be pH dependent; below pH 2, a proton-assisted dissociation of the complex is important, while above pH 2, ligand displacement pathways are dominant.

For most methylmercury systems, except the methylamine and glutathione systems discussed above, exchange averaged NMR spectra were observed, indicating that ligand and methylmercury exchange is fast on the NMR time scale, even when very strong complexes are formed. This has been attributed to two types of reactions (42), represented by Equations 5 and 6 which have the effect of labilizing



the mercury-ligand bond. The first of these reactions, Equation 5, is known to be important because of the ability of methylmercury to form polynuclear complexes. The second reaction, Equation 6 is important because of the ability of methylmercury to react with excess ligand. Earlier in this chapter, it was pointed out that 2:1 methylmercury-ligand complexes form only in small amounts, but these small concentrations are apparently kinetically important (10).

Some quantitative work has been reported on the

complexation of methylmercury by inorganic anions. Woodward and coworkers have determined the degree of dissociation of methylmercuric salts in aqueous solution by Raman spectroscopy (25,43,44). They reported that methylmercuric perchlorate is completely dissociated in concentrated aqueous solution (25), while methylmercuric nitrate is only partly dissociated (25). By intensity measurements on the nitrate bands in the Raman spectra of concentrated methylmercuric nitrate solutions, they estimated the degree of dissociation of methylmercuric nitrate to be similar to the degree of dissociation of nitric acid (43). Similar investigations on the methylmercury complexes of methanesulfonate and sulfate showed that these salts also are only partially dissociated in aqueous solution (44).

In 1961, Simpson (5) reported a polarographic study of the binding of methylmercury by a variety of ligands. Formation constants were calculated for methylmercuric hydroxide, chloride, acetate, and thiocyanate and for several amino acid complexes of methylmercury. These results were evaluated in terms of the aqueous solution model of Waugh, Walton, and Laswick (18) which, as mentioned above, did not include the methylmercury dimer  $(\text{CH}_3\text{Hg})_2\text{OH}^+$  or trimer  $(\text{CH}_3\text{Hg})_3\text{O}^+$ . Nevertheless, he obtained semi-quantitative information about the complexation behavior of methylmercury. Simpson concluded from these studies that, of the potential sites for the binding

of methylmercury to proteins, the sulfhydryl group is the most important followed by the imidazole nitrogen and the amino group.

In a separate study, Simpson (6) investigated the binding of methylmercury by nucleosides. From absorption spectroscopy data, he evaluated formation constants for the methylmercury-nucleoside complexes and determined the nitrogen sites involved in the binding of methylmercury. Recently, Tobias and coworkers have reported studies of the binding of methylmercury by pyrimidine nucleosides and nucleotides (45) and by purine nucleosides and nucleotides (3). Using Raman difference spectroscopic data, they concluded that the methylmercury binds preferentially to one of the deprotonated ring nitrogens rather than to an oxygen site.

In 1965, Schwarzenbach and Schellenberg (1) reported a study of the methylmercury complexes of a wide variety of organic and inorganic ligands. From potentiometric titration data, they calculated formation constants for a number of complexes; those which are of interest to this thesis are listed in Table 1. The results they obtained are consistent with the unifunctional, soft acid theory of methylmercury which predicts strongest methylmercury complexation to sulfur-binding ligands, followed by nitrogen and then oxygen-binding ligands. It was pointed out by Schwarzenbach and Schellenberg that,



TABLE 1  
 Formation Constants of Methylmercury Complexes  
 of Selected Ligands<sup>a</sup>

Ligand	log K <sub>F</sub>
F <sup>-</sup>	1.50
Cl <sup>-</sup>	5.25
Br <sup>-</sup>	6.62
I <sup>-</sup>	8.60
HPO <sub>3</sub> <sup>2-</sup>	4.67
S <sup>2-</sup>	21.2
CH <sub>3</sub> HgS <sup>-</sup>	16.3
(CH <sub>3</sub> Hg) <sub>2</sub> S	7
HO-CH <sub>2</sub> -CH <sub>2</sub> -S <sup>-</sup>	16.12
HO-CH <sub>2</sub> -CH <sub>2</sub> -S-HgCH <sub>3</sub>	6.27
SO <sub>3</sub> <sup>2-</sup>	8.11
NH <sub>3</sub>	7.60
CN <sup>-</sup>	14.1

a) , Reference 1.

although the methylmercury cation has been compared to the proton in the simple stoichiometry of its reactions, the tendency for complexation with various ligands is different because the proton is a hard acid, preferring oxygen to sulfur-binding ligands.

The binding of methylmercury by carboxylic acids (46), amines (7), sulfhydryl-containing amino acids (8-10), and glutathione (10) has been quantitatively characterized in aqueous solution by nuclear magnetic resonance spectroscopy. The conditional formation constants calculated for these complexes (42), show that the sulfhydryl group always binds methylmercury most strongly. At low pH, the carboxyl group and  $H_2O$  compete more effectively than the amino group for the methylmercury, while at high pH the methylmercury prefers the amino group or hydroxide to the carboxyl site.

### C. Overview of Part I

As indicated at the beginning of this chapter, little beyond formation constants has been reported for the complexation of methylmercury by inorganic anions in aqueous solution. It was decided to attempt to obtain more information about these systems at the molecular level. Nuclear magnetic resonance spectroscopy was chosen as the technique for this study. It can monitor the behavior of the methylmercury at the molecular level, providing information about both the structure and stability

of the complex, in contrast to potentiometric titration methods which only can provide formation constants. NMR has proven useful in other studies of methylmercury complexes, in which formation constants (7,8,10), ligand exchange kinetics (10) and ligand binding sites (8-10) have been determined.

The proton NMR spectrum of methylmercury consists of a methyl singlet flanked symmetrically by two less intense satellite peaks. The singlet is due to the protons of methyl groups bound to mercury atoms having a nuclear spin of zero, while the satellites are due to protons of methyl groups bound to the 16.9% of mercury having nuclear spin one-half ( $^{199}\text{Hg}$ ). Both the chemical shift of the methyl singlet and the mercury-proton spin-spin coupling constant of  $\text{CH}_3\text{HgX}$  are dependent on the nature of the ligand, X, coordinated to the methylmercury.

An early study by Hatton et al. (23) of methylmercury complexes of cyanide, acetate, hydroxide, chloride, nitrate, and perchlorate suggested that the magnitude of the spin-spin coupling constant decreases as the substituent is made more electronegative. A linear relationship between the spin-spin coupling constant of complexed methylmercury and the  $\text{pK}_a$  of the ligand has been observed in several instances. Sytsma and Kline (36) reported such a relationship in methylmercury complexes of organic acids. They attributed it to the fact that both the

spin-spin coupling constant and the  $pK_a$  are related to the polarizability of the basic site to which the proton or the methylmercury is bonded. Similar relationships of the spin-spin coupling constant of methylmercury carboxylates in chloroform solution (47) and in aqueous solution (46) to the  $pK_a$  of the carboxylic acid have been reported. Goggin and coworkers (48) also found that the spin-spin coupling constant depends on the ligand in methylmercury complexes, concluding that the coupling constant gives a measure of the metal-ligand bond strength or at least the s-orbital contribution to it. Scheffold (49) reported a linear relationship between the spin-spin coupling constants and the formation constants of methylmercury complexes of cyanide, thiosulfate, and the halides.

The spin-spin coupling constants of a number of methylmercury complexes reported in the literature are given in Table 2. This data indicates that this coupling constant depends on the nature of the metal-ligand bond, and that its magnitude can be correlated to the donor atom of the ligand. Because of this dependence, it would seem that the ligand to which methylmercury is bonded in natural and biological systems could possibly be identified from the magnitude of the coupling constant of methylmercury in these systems.

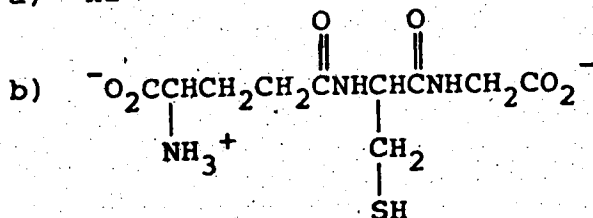
In Chapter IV, the nature of the binding

TABLE 2

The Mercury-Proton Coupling Constant of Methylmercury  
in Selected Methylmercury Complexes

Complex	Donor Atom of Ligand	$J_{\text{CH}_3\text{Hg}}^a$
$\text{CH}_3\text{HgCN}$	C	178.0 <sup>c</sup>
$\text{CH}_3\text{HgCl}$	Cl	215.2 <sup>c</sup>
$\text{CH}_3\text{HgOH}_2^+$	O	260.0 <sup>d</sup>
$\text{CH}_3\text{HgNO}_3$	O	227.0 <sup>c</sup>
$\text{CH}_3\text{HgO}_2\text{CCH}_3$	O	233.3 <sup>d</sup>
$\text{CH}_3\text{HgNH}_2\text{CH}_3^+$	N	211.5 <sup>e</sup>
Glutathione <sup>b</sup>	S	170.0 <sup>f</sup>

a) Hz



- c) Pyridine solution; Reference 23.  
d) Aqueous solution; Reference 46.  
e) Aqueous solution; Reference 7.  
f) Aqueous solution; Reference 10.

of methylmercury by selected inorganic anions is characterized by nuclear magnetic resonance spectroscopy. The spin-spin coupling constants of these methylmercury complexes is of interest because of the sensitivity of its magnitude to the nature of the ligand. The selenite complex of methylmercury was studied because of the reported protecting ability of the selenite anion against methylmercury. The sulfite complex was studied because of the similarity of the sulfite and selenite anions. Other selenium and sulfur complexes of methylmercury were studied to provide more information about methylmercury-selenium and methylmercury-sulfur complexes. Where possible, formation constants have been determined for the complexation reactions. In several complexes, structural information has been obtained from Raman spectroscopic studies to support the conclusions from the NMR studies.

## CHAPTER II

### EXPERIMENTAL

#### A. Chemicals

Sodium sulfite (Shawinigan Chemicals), sodium bisulfite (British Drug Houses), sodium sulfate (Allied Chemicals), sodium selenide (Alfa Inorganics), potassium selenocyanate (Alfa Inorganics), potassium thiocyanate (Baker Chemicals), and t-butanol (Fisher Scientific Company) were used as received and, if necessary, their solutions were standardized as described below. Sodium selenite (Alfa Inorganics), sodium sulfide (Baker Chemicals), sodium selenate (Alfa Inorganics), and methylmercuric hydroxide (Alfa Inorganics) were purified before their solutions were standardized. Purification and standardization procedures are described below.

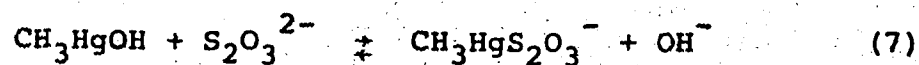
All other chemicals were of the highest grade commercially available and were used without further purification.

#### B. Preparation and Standardization of Methylmercuric Hydroxide Solutions

The commercial methylmercuric hydroxide contained insoluble material and an acetate impurity. The acetate impurity was indicated by a singlet in the proton magnetic resonance spectrum at 1.91 ppm downfield from the methyl resonance of sodium 2,2-dimethyl-2-silapentane-5-sulfonic

acid (DSS). To remove the insoluble fraction, an approximately 0.4 M solution of methylmercuric hydroxide in triply-distilled water was passed through a 0.2 micron membrane filter three times, or until the solution remained clear. The filtrate was then passed through an anion exchange column (Dowex 1-X8) in the hydroxide form, to replace the acetate ions by hydroxide ions. The acetate could have been present as  $\text{CH}_3\text{HgOAc}$  or as some other acetate salt. The cation of the acetate impurity was determined by analyzing the stock methylmercury solution.

First, the total hydroxide concentration of the solution was determined by adding a small excess of sodium thiosulfate to displace the hydroxide from the methylmercuric hydroxide, according to Equation 7. The hydroxide was then determined by potentiometric titration

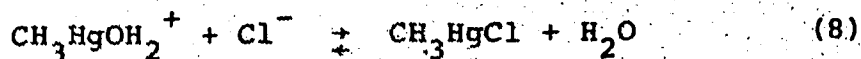


with standard nitric acid. This total hydroxide concentration would be equal to the methylmercury concentration only if no other cations were present in the solution. The presence of sodium was indicated and its concentration was determined by flame photometry. The methylmercury concentration of the same solution was determined by the sodium chloride titration method described below. The



results of these analyses showed that the total hydroxide concentration was equal to the sum of the methylmercury concentration and the sodium ion concentration. This indicated that the methylmercury stock solution contained methylmercuric hydroxide and sodium hydroxide. The sodium hydroxide was formed when the sodium acetate originally present in the commercial reagent was passed through the anion exchange column.

The stock solution of methylmercuric hydroxide was standardized by a potentiometric titration with standard sodium chloride solution, which was prepared by weighing dried reagent sodium chloride as a primary standard. This methylmercury standardization procedure is based on the reaction of chloride ions with the methylmercury cation to form methylmercuric chloride. This equilibrium is described by Equations 8 and 9. The formation constant of methylmercuric chloride in aqueous



$$K_F = \frac{[\text{CH}_3\text{HgCl}]}{[\text{CH}_3\text{HgOH}_2^+][\text{Cl}^-]} \quad (9)$$

solution is  $1.78 \times 10^5$  (1). To minimize competition between hydroxide and titrant for  $\text{CH}_3\text{Hg}^+$ , the titration was performed at pH 2, where the major fraction of methyl-

mercury exists as the hydrated cation. The titration was carried out in an ethanol-water solvent system to increase the formation constant of the methylmercuric chloride complex, and thus increase the sharpness of the break in the titration curve at the endpoint. An 80% ethanol by volume solvent system was adopted as the optimum titration medium. The endpoint was determined potentiometrically using a silver/silver chloride indicating electrode and a saturated calomel reference electrode. In the 80% ethanol by volume titration medium, the potential changed approximately 200 mv on going from 1% before to 1% after the endpoint. The concentration of a typical stock solution was found after four such titrations to be  $0.4303 \pm 0.0004$  M methylmercury.

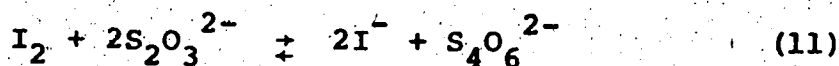
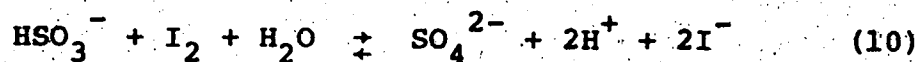
### C. Preparation and Standardization of Ligand Solutions

Sodium sulfate and sodium selenate were used as the source of the sulfate and selenate ligands. The sodium selenate was recrystallized from ammoniacal solution to remove traces of acetate which co-precipitated from water. Stock solutions of about 0.4 M sodium sulfate or 0.4 M sodium selenate in triply-distilled water were standardized by a precipitation titration with standard lead nitrate in acidic 80% acetone medium (50). Dithizone was used to locate the endpoint. The lead nitrate was standardized by passing aliquots of the stock

solution through a cation exchange column (Dowex 50W-X8) in the hydrogen form to replace the lead ions by protons. The number of moles of acid in the effluent, equal to twice the number of moles of lead ion in the aliquot, was then determined by titration with standard sodium hydroxide to a methyl red endpoint.

A solution of sodium selenite, the source of the selenite ligand, was purified by first filtering off the insoluble materials. The sodium selenite then was isolated from water soluble impurities by recrystallization. Stock solutions of approximately 0.4 M sodium selenite in triply-distilled water were prepared from the purified solid and were standardized by potentiometric titration with standard nitric acid.

Sodium sulfite or sodium bisulfite was used as the source of the sulfite-ligand. The solids were analyzed by oxidation with excess iodine followed by back-titration with standard thiosulfate, according to the equilibria represented by Equations 10 and 11. The standard thio-



sulfate solution was prepared by weighing the anhydrous reagent as a primary standard, and the resultant solution

was used to standardize the iodine solution. Starch was used to locate the endpoint.

Approximately 0.4 M stock solutions of potassium thiocyanate in triply-distilled water were standardized by a Volhard titration with silver nitrate using ferric alum to locate the endpoint (51). The standard silver nitrate was prepared by weighing the reagent as a primary standard and dissolving it in chloride-free distilled water.

Nitric acid solutions were prepared by diluting concentrated nitric acid and were standardized against primary standard mercuric oxide (52). Accurately weighed samples of dry mercuric oxide plus a five-fold excess of potassium iodide were dissolved in water. The mercuric oxide reacts with the iodide to form two equivalents of hydroxide, according to Equation 12. The nitric acid



solution was standardized by titration of the hydroxide to a phenolphthalein endpoint.

Standard solutions of base were prepared by dilution of saturated, carbonate-free sodium hydroxide with carbon dioxide-free distilled water. These solutions were standardized either by titration with standard nitric acid, or by titration against known amounts of primary standard potassium hydrogen phthalate.

#### D. pH Measurements

pH measurements were carried out at  $25 \pm 1^\circ\text{C}$  with an Orion Model 801 pH meter equipped with a standard glass electrode and a fibre junction saturated calomel reference electrode. Fisher Certified standard solutions having pH values of 4.00, 7.00 and 10.00 at  $25^\circ\text{C}$  (potassium biphthalate, potassium phosphate, and sodium borate, respectively) were used to standardize the pH meter.

pH measurements were converted to hydrogen ion concentrations using activity coefficients calculated by the Davies Equation (53), Equation 13. The Davies equation estimates the activity coefficient  $\gamma_i$  of an ion,

$$-\frac{\log \gamma_i}{z_i^2} = \frac{0.511(I)^{1/2}}{1 + 1.5(I)^{1/2}} - 0.2 I \quad (13)$$

$i$ , of charge  $z_i$  from the ionic strength,  $I$ , of the solution.

#### E. Solutions for Nuclear Magnetic Resonance and Raman Spectroscopic Measurements

##### 1. NMR Experiments

Solutions used in the nuclear magnetic resonance measurements were prepared in triply-distilled water from pipetted amounts of stock methylmercuric hydroxide solution

and weighed or pipetted amounts of the ligand. T-butanol was added for an internal chemical shift reference at an approximate concentration of one third the methylmercury concentration. These solutions were, typically, 0.1 M in methylmercury. The sulfite, selenocyanate, and selenide ligands are sensitive to air, and solutions containing these anions were prepared in an argon or nitrogen atmosphere, using an appropriate amount of the crystalline salt of the ligand and spectra were obtained immediately after sample preparation.

For chemical shift or spin-spin coupling constant measurements as a function of pH, solutions of methylmercury to ligand ratios varying from one-quarter to four were prepared. Initially, the solution was acidified to about pH 1. Then base was added and samples were withdrawn at approximately 0.4 pH unit intervals until about pH 12. Typically, twenty to thirty 0.4 ml samples were required to cover the pH range 1-12. In this way, the solution ionic strength remains almost constant throughout the experiment. For example, a solution containing 0.0538 M methylmercury and 0.201 M sodium sulfate was acidified with nitric acid before samples were withdrawn. Using the formation constant of methylmercuric sulfate calculated in Chapter IV and the  $K_a$ 's of the ligand, the concentration of each solution species, and thus the ionic strength of the solution, can be calculated at any pH.

The ionic strength of this solution varied from 0.55 to 0.74 on going from pH 1 to pH 5, the data region used for calculating formation constants of this system. Concentrated nitric acid and potassium hydroxide solutions were used to adjust the pH. Sodium hydroxide was used rather than potassium hydroxide if the solution contained the perchlorate anion. In some experiments 0.3 M potassium nitrate or sodium perchlorate was added to maintain a high but constant ionic strength.

For mole ratio experiments performed at constant pH the requisite amount of ligand and methylmercury were mixed, the pH adjusted and a sample withdrawn. More ligand or methylmercury was added to the solution and the same procedure followed for adjusting the pH and withdrawing the sample. The concentrations of ligand and methylmercury were corrected for the changing solution volume, but because of the high concentrations necessary for NMR experiments (greater than 0.05 M methylmercury to observe the satellite resonances), no attempt was made to control the ionic strength, which therefore varies more in mole ratio experiments than in pH variation experiments.

## 2. Raman Experiments

Solutions used in the Raman spectroscopy measurements were prepared in distilled water from the requisite amounts of methylmercuric hydroxide solution

and ligand. Solutions containing the sulfite ligand were prepared in an argon atmosphere to minimize air oxidation. The methylmercury to ligand ratios and solution pH's chosen were those which, based on calculations using the formation constants derived from the NMR experiments, contained a maximum concentration of the desired methylmercury species. The samples were sealed into glass capillaries (o.d. 1.5 mm).

For experiments in which quantitative information was obtained from the intensity of selected Raman bands, the methylmercury solution was titrated with standard perchloric acid, while withdrawing samples at approximately 0.5 pH unit intervals. The known amount of perchlorate ion present in each sample served as an internal intensity standard for the measurement of each spectrum.

#### F. Proton Magnetic Resonance Measurements

Proton magnetic resonance spectra were obtained on a Varian A60-D spectrometer at a probe temperature of  $25 \pm 1^\circ\text{C}$ . The temperature of the probe was determined by measuring the potential of a copper vs. constantan thermocouple inserted in the probe.

Spectra were recorded at sweep rates of 0.1 Hz/sec for the chemical shift measurements and 0.5 Hz/sec for the spin-spin coupling measurements. Reported data are the average of at least three scans. Chemical shifts were



measured relative to the t-butyl resonance of internal t-butanol but are reported relative to the methyl resonance of sodium 2,2-dimethyl-2-silapentane-5-sulfonic acid (DSS). Positive shifts correspond to resonances of protons less shielded than those of the reference. The t-butyl resonance of t-butanol is 1.24 ppm downfield from the methyl resonance of DSS.

The sweep widths of the NMR recorder were calibrated by a sideband procedure. A Hewlett-Packard, Model 200AB audio oscillator was used to provide sideband signals of a TMS resonance in a chloroform sample. The frequency of the sideband was counted with a Hewlett-Packard, Model 5307A High Resolution Counter. For recorder calibration, the shift of the sideband from the main signal, as indicated by the calibration markings of the recorder paper, was matched to the counted frequency generated by the audio oscillator.

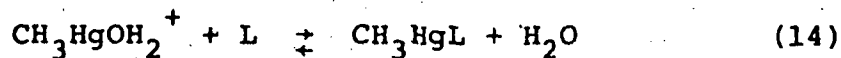
#### G. Raman Spectroscopic Measurements

Raman spectra were excited with the 4880 Å line of a Coherent Radiation Model 52 Ar<sup>+</sup> laser, which produced ca. 200 mw at the sample. The Raman scattering was dispersed with a Spex 1401 double monochromator and detected with an RCA C31034 photomultiplier tube. Raman spectra were recorded throughout the range  $\Delta\nu = 50 - 4000 \text{ cm}^{-1}$ .

To obtain intensity measurements on selected Raman bands, the  $\nu_1$  of the perchlorate ion (at  $929 \text{ cm}^{-1}$ ) was used as an internal intensity standard. It was recorded before and after running each spectrum and the intensities averaged. The intensity of the  $504 \text{ cm}^{-1}$  band of  $\text{CH}_3\text{HgOH}$ , relative to the intensity of the perchlorate  $\nu_1$ , was determined by adding sodium perchlorate to a standard methylmercuric hydroxide solution. Because of the approximations necessary in the use of intensity data, the observed Raman intensities were not corrected for difference in refractive index; such corrections are expected to be small relative to the uncertainties introduced by the approximations (44).

#### H. Determination of Formation Constants by NMR Spectroscopy

The formation constants of the methylmercury complexes described in Part I of this thesis were calculated from the chemical shift and the mercury-proton coupling constant of the methyl protons of methylmercury in solutions of known pH and known methylmercury and ligand concentrations. Formation constants of methylmercury complexation reactions, represented by  $K_F$ , are defined by Equations 14 and 15, where L is the ligand and  $\text{CH}_3\text{HgL}$  is the complex.



$$K_F = \frac{[\text{CH}_3\text{HgL}]}{[\text{CH}_3\text{HgOH}_2^+][\text{L}]} \quad (15)$$

In labile systems such as those studied in this thesis, the methylmercury is exchanging between its various free and complexed forms. The rate of this exchange is fast on the NMR time scale, that is, the inverse of the lifetime of the free and complexed forms is somewhat greater than  $2\pi\Delta\delta$ , where  $\Delta\delta$  represents the separation in Hz of the resonances of the free and complexed forms.

When this exchange is fast, an exchange-averaged resonance is observed for the methylmercury. The observed chemical shift, and similarly the spin-spin coupling constant, is a weighted average of the chemical shifts of the various methylmercury forms. The observed chemical shift,  $\delta_{\text{obs}}$ , is described by Equation 16 where  $\delta_f$  represents the

$$\delta_{\text{obs}} = P_f \delta_f + P_c \delta_c \quad (16)$$

chemical shift of the free methylmercury and  $\delta_c$  that of the complexed methylmercury.  $P_f$  and  $P_c$  are the fractions of methylmercury in the free and complexed forms, such that  $P_f + P_c = 1$ . Using this relationship, Equation 16.

can be rearranged to Equation 17 which shows that the fraction of methylmercury in the complexed form can be

$$P_c = \frac{\delta_{\text{obs}} - \delta_f}{\delta_c - \delta_f} \quad (17)$$

calculated from the observed chemical shift and the chemical shifts of the free and complexed methylmercury. Thus, for each data point, the concentration of complex is equal to  $P_c$  times the total methylmercury concentration and the free ligand concentration is equal to the total ligand concentration minus the complex concentration. The formation constant of the complex was calculated for each data point from Equation 18 and the total methylmercury

$$K_F = \frac{P_c [\text{CH}_3\text{Hg}^+]_{\text{total}}}{[\text{CH}_3\text{Hg}^+] \cdot \alpha \{ [\text{L}]_{\text{total}} - P_c [\text{CH}_3\text{Hg}^+]_{\text{total}} \}} \quad (18)$$

and ligand concentrations,  $[\text{CH}_3\text{Hg}^+]_{\text{total}}$  and  $[\text{L}]_{\text{total}}$ .  $\alpha$  represents the fraction of ligand in the form available for complexation and depends only on pH.  $[\text{CH}_3\text{Hg}^+]$  is dependent on the total concentration of free methylmercury and is calculated from the formation constants of the hydroxide and dimeric methylmercury species.

For the systems studied in this thesis,  $P_c$  and  $P_f$  vary between zero and one as the pH is changed. This is due to competing equilibria; at low pH, protons and the

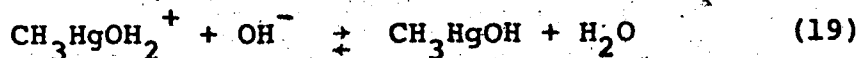
methylmercury cation are competing for the ligand, while at high pH, hydroxide and ligand are competing for the methylmercury. In order to determine accurate formation constants by the method described above, it is necessary to adjust solution conditions to ensure a significant fraction of methylmercury in each form, usually at least ten percent. When this is the case,  $\delta_{\text{obs}}$  generally differs significantly from both  $\delta_{\text{c}}$  and  $\delta_{\text{f}}$ , and the  $P_{\text{c}}$  and formation constant can be calculated from Equations 17 and 18.

### CHAPTER III

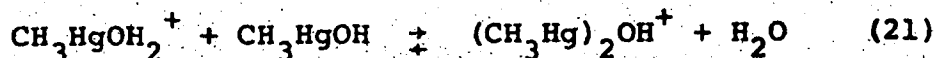
#### METHYLMERCURY SPECIES AND EQUILIBRIA IN AQUEOUS SOLUTION

##### A. Introduction

The aqueous solution model usually used in methylmercury complexation studies is that reported in 1965 by Schwarzenbach and Schellenberg (1). From potentiometric titration data for solutions of total methylmercury concentration ranging from  $5.85 \times 10^{-4}$  M to  $2.19 \times 10^{-2}$  M, they found evidence for three methylmercury species:  $\text{CH}_3\text{HgOH}_2^+$ ,  $(\text{CH}_3\text{Hg})_2\text{OH}^+$ , and  $\text{CH}_3\text{HgOH}$ . The equilibria relating these three species are described by Equations 19-22. Schwarzenbach and Schellenberg obtained values



$$K_1 = \frac{[\text{CH}_3\text{HgOH}]}{[\text{CH}_3\text{HgOH}_2^+][\text{OH}^-]} \quad (20)$$



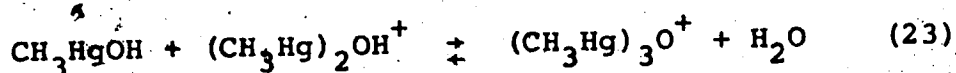
$$K_2 = \frac{[(\text{CH}_3\text{Hg})_2\text{OH}^+]}{[\text{CH}_3\text{HgOH}_2^+][\text{CH}_3\text{HgOH}]} \quad (22)$$

of  $2.34 \times 10^9$  and  $2.34 \times 10^2$  for  $K_1$  and  $K_2$  respectively, from their potentiometric titration data. According to

the Schwarzenbach model, methylmercury exists as a hydrated cation,  $\text{CH}_3\text{HgOH}_2^+$ , at low pH. At high pH, the methylmercury cation reacts with hydroxide to form methylmercuric hydroxide,  $\text{CH}_3\text{HgOH}$ . At intermediate pH, both these species are present, as well as the methylmercury dimer,  $(\text{CH}_3\text{Hg})_2\text{OH}^+$ , formed by reaction of the methylmercury cation with methylmercuric hydroxide.

Woodward and coworkers (54) identified the species  $\text{CH}_3\text{HgOH}$  in aqueous solution by Raman spectroscopy. They also assigned a band in the Raman spectra of methylmercury solutions at neutral pH to the species  $(\text{CH}_3\text{Hg})_2\text{OH}^+$  (43). This assignment of the Raman bands of  $\text{CH}_3\text{HgOH}$  and  $(\text{CH}_3\text{Hg})_2\text{OH}^+$  has been criticized by Green (20) on the basis of the report by Grdenic and Zado (19) that  $\text{CH}_3\text{HgOH}$  does not exist, except in dilute solution as the dissociation product of  $[(\text{CH}_3\text{Hg})_3\text{O}]\text{OH}$ . Grdenic and Zado claimed to have prepared  $[(\text{CH}_3\text{Hg})_3\text{O}]\text{OH}$  by a reaction between  $[(\text{CH}_3\text{Hg})_3\text{O}]\text{ClO}_4$  and  $\text{KOH}$  in methanol. They concluded from conductance data that  $(\text{CH}_3\text{Hg})_3\text{O}^+$  is stable in alkaline methanol solution and thus, that the compound previously thought to be  $\text{CH}_3\text{HgOH}$  is actually  $[(\text{CH}_3\text{Hg})_3\text{O}]\text{OH}$  or its dehydration product. Lorbeth and Weller (55) have shown that the compound reported to be  $[(\text{CH}_3\text{Hg})_3\text{O}]\text{OH}$  by Grdenic and Zado is a hydrate of  $(\text{CH}_3\text{Hg})_2\text{O}$ . However, Grdenic and Zado did observe the precipitation of a small amount of  $[(\text{CH}_3\text{Hg})_3\text{O}]\text{ClO}_4$  from a concentrated aqueous solution of

methylmercuric hydroxide titrated with perchloric acid, which indicates that some trismethylmercurioxonium ion must be present in aqueous solution. Thus, to fully describe the chemistry of aqueous methylmercury solutions more concentrated than those of Schwarzenbach and Schellenberg, it may be necessary to include the species  $(\text{CH}_3\text{Hg})_3\text{O}^+$ , the formation of which is represented by Equations 23 and 24.



$$K_3 = \frac{[(\text{CH}_3\text{Hg})_3\text{O}^+]}{[\text{CH}_3\text{HgOH}] [(\text{CH}_3\text{Hg})_2\text{OH}^+]} \quad (24)$$

In this chapter, NMR and Raman results are reported for the aqueous solution chemistry of methylmercury (26). These results indicate that the Schwarzenbach and Schellenberg model accounts for most of the methylmercury in solution, except at high methylmercury concentrations in which some trismethylmercurioxonium ion forms in the neutral pH region. The chemical shift and the spin-spin coupling constant of the cationic, hydroxide, and dimeric species of methylmercury in aqueous solution are also reported.



## B. Results and Discussion

The NMR spectrum of methylmercuric hydroxide in aqueous solution at pH 12.0 is shown in Figure 1. The central resonance is due to the protons of methyl groups bonded to isotopes of mercury having nuclear spin of zero, while the satellite resonances are due to protons of methyl groups bonded to  $^{199}\text{Hg}$ , the isotope having nuclear spin one-half (16.9% natural abundance). It was pointed out in Chapter I that both the chemical shift of the methyl resonance and the mercury-proton coupling constant (the separation between the satellite resonances) are dependent on the nature of the ligand coordinated to the methylmercury.

The chemical shift of the methyl resonance and the spin-spin coupling constant of methylmercury in a solution containing no coordinating ligand other than water are pH dependent. The chemical shift of methylmercury in a 0.190 M aqueous methylmercury solution is presented as a function of pH in Figure 2. The coupling constant of methylmercury in the same solution is presented as a function of pH in Figure 3. These chemical shift and coupling constant titration curves can be explained in terms of the model represented by Equations 19-24 which describes the aqueous solution chemistry of methylmercury. According to this model, the fractional concentrations of each methylmercury species at a given pH will be dependent

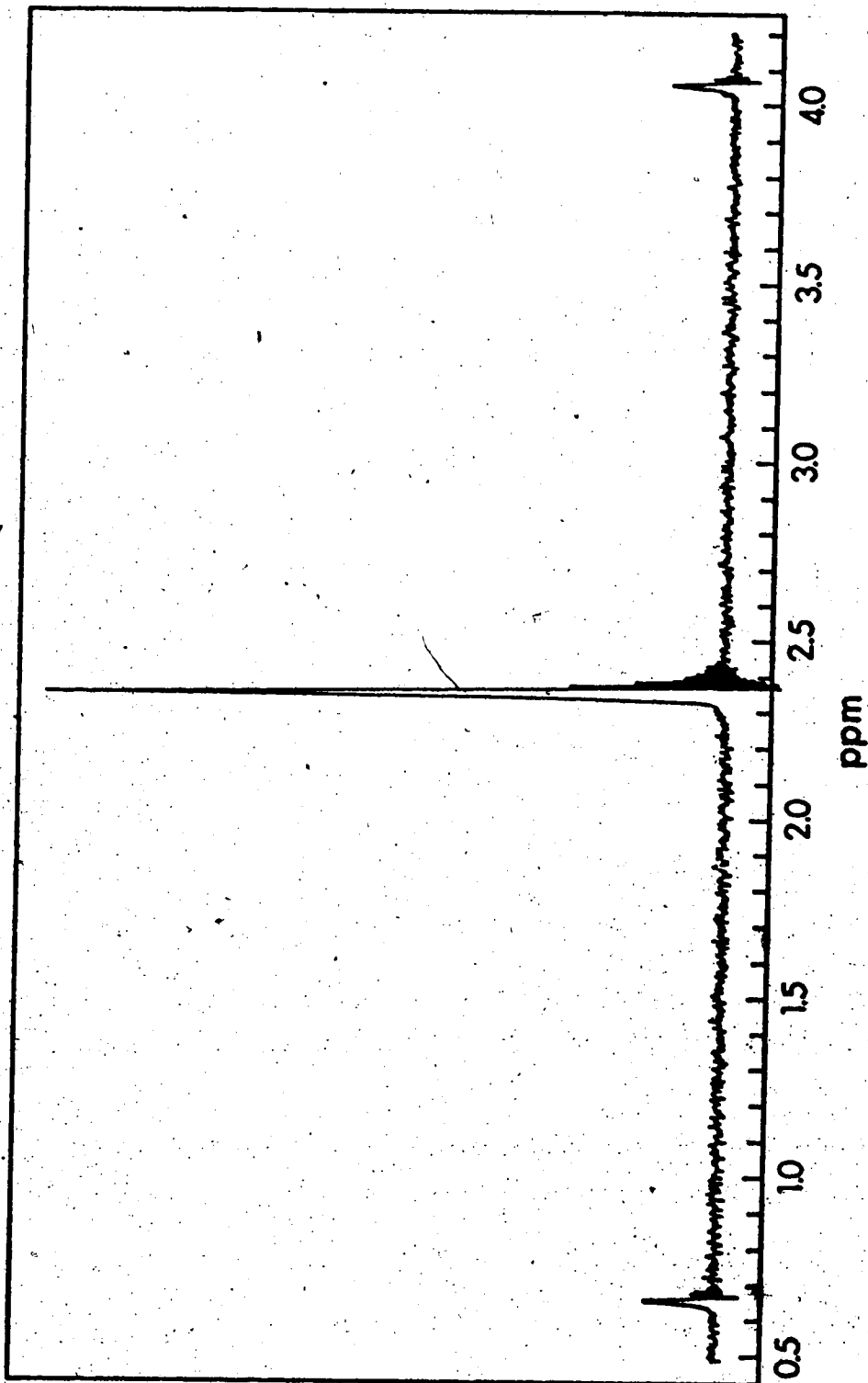


Figure 1. Proton NMR spectrum of methyl mercury in a 0.190 M aqueous solution at pH = 12.0.

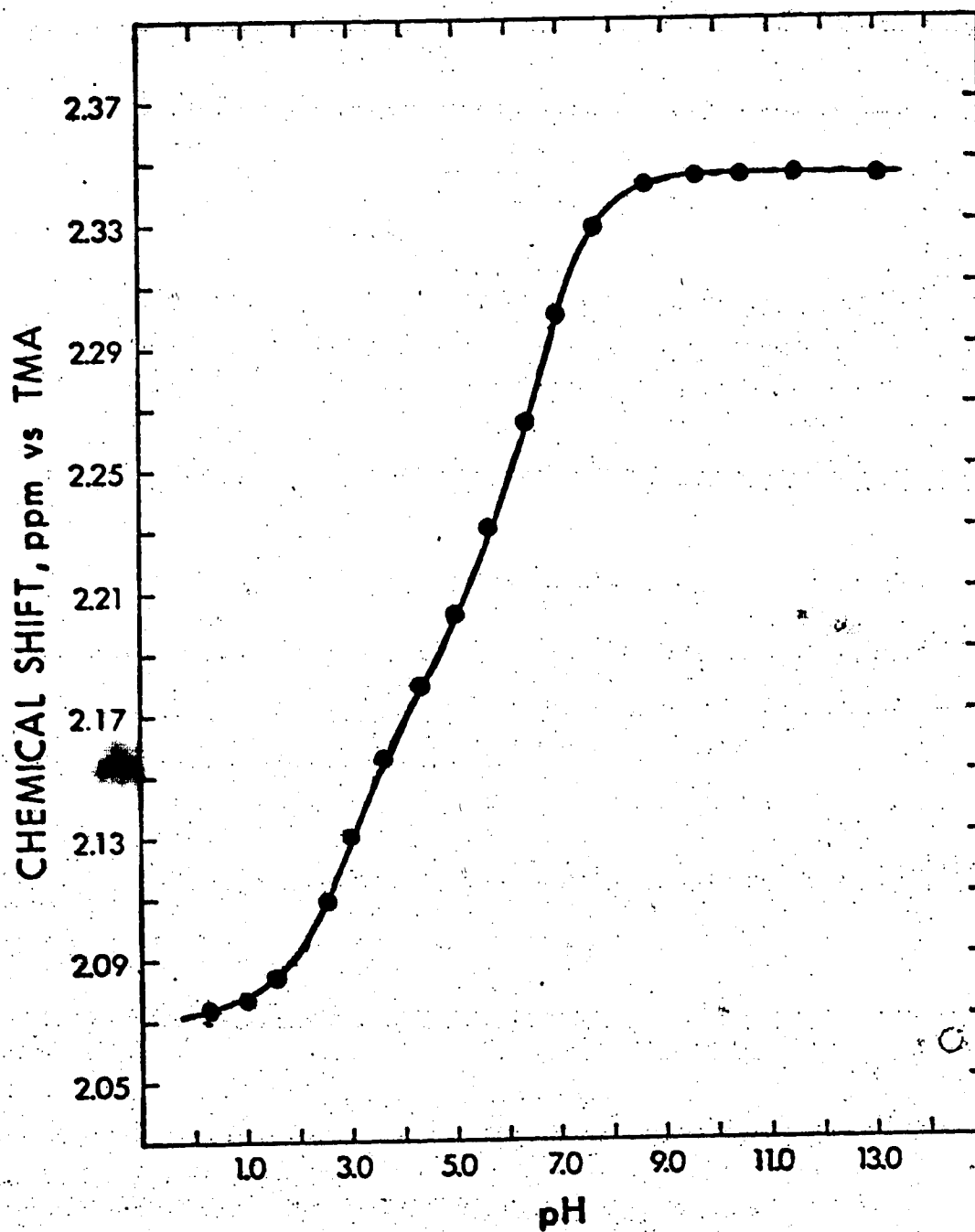


Figure 2. pH dependence of the chemical shift of the methyl protons of methylmercury in an aqueous solution containing 0.190 M methylmercury. The chemical shift is reported relative to the central resonance of the tetramethylammonium ion (TMA) triplet.

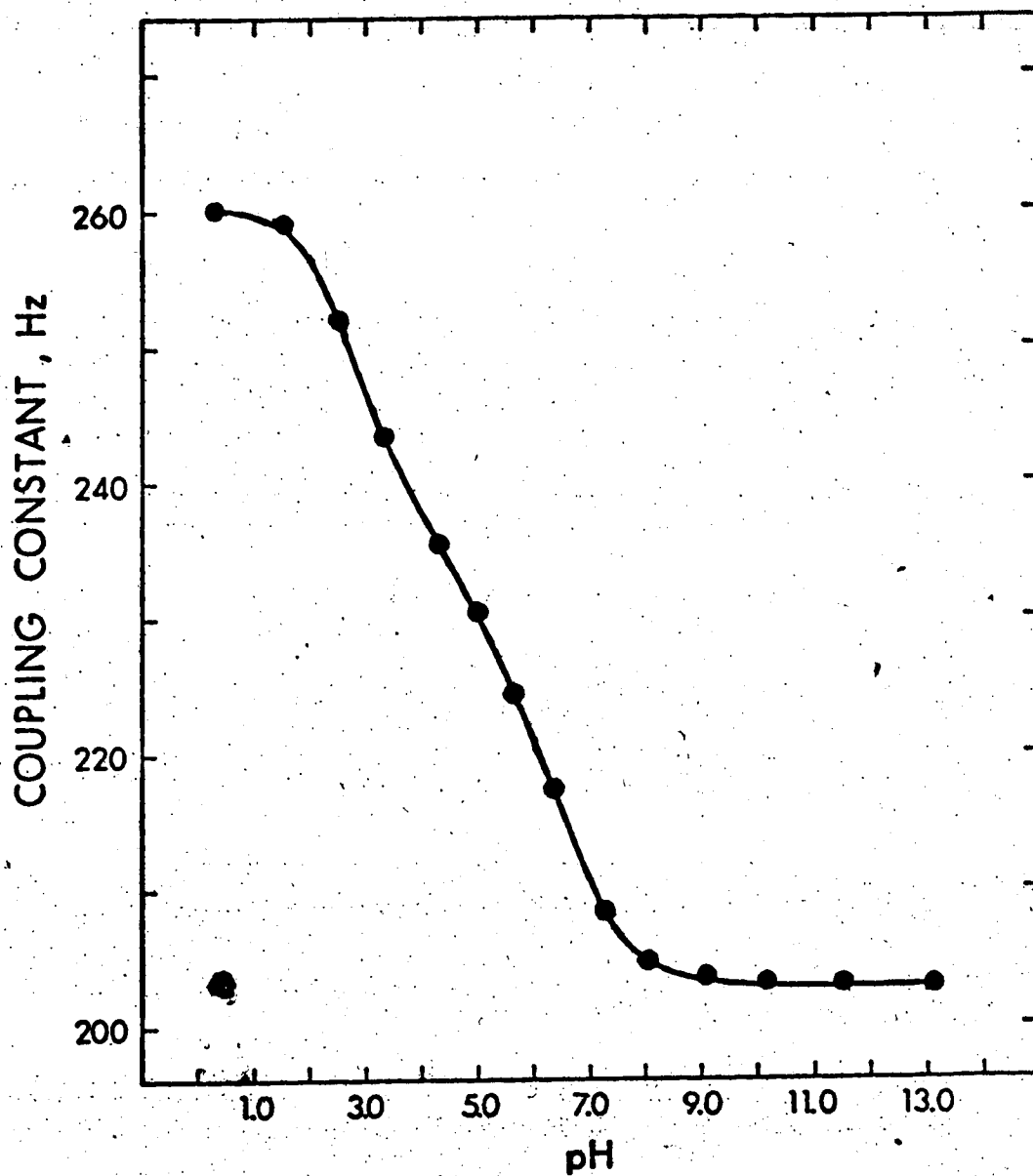


Figure 3. pH dependence of the mercury-proton spin-spin coupling constant of methylmercury in an aqueous solution containing 0.190 M methylmercury.

on the total methylmercury concentration, due to the unsymmetrical nature of the equilibria describing the formation of  $(\text{CH}_3\text{Hg})_2\text{OH}^+$  and  $(\text{CH}_3\text{Hg})_3\text{O}^+$ . Additional chemical shift data, shown in Figure 4, for total methylmercury concentrations ranging from 0.045 M to 0.213 M indicates that the predicted concentration dependence is observed in aqueous methylmercury solutions.

The aqueous solution model for methylmercury also predicts that the species distribution will be pH dependent, with  $\text{CH}_3\text{HgOH}_2^+$  predominant at low pH, a mixture of all species at intermediate pH, and  $\text{CH}_3\text{HgOH}$  predominating at high pH. The methylmercury chemical shift and coupling constant data presented in Figures 2 and 3 show that the chemical shift and the coupling constant change by 0.273 ppm and 57.0 Hz, respectively, as the pH is increased from 0.26 to 9 and then remain constant as the pH is increased further. Other experiments have shown that, at pH greater than 9, the chemical shift remains constant for solutions ranging from  $4.37 \times 10^{-3}$  M to 0.45 M methylmercury. Also,  $[(\text{CH}_3\text{Hg})_3\text{O}]\text{ClO}_4$  does not precipitate from a pH 12 solution containing 0.43 M methylmercury and 0.49 M  $\text{NaClO}_4$ , whereas it will form in a 0.51 M methylmercury and 0.25 M  $\text{NaClO}_4$  solution at neutral pH suggesting that the concentration of  $(\text{CH}_3\text{Hg})_3\text{O}^+$  is less in basic solution than at neutral pH. These results indicate that  $\text{CH}_3\text{HgOH}$  is the predominant species at pH

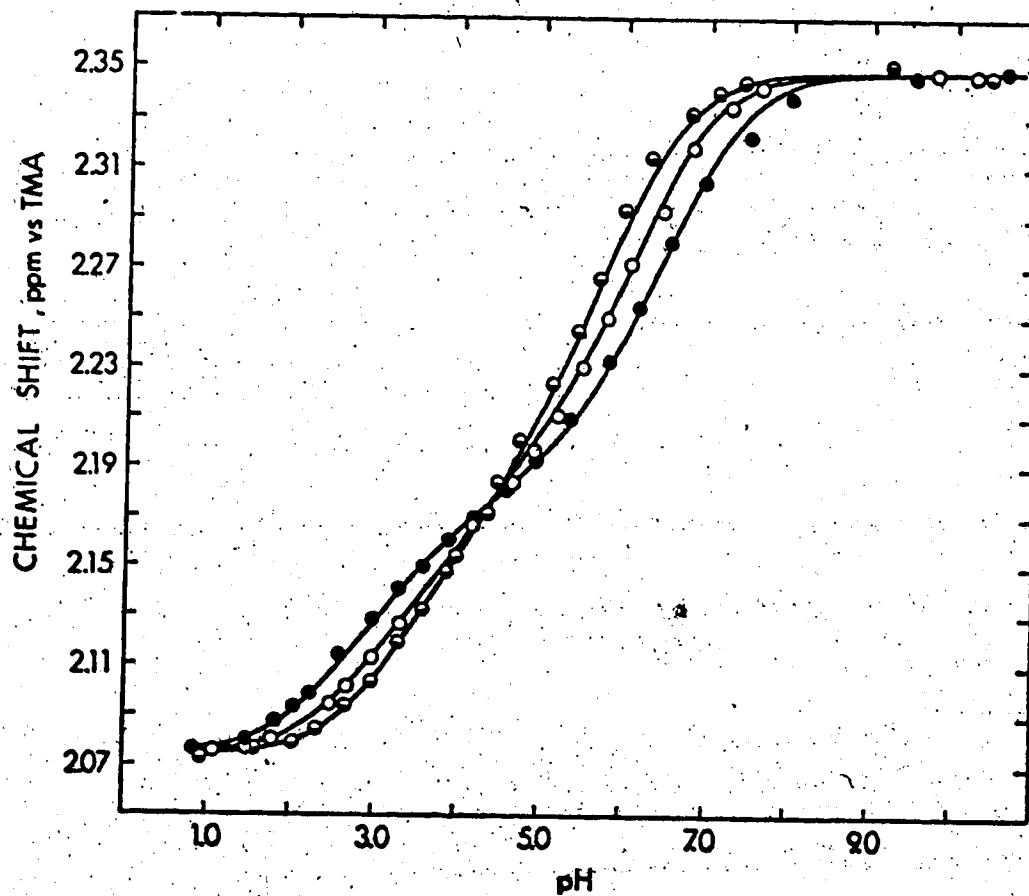


Figure 4. pH dependence of the chemical shift of the methyl protons of methylmercury in aqueous solutions containing 0.0451 M methylmercury (half-open points), 0.0901 M methylmercury (open points), and 0.213 M methylmercury (solid points). The chemical shift is reported relative to the central resonance of the tetramethylammonium ion (TMA) triplet.

greater than 9 at these, and lower total methylmercury concentrations, as predicted by the Schwarzenbach and Schellenberg model (1).

The non-sigmoidal nature of the chemical shift titration curves, presented in Figure 4, confirms that species in addition to  $\text{CH}_3\text{HgOH}$  and  $\text{CH}_3\text{HgOH}_2^+$  are present in the pH region 1 to 8. It is not possible to observe the different species directly by NMR since time-averaged spectra are observed for rapidly exchanging systems such as methylmercury. However, Raman spectroscopy is capable of establishing the presence of possible methylmercury species in solution if bands specific to the individual species are observable.

Woodward and coworkers have reported the position of Raman bands specific to the species  $\text{CH}_3\text{HgOH}$  (54),  $(\text{CH}_3\text{Hg})_2\text{OH}^+$  (43), and  $\text{CH}_3\text{HgOH}_2^+$  (25, 48), and the Raman spectrum of the  $(\text{CH}_3\text{Hg})_3\text{O}^+$  ion (56). In collaboration with Dr. C.A. Evans, Raman and infrared spectra of crystalline  $[(\text{CH}_3\text{Hg})_3\text{O}]\text{ClO}_4$ , prepared by the method of Grdenic and Zado (19), were recorded to determine the bands characteristic of  $(\text{CH}_3\text{Hg})_3\text{O}^+$ . The Raman spectrum showed bands at 63, 134, 550, 562 and  $919\text{ cm}^{-1}$ , excluding the  $\text{ClO}_4^-$  bands. Except for solvent bands, the Raman spectrum of methanol and nitromethane solutions of  $[(\text{CH}_3\text{Hg})_3\text{O}]\text{ClO}_4$  are similar to those of the solid, which indicates that the tris species is undissociated in these

solvents. However, the spectrum of a saturated aqueous solution of  $[(\text{CH}_3\text{Hg})_3\text{O}]\text{ClO}_4$  shows only one intense band in the region  $500\text{-}600\text{ cm}^{-1}$ , and some weak bands in the region  $400\text{-}500\text{ cm}^{-1}$ . These changes in the Raman spectrum can be interpreted in terms of hydrolysis of the cation.

Grdenic and Zado (19) concluded from conductimetric titrations of methanolic solutions of trimethylmercurioxonium salts with methanolic KOH that  $(\text{CH}_3\text{Hg})_3\text{O}^+$  is undissociated in alkaline methanol solution. To determine if this is the case, the chemical shift and mercury proton coupling constant of methylmercury were monitored as methanol solutions of  $[(\text{CH}_3\text{Hg})_3\text{O}]\text{ClO}_4$  were titrated with methanolic KOH. A similar experiment was performed in aqueous solution. The chemical shift results, which are presented in Figure 5, indicate that  $(\text{CH}_3\text{Hg})_3\text{O}^+$  is not stable in either alkaline methanol or alkaline aqueous solution. The Raman results described above, and the stoichiometry of the titration suggest that, in aqueous solution,  $(\text{CH}_3\text{Hg})_3\text{O}^+$  hydrolyzes to form  $\text{CH}_3\text{HgOH}$  and  $(\text{CH}_3\text{Hg})_2\text{OH}^+$ . When base is added, the  $(\text{CH}_3\text{Hg})_2\text{OH}^+$  then reacts to form  $\text{CH}_3\text{HgOH}$ . In methanol, undissociated  $(\text{CH}_3\text{Hg})_3\text{O}^+$  reacts with hydroxide, probably to form  $\text{CH}_3\text{HgOH}$  and  $(\text{CH}_3\text{Hg})_2\text{O}$ . These results are consistent with the report of Lorbeth and Weller (55), that the substance claimed to be  $[(\text{CH}_3\text{Hg})_3\text{O}]\text{OH}$  (19) is actually the hydrated oxide,  $(\text{CH}_3\text{Hg})_2\text{O}\cdot x\text{H}_2\text{O}$ .



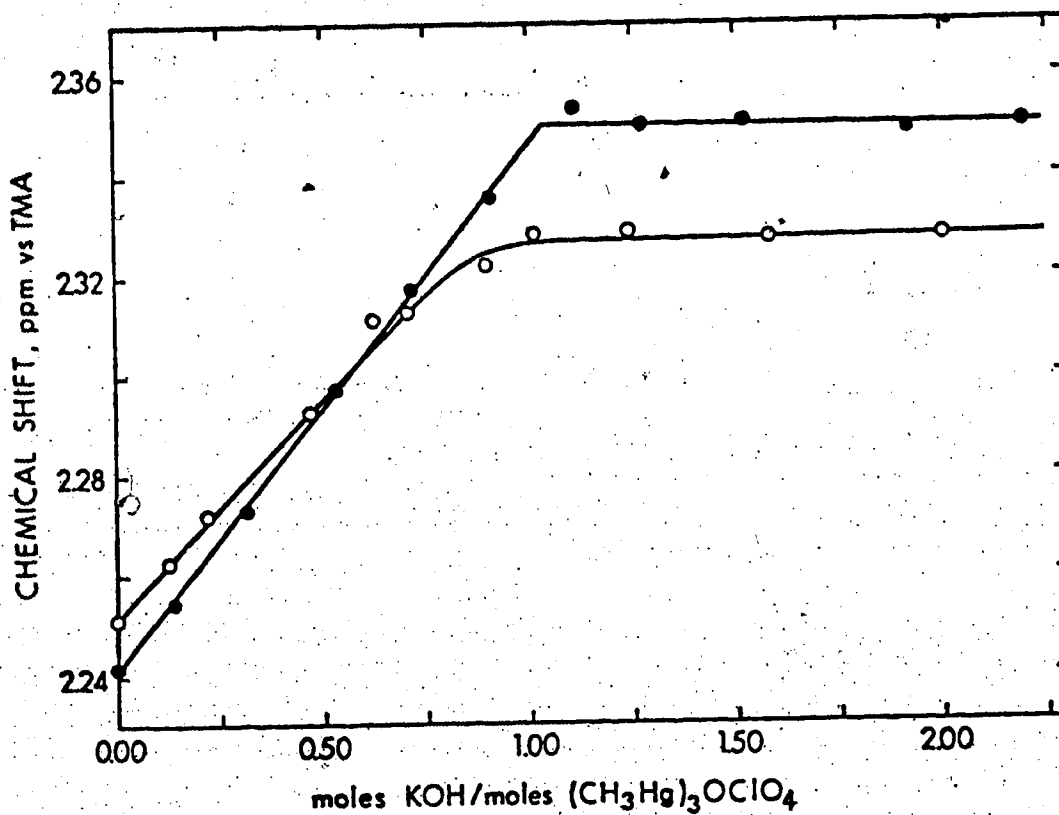


Figure 5. NMR chemical shift titration curves for the titration of 0.076 g of  $[(\text{CH}_3\text{Hg})_3\text{O}]\text{ClO}_4$  in 80 ml of water with 1.0 M aqueous KOH (open points) and for the titration of 0.076 g of  $[(\text{CH}_3\text{Hg})_3\text{O}]\text{ClO}_4$  in 80 ml of methanol with 1.0 M methanolic KOH (solid points). The chemical shift is reported relative to the central resonance of the tetramethylammonium ion (TMA) triplet.

Thus, the Raman spectrum of a saturated solution of  $[(\text{CH}_3\text{Hg})_3\text{O}]\text{ClO}_4$  indicates that there is very little  $(\text{CH}_3\text{Hg})_3\text{O}^+$  present in aqueous solution, even when the solution is saturated. Therefore  $K_1$  and  $K_2$ , the formation constants of the methylmercuric hydroxide and methylmercury dimer species (Equations 19-22) were calculated from the NMR data by assuming that no  $(\text{CH}_3\text{Hg})_3\text{O}^+$  was present. Then  $K_3$ , the formation constant of the tris species,  $(\text{CH}_3\text{Hg})_3\text{O}^+$  was determined by measurements. The small value obtained for  $K_3$  indicates that this assumption was justified.

The values of  $K_1$  and  $K_2$ , the formation constants of methylmercuric hydroxide and the methylmercury dimer, were obtained from a nonlinear least-squares fit of the NMR titration curve data. It was necessary first to evaluate the NMR parameters for each of the methylmercury species detectable in an NMR experiment. The chemical shift of each methylmercury species was obtained from the chemical shift titration curve data shown in Figure 4. The spin-spin coupling constants were obtained from the coupling constant titration curve data shown in Figure 3. The chemical shift and coupling constant of the cationic species,  $\text{CH}_3\text{HgOH}_2^+$ , have been taken as the limiting shift and the limiting coupling constant at the acidic end of the titration curves. This is dependent on the assumption that all the methylmercury is dissociated in this pH

region and does not exist as  $\text{CH}_3\text{HgONO}_2$ . Clarke and Woodward (43) determined by Raman spectroscopy that the degree of dissociation of  $\text{CH}_3\text{HgONO}_2$  is similar to that of nitric acid, or that the degree of dissociation of  $\text{CH}_3\text{HgONO}_2$  is greater than 99.5% for the conditions of this experiment. Thus the assumption is valid. The chemical shift and coupling constant of the species  $\text{CH}_3\text{HgOH}$  have been taken as the limiting chemical shift and coupling constant observed above pH 9, where all the methylmercury has been shown to exist as  $\text{CH}_3\text{HgOH}$ . The NMR parameters of the dimeric species,  $(\text{CH}_3\text{Hg})_2\text{OH}^+$ , cannot be obtained directly from the titration curves because the methylmercury does not exist entirely in that one form at any pH. However, these parameters can be obtained from the nonlinear least-squares analysis of the titration data.

By varying  $K_1$ ,  $K_2$ , and  $\delta_{(\text{CH}_3\text{Hg})_2\text{OH}^+}$ , the observed chemical shift data was fitted to Equation 25 which expresses the chemical shift as a function of P, the

$$\begin{aligned} \delta_{\text{obs}} = & P_{\text{CH}_3\text{Hg}^+} \delta_{\text{CH}_3\text{Hg}^+} + P_{(\text{CH}_3\text{Hg})_2\text{OH}^+} \delta_{(\text{CH}_3\text{Hg})_2\text{OH}^+} \\ & + P_{\text{CH}_3\text{HgOH}} \delta_{\text{CH}_3\text{HgOH}} \end{aligned} \quad (25)$$

fraction of methylmercury existing as the indicated

species, and  $\delta$ , the chemical shift of the indicated species. The observed coupling constant data was fitted to a similar equation expressed in terms of the coupling constant of each species, thus independently evaluating the coupling constant of the dimeric species as well as  $K_1$  and  $K_2$ . For a given data point, the fraction of each methylmercury species was calculated from its formation constant (Equations 19-22) and the concentration of  $\text{CH}_3\text{HgOH}_2^+$ . The concentration of  $\text{CH}_3\text{HgOH}_2^+$  was calculated for each value of  $K_1$  and  $K_2$  from Equation 26, which is derived from the methylmercury mass balance. The values

$$2K_1K_2[\text{OH}^-][\text{CH}_3\text{Hg}^+]^2 + \{1 + K_1[\text{OH}^-]\}[\text{CH}_3\text{Hg}^+] - [\text{CH}_3\text{Hg}]_{\text{total}} = 0 \quad (26)$$

of  $K_1$ ,  $K_2$ , and  $\delta_{(\text{CH}_3\text{Hg})_2\text{OH}^+}$  were varied until the best agreement was reached between the observed titration curve and that calculated by Equation 26. This results in values of  $\log K_1 = 9.29$  and  $\log K_2 = 2.31$  for the formation constants of methylmercuric hydroxide and the methylmercury dimer. A summary of the NMR parameters determined above for the  $\text{CH}_3\text{HgOH}_2^+$ ,  $(\text{CH}_3\text{Hg})_2\text{OH}^+$ , and  $\text{CH}_3\text{HgOH}$  species is given in Table 3.

To determine the pH dependence of the tris methylmercury species, Raman spectra of a 0.510 M  $\text{CH}_3\text{HgOH}$  solution titrated with 5.68 M perchloric acid were

TABLE 3

Chemical Shift of the Methyl Protons and the Mercury-Proton Coupling Constant of Methylmercury in Aqueous Methylmercury Species

Species	$\delta_{\text{CH}_3}^{\text{a}}$	$J_{\text{CH}_3\text{Hg}}^{\text{b}}$
$\text{CH}_3\text{HgOH}_2^+$	1.095 <sup>c</sup>	260.0
$(\text{CH}_3\text{Hg})_2\text{OH}^+$	0.997 <sup>c</sup>	233.1
$\text{CH}_3\text{HgOH}$	0.822 <sup>c</sup>	203.2

a) ppm vs. DSS

b) Hz

c) Uncertainty in this value is  $\pm 0.002$  ppm

recorded over the pH range 9 to 0.5 at intervals of approximately 0.5 pH unit. The high concentration was chosen to favor the formation of  $(\text{CH}_3\text{Hg})_3\text{O}^+$ . In two of the samples, at pH 6.84 and 6.26, crystals of  $[(\text{CH}_3\text{Hg})_3\text{O}]\text{ClO}_4$  slowly appeared. Figure 6 shows the Raman spectrum of the solution at pH 6.26 and of the crystals which slowly appeared from this solution. In spectrum A, absence of the band at  $500\text{ cm}^{-1}$ , the small shift in the frequency and the change in the intensity of the composite band at  $130\text{ cm}^{-1}$ , as well as the presence of the  $\text{CH}_3\text{HgOH}$  band at  $415\text{ cm}^{-1}$  indicate that the  $(\text{CH}_3\text{Hg})_3\text{O}^+$  cation is not a major species in aqueous solution, even when the solution is super-saturated with respect to  $[(\text{CH}_3\text{Hg})_3\text{O}]\text{ClO}_4$ .

By monitoring the intensity of the  $504\text{ cm}^{-1}$  Raman band of  $\text{CH}_3\text{HgOH}$  (normalized relative to the perchlorate  $\nu_1$ ) as a function of pH, the equilibrium constant for the formation of the  $(\text{CH}_3\text{Hg})_3\text{O}^+$  species,  $K_3$ , was determined. From a consideration of mass and charge balance equations, Equation 27 was derived. Equation 27 expresses  $K_3$  in terms of  $\text{MM}_t$ , the total methylmercury concentration,

$$K_3 = \frac{x + 2K_2xy - (\text{MM}_t - y)(1 + K_2y)}{(\text{MM}_t - y)K_2y^2 - 3K_2xy^2} \quad (27)$$

$x$ , the concentration of  $\text{ClO}_4^-$ , and  $y$ , the concentration of  $\text{CH}_3\text{HgOH}$  determined from the Raman spectrum. In the derivation of this equation, it was assumed that

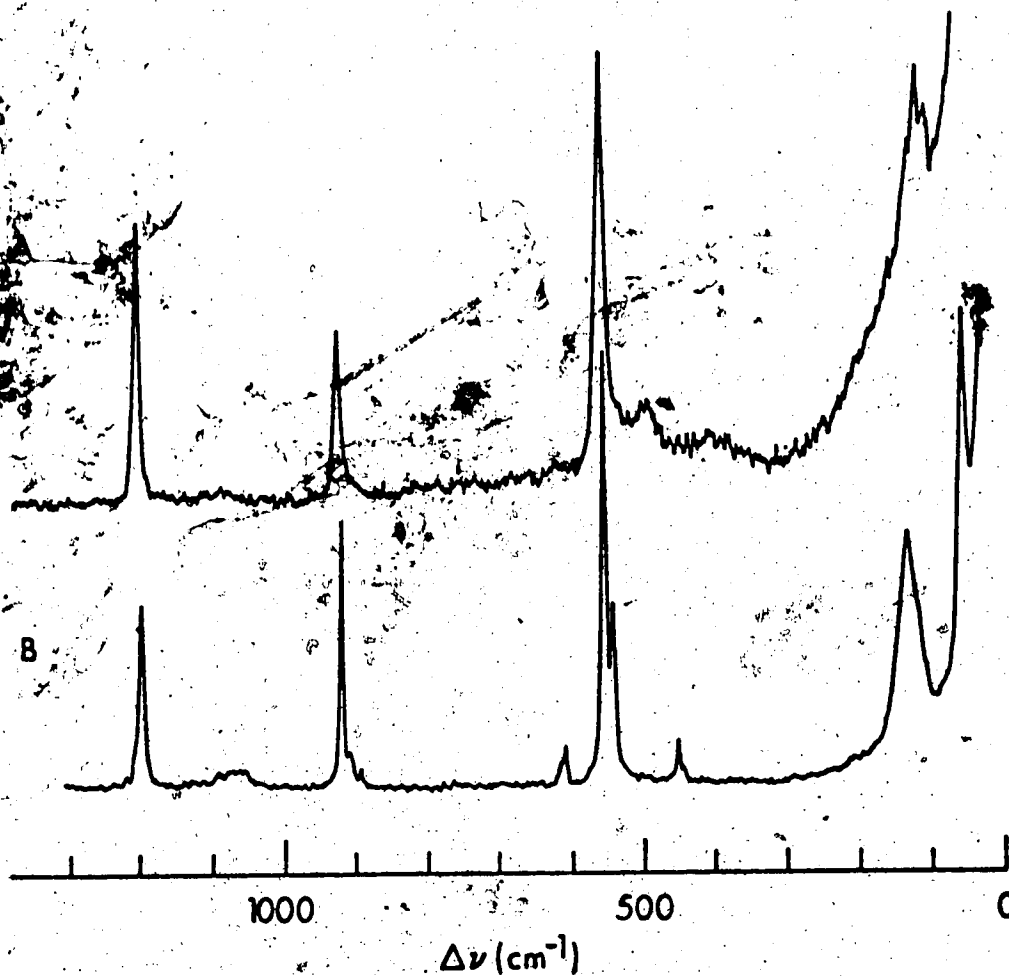


Figure 6. Raman spectra of (A) a solution supersaturated with respect to  $[(\text{CH}_3\text{Hg})_3\text{O}]\text{ClO}_4$  and of (B) the crystals which separated from the solution.

$[\text{ClO}_4^-] \gg [\text{OH}^-]$  once the titration has begun.  $K_3$  was estimated in this manner at each point in the titration, where the intensity of the  $504 \text{ cm}^{-1}$  band indicated that a significant concentration of  $\text{CH}_3\text{HgOH}$  was present, resulting in a value of  $K_3 = 0.7 \pm 0.3$ .

Although this value of  $K_3$  lacks precision, it is expected to be of the correct order of magnitude and leads to some important conclusions. Calculations of species distribution as a function of pH indicate that, for  $0.51 \text{ M}$  methylmercury solution, the maximum concentration of  $(\text{CH}_3\text{Hg})_3\text{O}^+$  is  $0.019 \text{ M}$  and this occurs at a pH of 6.75, while, at methylmercury concentrations of  $0.2$  and  $0.05 \text{ M}$ , the maximum  $(\text{CH}_3\text{Hg})_3\text{O}^+$  concentrations are  $3.1 \times 10^{-3} \text{ M}$  (at pH 6.4) and  $2.0 \times 10^{-4} \text{ M}$  (at pH 5.8). The pH dependence of the fractional concentrations of the various species in a  $0.2 \text{ M}$  methylmercury solution is shown in Figure 7. These results are based on the aqueous methylmercury solution model described by Equations 19-24 with  $\log K_1 = 9.29$ ,  $\log K_2 = 2.31$ , and  $K_3 = 0.7$ . They indicate that the Schwarzenbach and Schellenberg model accounts for all but a small fraction of methylmercury over the pH range less than 1 to greater than 13, at the methylmercury concentrations which have been used in most previous studies of the solution chemistry of methylmercury and in those described in Chapter IV of this thesis.



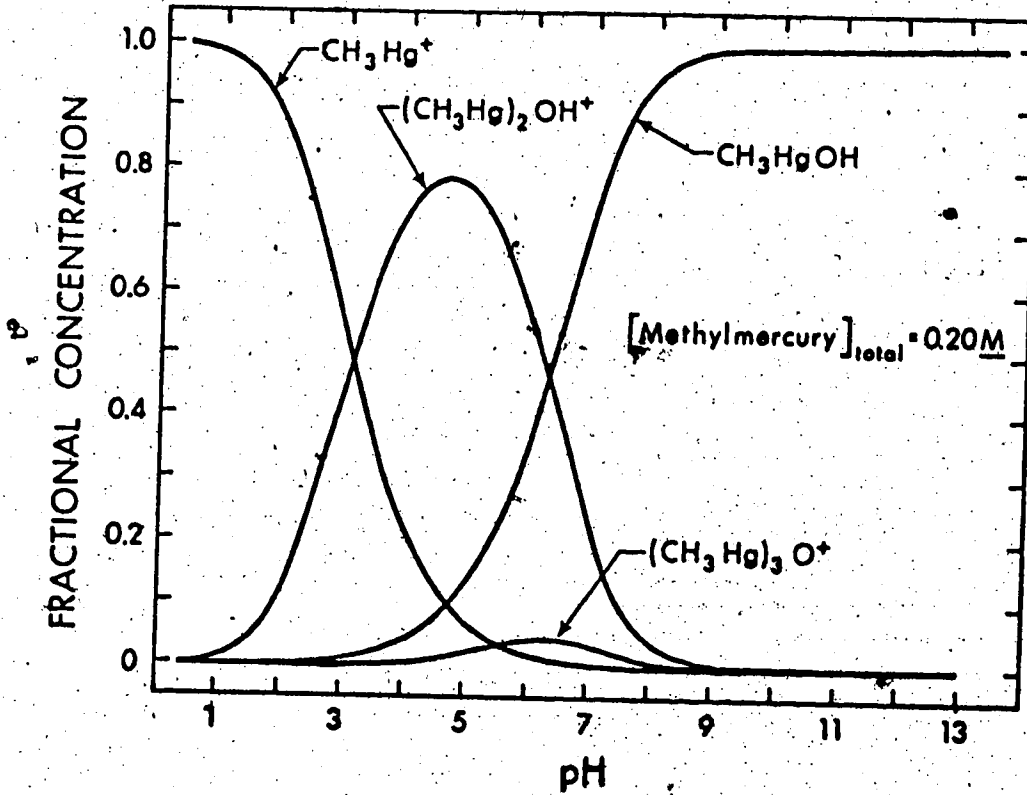


Figure 7. pH dependence of the fractional concentrations of the methylmercury-containing species in an aqueous solution containing 0.200 M methylmercury. The fractional concentrations were calculated using constants determined in this thesis.

## CHAPTER IV

### METHYLMERCURY COMPLEXES OF SELECTED INORGANIC

#### ANIONS

##### A. Introduction

The results of a study of the coordination of methylmercury by the inorganic anions sulfate, selenate, sulfite, selenite, thiocyanate, selenocyanate, sulfide, and selenide are presented in this chapter. These ligands were chosen because of the known affinity of methylmercury for sulfur-binding ligands (1), and the reported ability of  $\text{Na}_2\text{SeO}_3$  to act as a protecting agent against methylmercury poisoning (16). The complexation of these ligands by methylmercury was studied by NMR (57). In addition, structural information was obtained for some of these complexes by Raman spectroscopy (57).

##### B. Results

###### 1. The Sulfate and Selenate Complexes of Methylmercury.

The binding of methylmercury by the sulfate and selenate ligands,  $\text{SO}_4^{2-}$  and  $\text{SeO}_4^{2-}$ , was investigated by monitoring the chemical shift and the mercury-proton coupling constant of the methyl protons of methylmercury as a function of solution conditions. Sulfate has been reported to interact only weakly with methylmercury (44),

therefore solutions containing four times as much ligand as methylmercury were used in these studies to maximize the fraction of methylmercury complexed.

The chemical shift of the methyl protons of methylmercury is presented in Figure 8 for both a solution containing only methylmercury (open points) and a solution containing methylmercury and sodium sulfate in a ratio of one to four (solid points). The mercury-proton spin-spin coupling constant data for solutions containing methylmercury and sodium sulfate in a ratio of one to two is presented in Table 4. The spin-spin coupling constant of the one to four methylmercury-sulfate solution was too broad to measure, presumably due to exchanging ligand, and therefore the coupling constant data was obtained for the less ideal, one to two methylmercury-sulfate solution. The chemical shift titration curves for methylmercury alone and for methylmercury plus sulfate coincide above pH 7, but diverge as the pH is decreased, and approach each other again at very low pH (<1.). At low pH, there is competition between hydrogen ions and methylmercury for the  $\text{SO}_4^{2-}$ . At very low pH, the proton is more successful than the methylmercury, so that a large fraction of methylmercury exists as  $\text{CH}_3\text{HgOH}_2^+$  rather than as the sulfate complex. This is indicated by the similarity of the chemical shift titration curve of the methylmercury-sulfate solution to that of

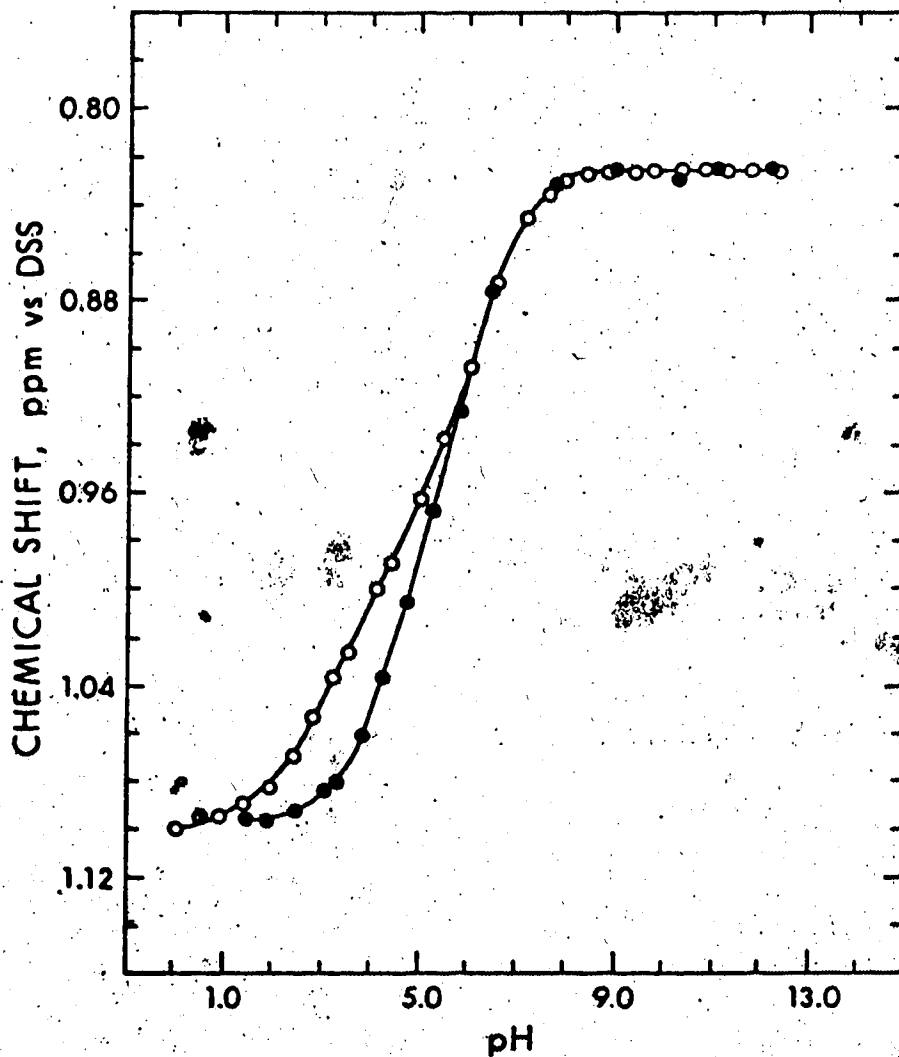


Figure 8. pH dependence of the chemical shift of the methyl protons of methylmercury in an aqueous solution containing 0.100 M methylmercury (open points) and in an aqueous solution containing 0.0532 M methylmercury and 0.213 M sodium sulfate (solid points).

TABLE 4

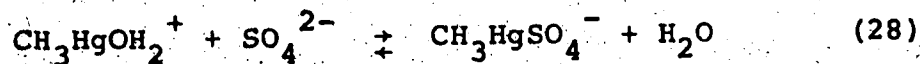
Mercury-Proton Coupling Constant as a Function of pH for  
the Methylmercury in an Aqueous Solution Containing  
0.106 M Methylmercury and 0.211 M Sodium Sulfate

pH	$J_{\text{CH}_3\text{Hg}}^a$
13.01	203.0
12.00	203.0
10.98	202.9
9.41	203.6
8.97	204.0
8.51	203.9
8.01	204.4
7.50	205.9
7.14	208.1
6.67	212.2
6.20	219.0
5.62	225.2
5.07	231.9
4.53	237.1
4.01	242.3
3.50	247.7
3.02	250.9
2.60	253.7
2.03	255.8
1.50	256.0
1.03	257.2
0.68	257.2

a) Hz

methylmercury alone in the very low pH region. At high pH, there is competition between hydroxide ions and ligand for the methylmercury. The coincidence of the chemical shift titration curve, above pH 7, for methylmercury alone with that of the methylmercury plus sulfate solution indicates that, in this pH region, the methylmercuric sulfate complex is completely dissociated. Thus, the chemical shift titration curves in Figure 8 indicate that a methylmercury-sulfate complex is formed between pH 1.5 and 7.

The binding of methylmercury by the sulfate anion is described by Equations 28 and 29. The formation



$$K_F = \frac{[\text{CH}_3\text{HgSO}_4^-]}{[\text{CH}_3\text{HgOH}_2^+][\text{SO}_4^{2-}]} \quad (29)$$

constant,  $K_F$ , and the chemical shift of the sulfate-complexed methylmercury were calculated from the chemical shift versus pH data of Figure 8 for the methylmercury-sulfate solution. The spin-spin coupling constant and an independent measure of the formation constant of the methylmercuric sulfate complex, were obtained from similar calculations with the coupling constant versus pH data of Table 4. The fractional concentration of sulfate-

complexed methylmercury,  $P_c$ , is given by Equation 30 where

$$P_c = \frac{\delta_{\text{obs}} - \delta_f}{\delta_c - \delta_f} \quad (30)$$

$\delta_c$  is the chemical shift of the complexed methylmercury,  $\delta_f$  is the shift of "free" methylmercury, and  $\delta_{\text{obs}}$  is the observed chemical shift. In the pH range 1.5 to 7 where complexation takes place, the "free" methylmercury is a mixture of  $\text{CH}_3\text{HgOH}_2^+$ ,  $(\text{CH}_3\text{Hg})_2\text{OH}^+$ , and  $\text{CH}_3\text{HgOH}$ . The concentration of the tris methylmercury species,  $(\text{CH}_3\text{Hg})_3\text{O}^+$  was shown in Chapter III to be negligible at the methylmercury concentrations used in this work, and therefore has been ignored. The relative concentration of each free methylmercury species is dependent on pH and on  $P_f$ , due to the unsymmetrical nature of the equilibria described in Chapter III. Therefore  $\delta_f$ , the shift of the free methylmercury also depends on pH and on  $P_f$  (26). The chemical shift of the complexed methylmercury cannot be determined directly, because at no pH is all the methylmercury in the complexed form. Consequently, an iterative procedure was used to simultaneously determine  $\delta_c$  and the formation constant. Initially, a chemical shift of 1.12 ppm was used for  $\delta_c$ , which is estimated from considering the two titration curves of Figure 8.  $P_c$  was calculated from Equation 30 using this initial value for  $\delta_c$  for each data point between pH 1.5 and 7.0.

Since  $\delta_f$  is dependent on  $P_f$  in this pH region, its value must be determined in a separate iteration loop. Thus, the chemical shift of methylmercury alone at the same pH as the data point in question was used as an initial estimate of  $\delta_f$  in the calculation of  $P_c$  from Equation 30.  $P_f$  was then calculated from the equation  $P_f = 1 - P_c$ , and a better value of  $\delta_f$  was determined for this  $P_f$  from Equation 25, using the NMR parameters of the free methylmercury determined in Chapter III and the concentration of each free methylmercury species. The concentration of the methylmercury cation was calculated for a particular  $P_f$  from Equation 31 which is derived from a mass balance on methylmercury and Equations 20 and 22. The concentrations of  $(\text{CH}_3\text{Hg})_2\text{OH}^+$  and  $\text{CH}_3\text{HgOH}$  were then calculated

$$2K_1K_2[\text{OH}^-][\text{CH}_3\text{Hg}^+]^2 + (1 + K_1[\text{OH}^-])[\text{CH}_3\text{Hg}^+] - P_f[\text{CH}_3\text{Hg}^+]_{\text{total}} = 0 \quad (31)$$

from Equations 20 and 22 and the concentration of the cationic species obtained from Equation 31. This procedure was repeated until convergence was reached in the value of  $\delta_f$  and in the corresponding value of  $P_c$ , usually in less than five iterations. For each data point, the concentration of the complex,  $\text{CH}_3\text{HgSO}_4^-$  was then calculated from Equation 32 where  $[\text{CH}_3\text{Hg}^+]_{\text{total}}$  is the total



$$[\text{CH}_3\text{HgSO}_4^-] = P_c [\text{CH}_3\text{Hg}^+]_{\text{total}} \quad (32)$$

methylmercury concentration. The concentration of  $\text{CH}_3\text{Hg}^+$  was obtained from Equation 31 for  $P_f = 1 - P_c$ . The concentration of uncomplexed ligand was calculated from Equation 33 where  $[\text{SO}_4^{2-}]_{\text{total}}$  represents the total sulfate

$$[\text{SO}_4^{2-}] = \alpha_2 \{ [\text{SO}_4^{2-}]_{\text{total}} - [\text{CH}_3\text{HgSO}_4^-] \} \quad (33)$$

concentration and  $\alpha_2$  is the fraction of ligand available for binding and is dependent only on pH. Using values of  $\text{CH}_3\text{HgSO}_4^-$ ,  $\text{CH}_3\text{Hg}^+$ , and  $\text{SO}_4^{2-}$  calculated in this manner, a formation constant, as defined by Equation 29 was calculated from each data point. Using the median of the individual formation constants and the  $\delta_c$  used in their calculation, a chemical shift titration curve was then calculated.  $\delta_c$  was then changed slightly and a new set of formation constants obtained. The  $\delta_c$  and formation constant which resulted in the smallest standard deviation between calculated and observed chemical shift titration curves are 1.00 ppm and 8.8. The probable deviation of  $K_f$  is 0.2. The formation constants calculated from the individual data points using the value 1.100 ppm for the chemical shift of the complex,  $\delta_c$ , are given in Table 5.

TABLE 5

The Formation Constant of Methylmercuric Sulfate  
Calculated from Methylmercury Chemical Shift Data

<u>pH</u>	<u>K<sub>F</sub></u>
1.48	8.81
1.88	9.67
2.48	6.00
3.10	6.70
3.33	8.47
3.84	8.87
4.26	8.70
4.74	8.80

Similar calculations using the spin-spin coupling constant data, presented in Table 4 for a methylmercury-sulfate solution, result in a  $J_c$  and  $K_f$  of 251.4 Hz and  $7.2 \pm 0.4$  for the methylmercuric sulfate complex. The formation constants determined in these studies are concentration constants, determined by converting the meter pH readings to hydrogen ion concentrations by the method described in Chapter II, Section D of this thesis.

Clarke and Woodward (44) have studied the stoichiometry and dissociation of the methylmercury-sulfate complex in aqueous solution by Raman spectroscopy. Complex formation was indicated by the presence of a band at  $272 \text{ cm}^{-1}$ , most likely due to a Hg-O stretching mode. The complex was shown to be  $\text{CH}_3\text{HgOSO}_3^-$  by comparison with the spectra of aqueous sulfuric acid solutions. From intensity measurements of the  $982 \text{ cm}^{-1}$   $\text{SO}_4^{2-}$  band at various mole fractions of methylmercury and sulfate, the degree of dissociation of the complex was determined to be "approximately equal to that of  $\text{HSO}_4^-$ ". A formation constant of 3 can be estimated from their results, in reasonable agreement with the value determined in this research from NMR data, considering the approximate nature of the value estimated from their Raman data. As in sulfuric acid solutions where  $\text{H}_2\text{SO}_4$  molecules are not detectable at concentrations less than 1 M, no evidence for the presence of  $(\text{CH}_3\text{Hg})_2\text{SO}_4$  molecules was obtained

by Clarke and Woodward for solutions up to 0.8 M, even though the  $(\text{CH}_3\text{Hg})_2\text{SO}_4$  complex can be crystallized from concentrated aqueous methylmercury-sulfate solutions.

The basicity of  $\text{SeO}_4^{2-}$  and  $\text{HSeO}_4^-$  to protons is similar to that of  $\text{SO}_4^{2-}$  and  $\text{HSO}_4^-$  (57), and by analogy, the behavior of selenate anions towards methylmercury is expected to be similar to that of sulfate. The similarity of the NMR titration curves for methylmercury-selenate solutions to those of methylmercury-sulfate solutions indicates this to be the case. The chemical shift of the methyl protons of methylmercury is presented as a function of pH in Figure 9 for both a solution containing only methylmercury (open points) and a solution containing methylmercury and sodium selenate in a ratio of one to four (closed points). The spin-spin coupling constant of methylmercury in the same solutions is presented as a function of pH in Figure 10. Comparison of this chemical shift and coupling constant data with that of the methylmercury-sulfate solutions (Figure 8 and Table 4) suggests strong similarity between the methylmercury-sulfate and methylmercury-selenate systems. The formation constant and chemical shift of the methylmercuric selenate complex was determined from the chemical shift versus pH data by the method described above for the methylmercuric sulfate complex. The  $\delta_c$  and  $K_f$  which resulted in the smallest probable deviation between the calculated and observed

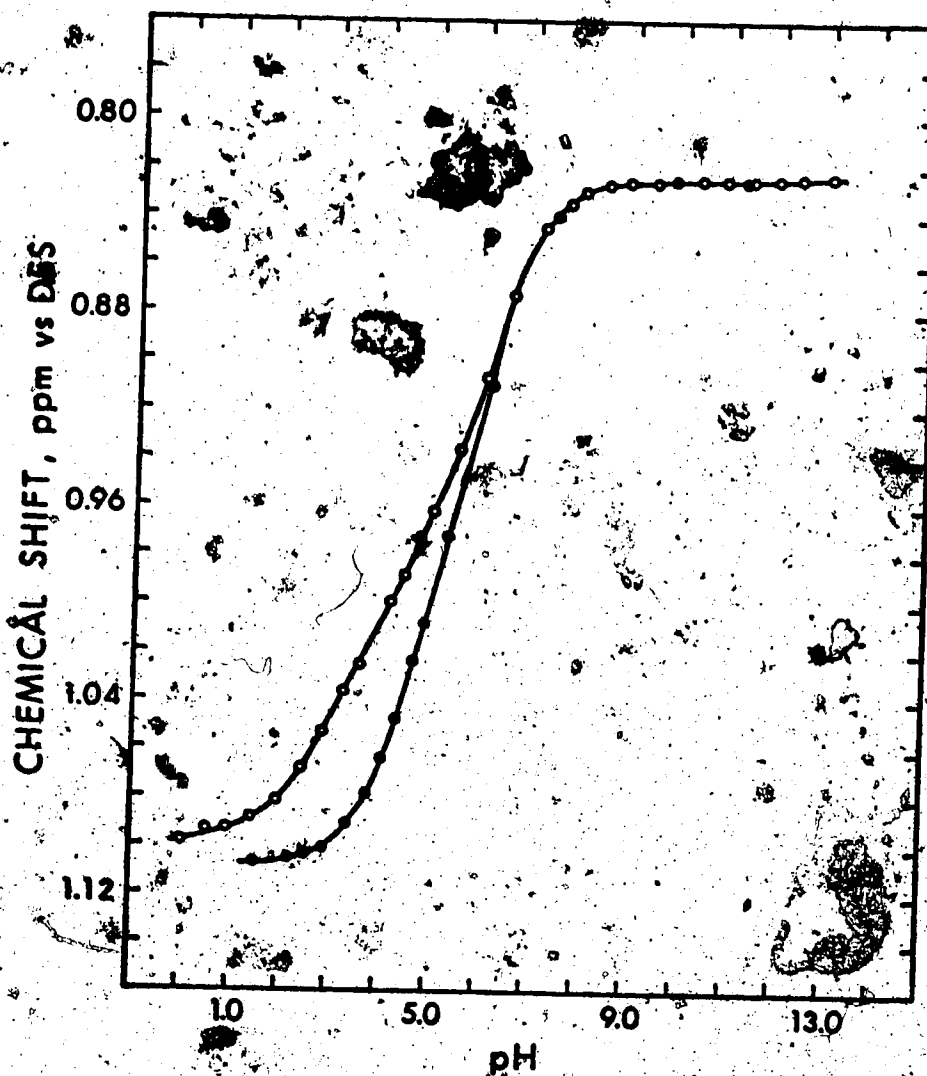


Figure 9. pH dependence of the chemical shift of the methyl protons of methylmercury in an aqueous solution containing 0.100 M methylmercury (open points) and in an aqueous solution containing 0.0521 M methylmercury and 0.208 M sodium selenate (solid points).

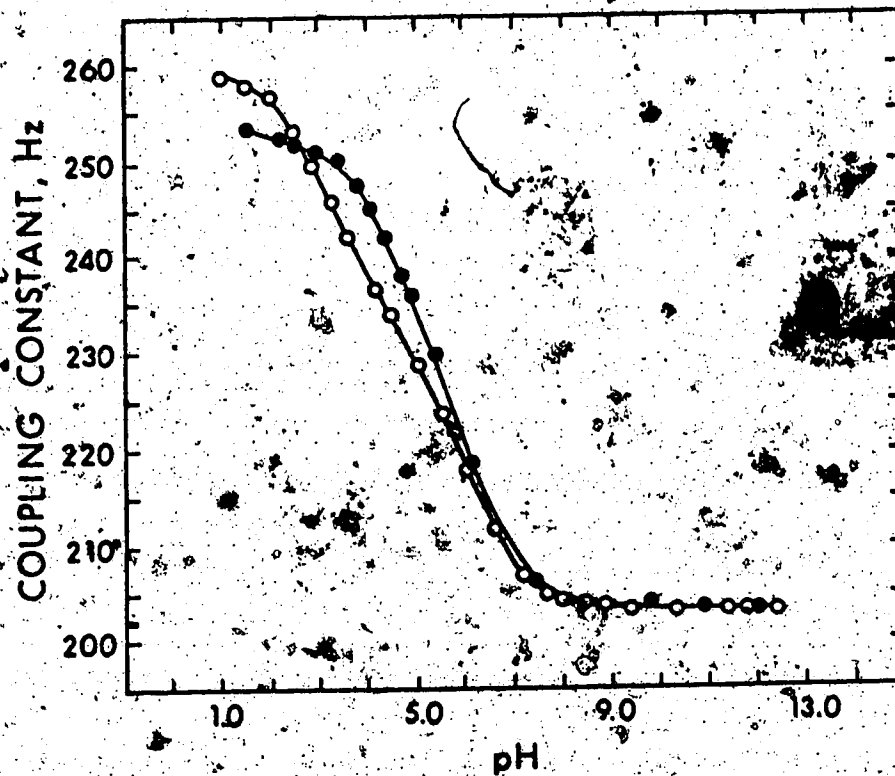


Figure 10. pH dependence of the mercury-proton spin-spin coupling constant of methylmercury in an aqueous solution containing 0.100 M methylmercury (open points) and in an aqueous solution containing 0.521 M methylmercury and 0.208 M sodium selenate (solid points).

chemical shift titration curves were 1.112 ppm and 13.2 ppm. Similar calculations with the coupling constant versus  $pK_a$  data resulted in values of 248.5 Hz and 17.3  $\pm$  0.8 for the coupling constant and formation constant of methylmercuric selenate.

The results of the calculations for the methylmercury-sulfate and methylmercury-selenate systems are summarized in Table 6. These results indicate that the methylmercuric sulfate and methylmercuric selenate complexes are both weak, with the methylmercuric selenate complex having a slightly larger formation constant and a slightly smaller spin-spin coupling constant. In Chapter I, it was pointed out that the magnitude of the coupling constant of methylmercury is dependent on the ligand coordinated to the methylmercury, and can be correlated with the magnitude of the formation constant. The magnitudes of the coupling constants of the sulfate and selenate complexes of methylmercury are large, suggesting weak complexation. In addition, they are similar to the coupling constants listed in Table 2 for oxygen-binding ligands. These observations suggest that the sulfate and selenate anions bind to methylmercury through an oxygen atom, forming the  $CH_3HgOSO_3^-$  and  $CH_3HgOSeO_3^-$  species.

As discussed above, Clarke and Woodward (44) also concluded, from Raman spectroscopy, that the methylmercuric

TABLE 6  
 Formation Constants and NMR Parameters of Methylmercuric Sulfate and  
 Methylmercuric Selenate

(Complex)	$\delta_{CH_3}$ <sup>a</sup>	$K_F$ <sup>b</sup>	$J_{CH_3Hg}$ <sup>c</sup>	$K_F$ <sup>d</sup>
$CH_3HgOSO_3^-$	1.100 <sup>e</sup>	$8.9 \pm 0.2^f$	251.4	$7.2 \pm 0.4^f$
$CH_3HgOSeO_3^-$	1.112 <sup>e</sup>	$13.2 \pm 1.0^f$	248.5	$17.3 \pm 0.8^f$

a) ppm vs.  $\delta_{SS}$   
 b) Calculated from chemical shift data  
 c) Hz  
 d) Calculated, from coupling constant data  
 e) Uncertainty in this value is  $\pm 0.002$  ppm  
 f) Reported uncertainties are a measure of the fit of the data and not a measure of the uncertainty in the constant



sulfate complex has the structure  $\text{CH}_3\text{HgOSO}_3^-$ . Therefore, the Raman spectrum of methylmercuric selenate was studied to determine whether it also indicates binding of the ligand through an oxygen atom. The Raman studies of this complex and of other complexes reported in this thesis were obtained in collaboration with Dr. C.A. Evans. The selenate complex forms sufficiently weakly and the selenate moiety is a sufficiently weak Raman scatterer relative to  $\text{CH}_3\text{-Hg-}$ , that the complete Raman spectrum of the complex was not observed. Careful choice of solution conditions, however, made it possible to observe five bands which can be attributed to the complex. Two solutions were prepared, the first to maximize the fraction of methylmercury in the complexed form, the second to maximize the fraction of complexed selenate. Calculations using the formation constants given above show that for the first solution, which contained 0.8 M sodium selenate and 0.2 M methylmercury at pH = 3, 87% of the methylmercury is complexed. In the second solution, which contained 0.50 M methylmercury and 0.125 M sodium selenate at pH 2.4, 72% of the selenate is complexed. Table 7 lists the important Raman bands observed in these solutions as well as the corresponding bands of methylmercuric sulfate reported by Clarke and Woodward (44). For comparison, selected Raman bands of several oxygen-

TABLE 7  
Some Raman Bands of Methylmercuric Complexes,  $\text{CH}_3\text{HgX}$

Complex	Donor Atoms of Ligand	Frequency of Vibration <sup>a</sup>		
		$\text{CH}_3$ Deformation Sym.	Hg-C Stretch	Hg-X Stretch
$\text{CH}_3\text{HgOH}^g$	o	1211	577	511
$\text{CH}_3\text{HgOH}_2^f$	o	1207	570	463
$(\text{CH}_3\text{Hg})_2^g$	o	1206	563	132
$\text{CH}_3\text{HgSCH}_3^h$	s	1177	537	329
$\text{CH}_3\text{HgOSO}_3^-$	o	1207	566	272
$\text{CH}_3\text{HgOSeO}_3^-$	o	1203	565	290
$\text{CH}_3\text{Hg}^i$	o	1190	541	206
$\text{CH}_3\text{Hg}^j$	o	1207	568	290
$\text{CH}_3\text{Hg}^k$	s	1186	540	203
$\text{CH}_3\text{HgSeCN}^{b,k}$	se	1177, 1164	540, 516	- <sup>c</sup>
$(\text{CH}_3\text{Hg})_2^l$	s	1176	544	281
$\text{CH}_3\text{HgS}^m$	s	1188	537	353
$(\text{CH}_3\text{Hg})_2\text{Se}^n$	se	-	-	216 <sup>d</sup>
$(\text{CH}_3\text{Hg})_3\text{Se}^{b,n}$	se	-	-	207 <sup>d</sup>

- a)  $\text{cm}^{-1}$   
 b) Infrared spectrum of solid  
 c) Spectrum in this region not reported  
 d) Degeneracy weighted average of symmetric and asymmetric bands.  
 e) Reference 54.  
 f) Reference 25.  
 g) This work.  
 h) R.A. Nyquist and J.R. Mann, *Spectrochim. Acta*, **28A**, 511 (1972).  
 i) Reference 44.  
 j) Reference 63.  
 k) Reference 64.  
 l) Reference 55.  
 m) Reference 30.  
 n) Reference 30.

bound and sulfur-bound methylmercury complexes are also presented. In the Raman spectrum of methylmercuric selenate, the symmetric  $\text{CH}_3$  deformation at  $1203 \text{ cm}^{-1}$ , the mercury-carbon stretch at  $565 \text{ cm}^{-1}$  and a band at  $290 \text{ cm}^{-1}$  assigned to mercury-oxygen stretching are all typical of the  $\text{CH}_3\text{-Hg-O}$  grouping. This spectrum provides support for the  $\text{CH}_3\text{HgOSeO}_3^-$  structure of the selenate complex, similar to the structure of the sulfate complex. Other bands observed in the methylmercuric selenate spectrum were assigned to  $\text{SeO}_3$  stretching in the complex at  $856 \text{ cm}^{-1}$ , and  $\text{SeO}_3$  deformation in the complex at  $503 \text{ cm}^{-1}$  and  $406 \text{ cm}^{-1}$ . These positions are close to those for  $\text{SeO}_4^{2-}$  and  $\text{HSeO}_4^-$  quoted by Wacker (58) and confirmed in this work. In particular, the  $\text{SeO}_3$  stretching frequency falls nicely between the  $\nu_1$  frequency of  $\text{SeO}_4^{2-}$  ( $835 \text{ cm}^{-1}$ ) and the most intense band in the spectrum of  $\text{HSeO}_4^-$  ( $867 \text{ cm}^{-1}$ ).

## 2. The Sulfite Complex of Methylmercury

The binding of methylmercury by the sulfite ligand,  $\text{SO}_3^{2-}$ , was investigated by monitoring the chemical shift of the methylmercury protons and the mercury-proton spin-spin coupling constant of solutions containing varying amounts of methylmercury and ligand. The interaction of the sulfite anion with methylmercury is known to be orders of magnitude stronger than the methylmercury-sulfate interaction (1,44).

Because of the easy oxidation of sulfite by atmospheric or dissolved oxygen, this system was studied by mole ratio experiments at constant pH, in which each sample could be prepared individually and its spectrum obtained immediately. The data for one such experiment, in which the ratio of sodium sulfite to methylmercury is varied from 0 to 6, while maintaining the pH at 5, is presented in Table 8. The pH of this experiment was chosen so as to maximize the interaction of the sulfite with the methylmercury by minimizing competition from hydroxide ions for the formation of  $\text{CH}_3\text{HgOH}$ . The chemical shift and coupling constant of the methylmercuric sulfite complex, 0.928 ppm and 173.1 Hz respectively, are obtained directly from the limiting chemical shift and the limiting coupling constant of this experiment. At low ligand concentrations, the observed chemical shift and coupling constant vary as the ligand to methylmercury ratio is changed, indicating that the relative amounts of free and complexed methylmercury are changing. At ligand to methylmercury ratios greater than two, both the observed chemical shift and the observed coupling constant remain constant, suggesting that all the methylmercury is complexed under these conditions, and that the observed NMR parameters are those of the sulfite-complexed methylmercury.

The data for additional mole ratio experiments at

TABLE 8

NMR Data for the Methylmercury-Sulfite System at pH = 5.0

<u>[Methylmercury]<sub>total</sub></u>	<u>[Sulfite]<sub>total</sub></u>	$\delta_{\text{CH}_3}$ <sup>a</sup>	$J_{\text{CH}_3\text{Hg}}$ <sup>b</sup>
<u>M</u>	<u>M</u>		
0.108	0.	0.962	230.5
0.100	0.0239	0.954	216.0
0.0942	0.0870	0.932	172.9
0.0910	0.174	0.928	172.6
0.0860	0.315	0.92	173.5
0.0841	0.507	0.928	173.1

a) ppm vs. DSS

b) Hz

pH 10.5 and 11.0 are presented in Tables 9 and 10. In this pH region, complexation equilibria can be studied over a wider range of ligand-to-methylmercury ratios due to more successful competition of the hydroxide with the sulfite for the methylmercury ions. The data presented in Figures 9 and 10 was used to calculate the formation constant of the sulfite complex of methylmercury. For each data point, a formation constant was calculated from the observed chemical shift, and then similarly from the observed coupling constant. The fractional concentration of complexed methylmercury at each data point is given by Equation 30. The chemical shift (or similarly the coupling constant) of the complexed methylmercury, was determined above from the experiment at pH = 5.0. The chemical shift of the free methylmercury,  $\delta_f$ , is that of  $\text{CH}_3\text{HgOH}$ , since at these pH values all the free methylmercury exists in that form (26). Thus  $P_c$ , the fraction of methylmercury as the complex  $\text{CH}_3\text{HgSO}_3^-$ , and its concentration,  $P_c [\text{CH}_3\text{Hg}^+]_{\text{total}}$ , was calculated for each data point.  $P_f$  was obtained from the equation  $P_f = 1 - P_c$ . Since all the free methylmercury is methylmercuric hydroxide,  $[\text{CH}_3\text{HgOH}] = P_f [\text{CH}_3\text{Hg}^+]_{\text{total}}$ . The concentration of methylmercury in the cationic form was calculated from Equation 33 (using  $K_1$ , the formation constant of the hydroxide complex, determined in Chapter III). The free sulfite concentration was calculated from Equation 34

TABLE 9

NMR Data for the Methylmercury-Sulfite System at pH = 10.51

[Methylmercury] <sub>total</sub>	[Sulfite] <sub>total</sub>	$\delta_{CH_3}^a$	$\log K_F^b$	$J_{CH_3Hg}^c$	$\log K_F^d$
0.103	0.0198	0.840	7.79	198.3	7.62
0.101	0.0532	0.869	7.78	190.0	7.75
0.0984	0.0832	0.892	7.83	183.4	7.83
0.0978	0.1373	0.910	7.75	177.1	7.90
0.0934	0.0608	0.882	8.07	187.0	7.85
0.0907	0.0792	0.897	8.01	182.5	7.93
0.0859	0.0199	0.845	8.23	196.5	8.24
0.0824	0.0982	0.910	8.05	178.5	7.98
0.0822	0.0419	0.870	8.09	188.8	8.47
0.0807	0.0544	0.882	7.98	186.3	7.96
0.0779	0.1684	0.919	7.85	175.1	7.98

- a) ppm vs. DSS
- b) Calculated from chemical shift data
- c) Hz
- d) Calculated from coupling constant data

TABLE 10  
 NMR Data of the Methylmercury-Sulfite System at pH = 12.00

[Methylmercury] total M	[Sulfite] total M	$\delta_{CH_3}$	$\log K_F^b$	$J_{CH_3Hg}^c$	$\log K_F^d$
0.104	0	0.821	-	203.5	-
0.106	0.0177	0.830	8.77	201.0	8.20
0.105	0.0547	0.840	8.06	198.5	7.98
0.103	0.153	0.856	7.92	193.5	7.90
0.100	0.207	0.861	7.85	192.1	7.84
0.0990	0.282	0.868	7.80	189.8	7.83
0.0964	0.408	0.875	7.75	187.6	7.78
0.0950	0.602	0.883	7.70	185.9	7.69
0.0906	0.796	0.890	7.67	184.1	7.67
0.0926	0.980	0.894	7.66	182.5	7.68
0.0872	1.240	0.900	7.68	181.4	7.65
0.0827	2.154	0.911	7.70	179.4	7.56

a) ppm vs. DSS  
 b) Calculated from chemical shift data  
 c) Hz  
 d) Calculated from coupling constant data



$$[\text{CH}_3\text{Hg}^+] = \frac{[\text{CH}_3\text{HgOH}]}{K_1 [\text{OH}^-]} \quad (33)$$

$$[\text{SO}_3^{2-}] = \alpha_2 \{ [\text{SO}_3^{2-}]_{\text{total}} - [\text{CH}_3\text{HgSO}_3^-] \} \quad (34)$$

where  $[\text{SO}_3^{2-}]_{\text{total}}$  is the total concentration of sulfite in the solution and  $\alpha_2$  is the fraction of sulfite in a form available for binding, which is dependent only on pH. The formation constant of methylmercuric sulfite, defined by Equation 35, is calculated for each data

$$K_F = \frac{[\text{CH}_3\text{HgSO}_3^-]}{[\text{CH}_3\text{Hg}^+][\text{SO}_3^{2-}]} \quad (35)$$

point from both the observed chemical shift and coupling constant. The results of these calculations are given in Tables 9 and 10. The median of these values is  $\log K_F = 7.96 \pm 0.04$ . This is in reasonable agreement with the potentiometric titration results of Schwarzenbach and Schellenberg (1) who reported a value of  $\log K_F = 8.11$  for this complex. The large scatter in formation constants determined in these NMR experiments is due to changes in the ionic strength from sample to sample. Because the ionic strength of the samples was necessarily large, no attempt was made to control it or to correct for its variations.

The large formation constant of the sulfite complex of methylmercury compared to that of the sulfate and selenate complexes suggests that the sulfite binds to methylmercury through the sulfur atom. In addition, the methylmercuric sulfite coupling constant is much smaller than that of either the sulfate or selenate complex, but similar to those reported for methylmercury complexes of sulfur-binding ligands, examples of which are given in Table 2.

Confirmation of binding through the sulfur atom in the sulfite complex was obtained from the Raman spectrum of the complex in solution. Details of the Raman spectrum of  $\text{CH}_3\text{HgSO}_3^-$  are given in Table 11. The assignments given to the Raman bands listed in this table are straightforward and closely follow the known frequencies of the  $\text{CH}_3\text{Hg}^+$  species in other complexes, the isoelectronic molecule  $\text{NH}_3\text{HgSO}_3$  (59) and the free and complexed  $\text{SO}_3^{2-}$  anion (60,61). The mercury-carbon stretching frequency of  $541 \text{ cm}^{-1}$  is typical of complexes with a sulfur bound to mercury, as indicated by comparison with the Raman data given in Table 7 for selected methylmercuric complexes. The mercury-carbon stretching frequency at  $206 \text{ cm}^{-1}$  is lower than observed for other sulfur-bound methylmercury species, but not unreasonably so, and may to some extent, correlate with the rather small formation constant of this complex compared to other sulfur-bound complexes of methylmercury.

TABLE 11  
Raman Spectrum of  $[\text{CH}_3\text{-Hg-SO}_3]^-$  <sup>a</sup>

Frequency	Description	$[\text{NH}_3\text{-Hg-SO}_3]$ <sup>b</sup>	$\text{SO}_3^{2-}$
2928 m, - <sup>c</sup>	$\text{CH}_3$ stretch (sym.)	(3120)	
1190 s, br, pol	$\text{CH}_3$ deformation (sym.)	(1299)	
1100 w, br, dp	$\text{SO}_3$ stretch (asym.)	1109	933
997 m, pol	$\text{SO}_3$ stretch (sym.)	997	967
785 vw, dp	$\text{CH}_3$ rock	(732)	
649 w, pol	$\text{SO}_3$ deformation (sym.)	640	620
541 vs, pol	Hg-C stretch	(462)	
510 w, sh, dp	$\text{SO}_3$ deformation (asym.)	511	469
206 vs, pol	Hg-S stretch	- <sup>c</sup>	
105 s, dp	$\text{SO}_3$ rock	- <sup>c</sup>	

- a) Sample prepared under argon from 0.44 M  $\text{CH}_3\text{HgOH}$  and an equivalent amount of solid  $\text{NaHSO}_3$ .
- b) Infrared spectrum reported by K. Broderson, Chem. Ber., 57, 2703 (1957); values in parentheses are comparable to those in  $\text{CH}_3\text{HgSO}_3^-$  but involve the  $\text{NH}_3$  group. The assignment of the bands at 1109 and 997  $\text{cm}^{-1}$  has been reversed from that in the original work because the band at 997  $\text{cm}^{-1}$  in  $\text{CH}_3\text{HgSO}_3^-$  is polarized.
- c) Not measured.

### 3. The Selenite Complexes of Methylmercury

The binding of methylmercury by the selenite ligand,  $\text{SeO}_3^{2-}$ , was investigated by monitoring the chemical shift of the methylmercury protons and the  $^{199}\text{Hg}$ -proton coupling constant as a function of solution conditions. The chemical shift of the methylmercury protons is presented as a function of pH in Figure 11 for a solution containing methylmercury and sodium selenite in a ratio of one to two (solid points). For comparison, chemical shift data is also presented for a solution containing only methylmercury. The spin-spin coupling constant is presented as a function of pH for methylmercury in the same solutions in Figure 12. Neither the chemical shift, nor the coupling constant titration curves of the methylmercury-selenite solution coincide with the titration curves of methylmercury alone, indicating that some complexation occurs over the entire pH range 0.5 to 13. In addition, the chemical shift and coupling constant titration curves of the methylmercury-selenite solution show two inflection points, suggesting that more than one complex is formed in this solution. A formation constant and NMR parameters for the  $\text{SeO}_3^{2-}$  complex of methylmercury have been calculated from the data in the high pH region ( $\text{pH} > 7.0$ ) of the titration curves using the method, described earlier in this chapter, for the calculation of the methylmercuric sulfate formation

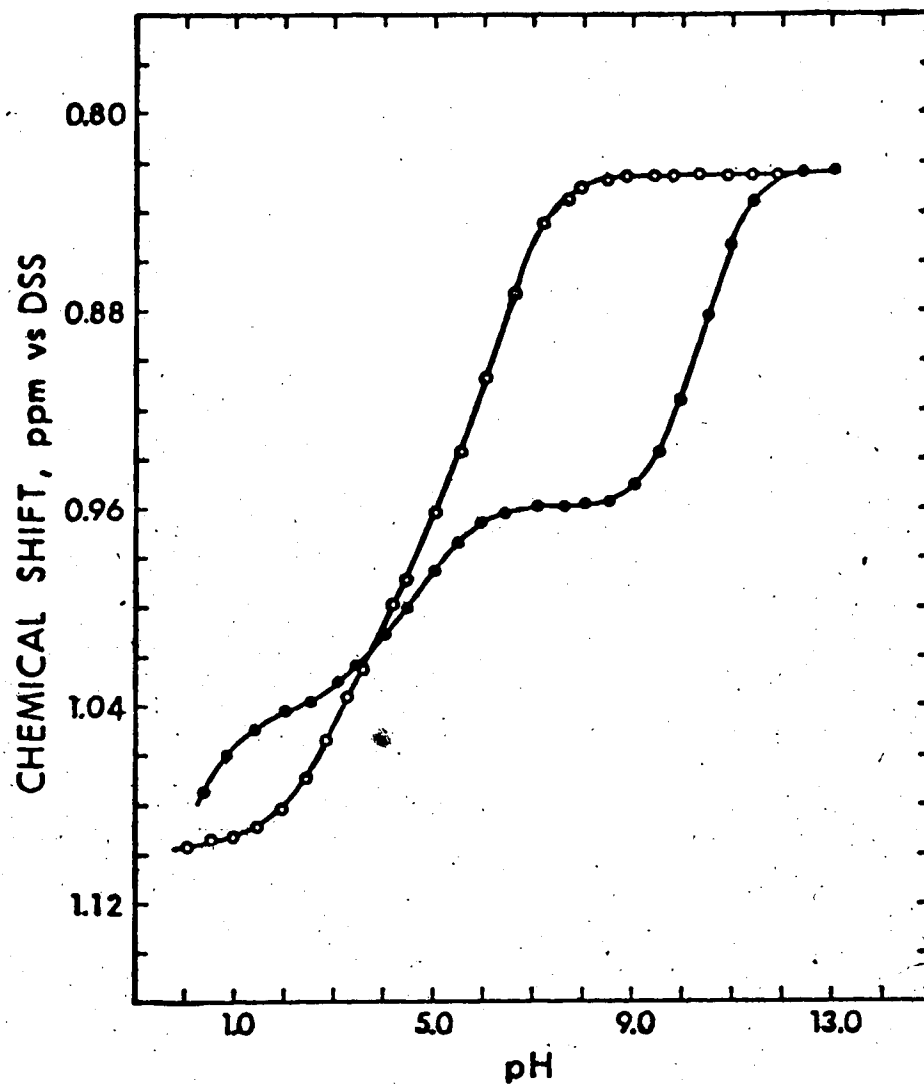


Figure 11. pH dependence of the chemical shift of the methyl protons of methylmercury in an aqueous solution containing 0.100 M methylmercury (open points) and in an aqueous solution containing 0.112 M methylmercury and 0.224 M sodium selenite (solid points).

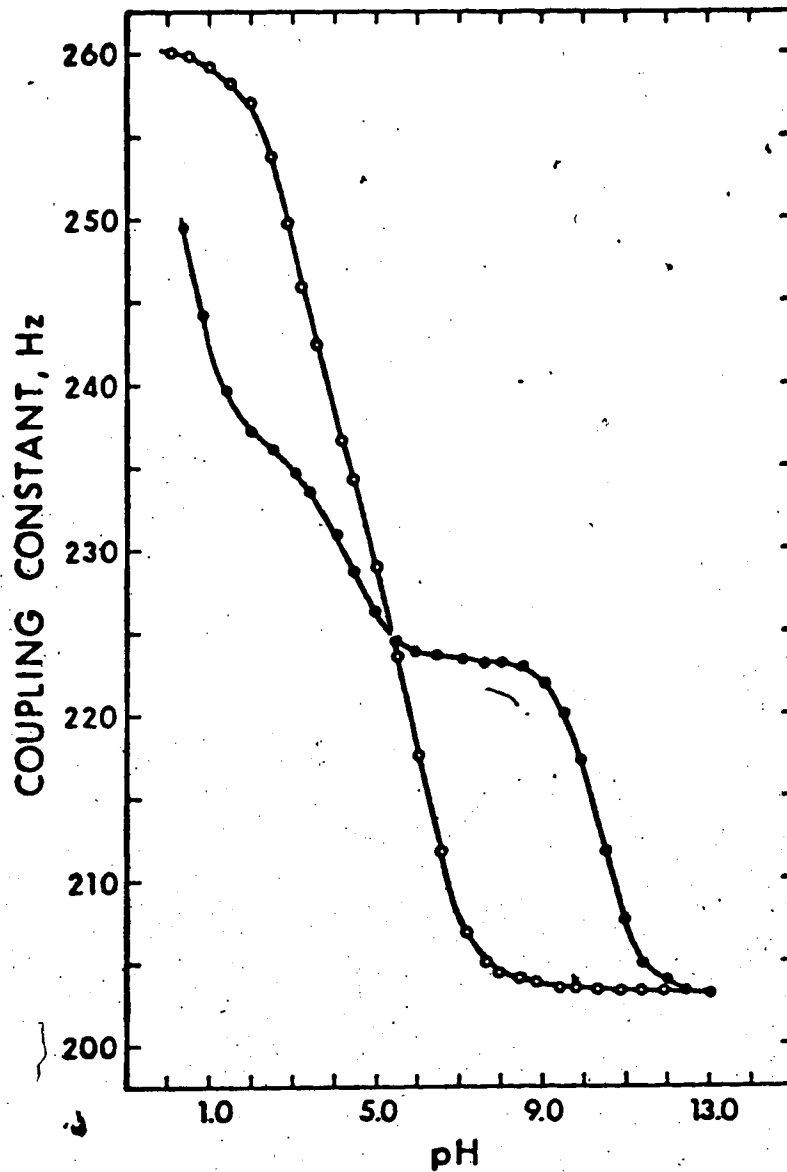


Figure 12. pH dependence of the mercury-proton spin-spin coupling constant of methylmercury in an aqueous solution containing 0.100 M methylmercury (open points) and in an aqueous solution containing 0.112 M methylmercury and 0.224 M sodium selenite (solid points).

constant and NMR parameters. From the chemical shift titration curve data, values of 0.958 ppm and  $6.46 \pm 0.02$  were obtained for the chemical shift and the logarithm of the formation constant of methylmercuric selenite. The formation constants calculated for each data point using  $\delta_c = 0.958$  ppm are given in Table 12. Similar calculations with the spin-spin coupling constant data resulted in values of 223.5 Hz and  $6.47 \pm 0.02$  for the coupling constant and the logarithm of the formation constant of the methylmercuric selenite complex.

Assuming that the  $\text{SeO}_3^{2-}$  complex of methylmercury is the only complex formed over the entire pH range, a chemical shift titration curve was calculated using the values of  $\delta_c$  and  $\log K_f$  determined above. This calculated titration curve and the experimental titration curve are presented in Figure 13. From a comparison of these curves, it is obvious that the formation of only methylmercuric selenite can account for the data at pH greater than six, however, another complex must be important at lower pH. Because the solution conditions were adjusted so that twice as much ligand as methylmercury was present, it is unlikely that this additional complex is  $(\text{CH}_3\text{Hg})_2\text{SeO}_3$ . Therefore, a model was adopted for the low pH data which included the formation of a complex between methylmercury and  $\text{HSeO}_3^-$  ( $\text{pK}_A = 8.18$ ). The formation constant and the NMR parameters of this complex

TABLE 12

Calculated Values of  $K_F$  for Methylmercuric Selenite from  
the Chemical Shift of the Methylmercury Protons in the  
High pH Region

---

<u>pH</u>	<u>log <math>K_F</math></u>
11.42	6.41
10.99	6.46
10.51	6.48
9.94	6.46
9.53	6.46
9.05	6.42
8.53	6.48
8.04	6.37
7.61	6.42
7.09	6.51



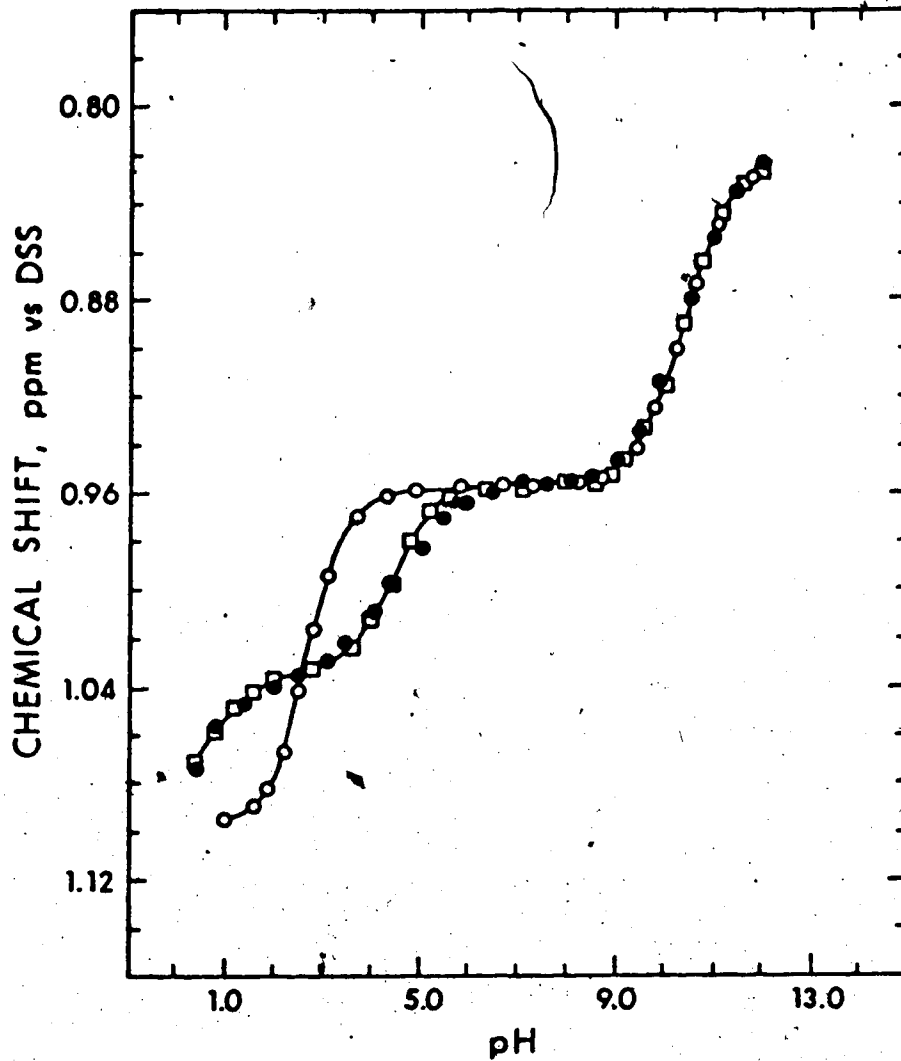


Figure 13. pH dependence of the chemical shift of the methyl protons of methylmercury in an aqueous solution containing 0.112 M methylmercury and 0.224 M sodium selenite. Squares: observed data points. Open points: calculated curve assuming only one complex,  $\text{CH}_3\text{HgSeO}_3^-$  is formed. Solid points: calculated curve assuming the formation of two complexes,  $\text{CH}_3\text{HgSeO}_3^-$  and  $\text{CH}_3\text{HgSeO}_3\text{H}$ .

were determined from the low pH region of the chemical shift and coupling constant curves in Figures 11 and 12. The nonlinear least-squares curvefitting computer program, KINFIT (62), was used to fit the data to this model. This program fit the observed chemical shift at each data point to that calculated by Equation 36, where P is the

$$\begin{aligned} \delta_{\text{obs}} = & P_{\text{CH}_3\text{Hg}^+} \delta_{\text{CH}_3\text{Hg}^+} + P_{(\text{CH}_3\text{Hg})_2\text{OH}^+} \delta_{(\text{CH}_3\text{Hg})_2\text{OH}^+} \\ & + P_{\text{CH}_3\text{HgOH}} \delta_{\text{CH}_3\text{HgOH}} + P_{\text{CH}_3\text{HgSeO}_3^-} \delta_{\text{CH}_3\text{HgSeO}_3^-} \\ & + P_{\text{CH}_3\text{HgSeO}_3\text{H}} \delta_{\text{CH}_3\text{HgSeO}_3\text{H}} \end{aligned} \quad (36)$$

fraction of methylmercury and  $\delta$  is the chemical shift of the species indicated. The sum of all the fractions of methylmercury species is equal to unity. For each data point, the concentration of the methylmercury cation was obtained by solving a mass balance equation for methylmercury in which the concentration of each methylmercury species was expressed in terms of the formation constants of the methylmercury species, the acid dissociation constants of the ligand, and the concentration of the methylmercury cation. The concentrations of all the other methylmercury species were then calculated from their formation constants and the methylmercury cation

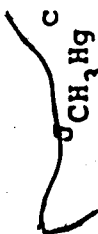
concentration. The chemical shifts and formation constants of all the methylmercury species, except  $\text{CH}_3\text{HgSeO}_3\text{H}$ , have been determined previously. The computer program, KINFIT, varies these two parameters to minimize the difference between the observed and calculated chemical shift at each data point. These calculations give values of 1.033 ppm and  $2.68 \pm 0.05$  for the chemical shift and logarithm of the formation constant of the  $\text{SeO}_3\text{H}^-$  complex of methylmercury. From the spin-spin coupling constant data, the coupling constant and logarithm of the formation constant of this complex were determined to be 234.6 Hz and  $2.71 \pm 0.03$ , respectively.

The values determined for the formation constant and the NMR parameters of the selenite and biselenite complexes of methylmercury are summarized in Table 13. Using these parameters, a chemical shift titration curve was calculated for comparison with the experimentally observed curve. Both these titration curves are presented in Figure 13. The agreement between these curves over the entire pH range indicates the model chosen for this system accurately describes the interaction of methylmercury with the  $\text{SeO}_3^{2-}$  and  $\text{HSeO}_3^-$  anions.

The value of the formation constant for the selenite complex of methylmercury is much larger than those of the sulfate and selenate complexes ( $\log K_F - 1$ ) but within two orders of magnitude of the formation

TABLE 13

Formation Constants and NMR Parameters for Selenite Complexes  
of Methylmercury

Complex	$\delta_{\text{CH}_3}^a$	$K_F^b$	 $\text{CH}_3\text{Hg}^c$	$K_F^d$
$\text{CH}_3\text{HgOSeO}_2^-$	.958 <sup>e</sup>	$6.46 \pm 0.02^f$	223.5	$6.47 \pm 0.02^f$
$\text{CH}_3\text{HgOSeO}_2\text{H}$	1.033 <sup>e</sup>	$2.68 \pm 0.05^f$	234.6	$2.71 \pm 0.03^f$

- a) ppm vs. DSS  
 b) Calculated from chemical shift data  
 c) Hz  
 d) Calculated from coupling constant data  
 e) Uncertainty in this value is  $\pm 0.002$  ppm  
 f) Reported uncertainties are a measure of the fit of the data and not a measure of the uncertainty in the constant

9

constant of methylmercuric sulfite. This might be taken to indicate that the selenite binds to methylmercury through the selenium atom. However, the mercury proton coupling constant of the selenite complex is much larger than that observed for methylmercury complexes of sulfur or selenium binding ligands but comparable to that of oxygen-bound methylmercury complexes. In addition, the results obtained for the methylmercuric selenite complex are similar to those obtained for methylmercuric carbonate. Dr. S. Libich determined values of 221.4 Hz and 6.10 for the coupling constant and the logarithm of the formation constant of the methylmercury-carbonate complex. These results suggest coordination of the selenite anion to the methylmercury through an oxygen atom, i.e.  $\text{CH}_3\text{HgOSeO}_2^-$ . The larger than expected value for the formation constant of this complex is perhaps related to the large  $\text{pK}_a$  of the ligand ( $\text{pK}_a = 8.18$  for the  $\text{HSeO}_3^-$  species), in the same manner as observed previously for the carboxylic acid complexes of methylmercury (46).

Confirmation of this structure for the methylmercuric selenite complex was obtained from its Raman spectrum. The Raman spectra of solutions containing about equal concentrations of methylmercury and ligand at various pH values were studied. The Raman bands of interest and their assignments are given in Table 7. The symmetric  $\text{CH}_3$  deformation at  $1207 \text{ cm}^{-1}$  and the mercury-carbon

stretch are typical of oxygen bonded methylmercury. Other bands in the spectrum are of low intensity compared to these, and the complete spectrum for the complex was not observed. The most intense band from selenium-oxygen stretching in the complex is at  $835 \text{ cm}^{-1}$ , intermediate in frequency between the strongest bands in  $\text{SeO}_3^{2-}$  at  $808 \text{ cm}^{-1}$  and  $\text{HSeO}_3^-$  at  $855 \text{ cm}^{-1}$ . A medium intensity band at  $290 \text{ cm}^{-1}$  may be from mercury-oxygen stretching, as its frequency is close to that assigned to similar vibrations in other complexes of oxy-anions, or it may be from a deformation mode of complexed selenite. Other bands are at  $730 \text{ cm}^{-1}$  (Se-O stretch) and  $365 \text{ cm}^{-1}$  (Se-O deformation). The spectra of aqueous solutions of  $\text{SeO}_3^{2-}$  and  $\text{HSeO}_3^-$  recorded in the present work are in excellent agreement with those reported by Walrafen (58).

The coupling constant determined above for the methylmercuric biselenite complex,  $234.6 \text{ Hz}$ , indicates that bonding occurs through oxygen in this complex also. Its small formation constant relative to that of the  $\text{CH}_3\text{HgSeO}_3^-$  complex correlates with the decreased basicity of  $\text{SeO}_3\text{H}^-$  (46).

The relatively small formation constant obtained for the selenite complex of methylmercury, compared to the formation constants of sulfhydryl (5,10) and nucleoside (6) complexes, is somewhat surprising considering reports that selenium-containing compounds, in particular

$\text{Na}_2\text{SeO}_3$ , are capable of protecting against methylmercury poisoning in animals (16,17). Ganther and coworkers (16) showed that when  $\text{Na}_2\text{SeO}_3$  was added to the diet of rats being fed methylmercuric hydroxide, the symptoms of methylmercury poisoning were delayed and decreased compared to those exhibited by rats being fed only methylmercury in the same doses. One possible explanation for this behavior is that the  $\text{Na}_2\text{SeO}_3$  is able to complex the methylmercury very strongly, preventing it from complexing with the sulfhydryl containing molecules found in the body. The magnitude of the formation constant determined above for the  $\text{CH}_3\text{HgSeO}_3^-$  complex indicates that this simple explanation cannot account for the detoxifying effect of methylmercury, and that some metabolized form of the selenite must be responsible for the observed behavior.

#### 4. The Thiocyanate and Selenocyanate Complexes of Methylmercury

The formation constant and the NMR parameters of the methylmercury-thiocyanate complex were determined by monitoring the NMR parameters of solutions containing methylmercury and thiocyanate as a function of pH. A solid, presumably the  $\text{CH}_3\text{HgSCN}$  complex, precipitates from aqueous solution containing 0.0901 M methylmercury and 0.0211 M potassium thiocyanate at a pH less than 8.5.

Therefore a solution which was half as concentrated and which contained four times as much methylmercury as thiocyanate ion was prepared. In this solution, the methylmercury was sufficiently concentrated for the NMR satellite resonances to be observable, and there was enough ligand for complexation to be detectable, but not enough complex to cause it to precipitate. The chemical shift of the methylmercury protons in this methylmercury-thiocyanate solution is presented as a function of pH in Figure 14. The spin-spin coupling constant of methylmercury in the same solution is presented as a function of pH in Figure 15. Chemical shift and coupling constant titration curves of solutions containing only methylmercury are given for comparison. The two chemical shift titration curves are different in the pH region 7 to 10.5, indicating that complexation is occurring in this pH region. The two coupling constant titration curves differ only at pH less than 8, indicating that a complex is also formed at low pH.

At pH greater than 8, where the chemical shift titration curve indicates complexation, the coupling constant titration curve of the methylmercury-thiocyanate solution is the same as that for a solution of methylmercury alone. This implies that the coupling constant of the methylmercury-thiocyanate complex formed at high pH is equal to the coupling constant of methylmercuric



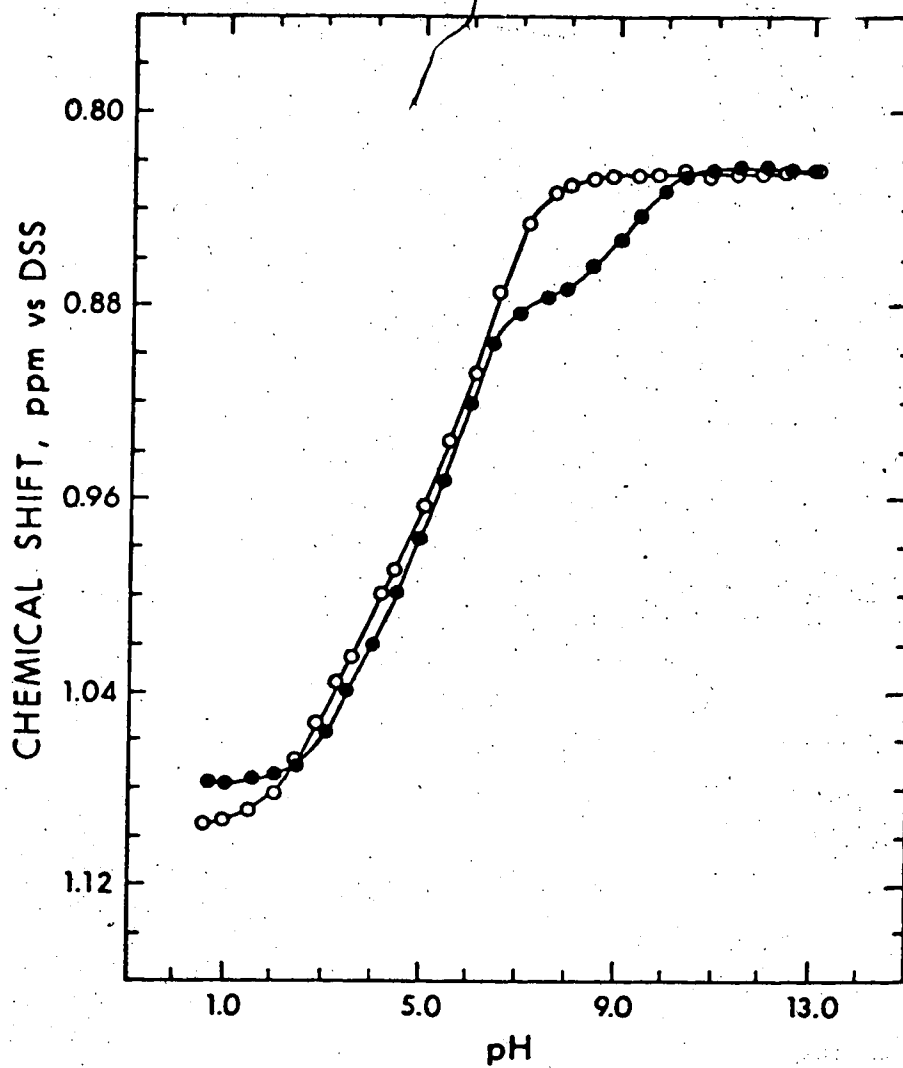


Figure 14. pH dependence of the chemical shift of the methyl protons of methylmercury in an aqueous solution containing 0.100 M methylmercury (open points) and in an aqueous solution containing 0.0563 M methylmercury and 0.0132 M potassium thiocyanate (solid points).

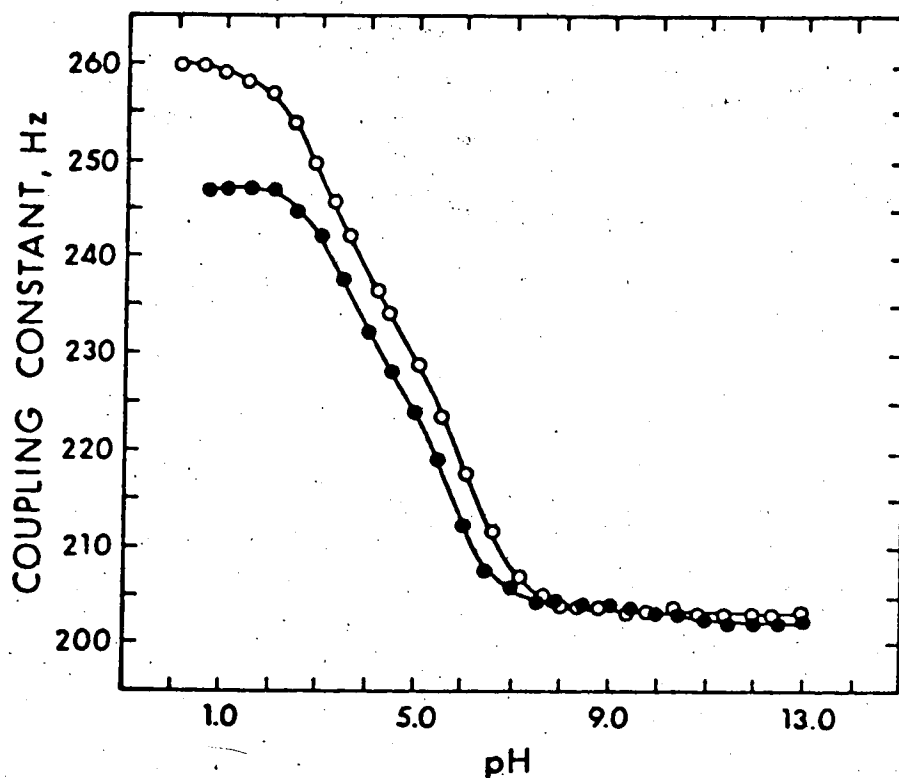


Figure 15. pH dependence of the mercury-proton spin-spin coupling constant of methylmercury in an aqueous solution containing 0.100 M methylmercury (open points) and in an aqueous solution containing 0.0563 M methylmercury and 0.0132 M potassium thiocyanate (solid points).

hydroxide, 203 Hz. The formation constant and chemical shift of this complex were determined from the chemical shift data in the high pH region, by the method described earlier in this chapter for the methylmercuric sulfate complex. The calculations were somewhat simplified, because in the high pH region all the free methylmercury exists as  $\text{CH}_3\text{HgOH}$ ; thus  $\delta_f$  is equal to the chemical shift of  $\text{CH}_3\text{HgOH}$  and does not need to be calculated at each data point. These calculations resulted in a value of 1.862 ppm for the chemical shift of  $\text{CH}_3\text{HgSCN}$  and a  $\log K_F = 6.05 \pm 0.01$ . This is in good agreement with the value  $\log K_F = 6.11$  determined potentiometrically by Schwarzenbach and Schellenberg for the same complex (1).

Schwarzenbach also detected a second methylmercury-thiocyanate complex,  $(\text{CH}_3\text{Hg})_2\text{SCN}^+$ , having a  $\log K_F = 1.65$ . This presumably would be present to the greatest extent at low pH where the concentration of  $\text{CH}_3\text{Hg}^+$  is the greatest. Thus the coupling constant titration curve seems to be a better indicator of 2:1 complex formation than is the chemical shift titration curve. However, a titration curve calculated by assuming that only one methylmercury-thiocyanate complex forms over the entire pH range, was compared to the experimental coupling constant titration curve and found to be identical. Thus, the 2:1 complex,  $(\text{CH}_3\text{Hg})_2\text{SCN}^+$ , is not present in large enough concentrations to be detected by the NMR experiment.

Schwarzenbach reported that the thiocyanate ion binds to methylmercury through the sulfur atom. The coupling constant of the complex is larger than usually observed for methylmercury complexes of sulfur-binding ligands. However, Cooney and Hall (63) concluded from Raman measurements that the ligand does bind through the sulfur. The Raman bands of interest for the  $\text{CH}_3\text{HgSCN}$  complex are listed in Table 7.

The selenocyanate anion is expected to show similar coordination behavior with methylmercury. In experiments similar to those performed in the study of the thiocyanate complex of methylmercury, samples were obtained from a four to one methylmercury to selenocyanate solution over the pH range 8.5 to 9.5. At pH less than 8.5 a solid, presumably the complex, precipitated from solution. At pH greater than 9.5 a black solid formed in the solution, presumably due to decomposition of the ligand. The data obtained from this experiment is presented in Table 14. As in the thiocyanate system at high pH, the observed coupling constant is the same as that observed at high pH for a solution containing only methylmercury, while the chemical shift varies with pH. This implies that the coupling constant of the methylmercury selenocyanate complex is very similar to the coupling constant of methylmercuric hydroxide, 203 Hz. The formation constant of the complex was calculated from

TABLE 14

NMR Data for the Methylmercury-Selenocyanate System<sup>a</sup>

<u>pH</u>	<u><math>\delta_{\text{CH}_3}^b</math></u>	<u><math>J_{\text{CH}_3\text{Hg}}^c</math></u>
9.49	0.885	202.4
9.28	0.890	202.5
9.11	0.893	202.0
8.67	0.894	202.6

a) Solution contains [methylmercury]<sub>Total</sub> = 0.0608 M  
and [selenocyanate]<sub>Total</sub> = 0.0161 M

b) ppm vs. DSS

c) Hz

the chemical shift data by the method described above for the calculation of the formation constant of  $\text{CH}_3\text{HgSCN}$ . The formation constants calculated for the individual data points are listed in Table 14. These values result in a median  $\log K_F = 6.79 \pm 0.01$  for the selenocyanate complex of methylmercury. This value is not expected to be too accurate owing to the inability to standardize the selenocyanate ligand, which decomposes in air. However, it does give an order of magnitude measure of the strength of the complex, and it can therefore be concluded that  $\text{SCN}^-$  and  $\text{SeCN}^-$  form similar complexes with methylmercury. This, in addition to the similarity of the coupling constants of the two complexes, implies that selenocyanate binds to methylmercury through the selenium atom. This structure is supported by the Raman spectrum of  $\text{CH}_3\text{HgSeCN}$ . Aynsley *et al.* (64) reported the spectrum of solid  $\text{CH}_3\text{HgSeCN}$ ; the bands of interest and their assignment are presented in Table 7. The position of the mercury-carbon stretch bands ( $540, 536 \text{ cm}^{-1}$ ) indicate that the selenocyanate ion coordinates to methylmercury through the selenium atom.

##### 5. Sulfide and Selenide Complexes of Methylmercury

As with oxide, multinuclear methylmercury complexes form readily with sulfide, although the nature of the complexes is slightly different in aqueous solution

due to the greater acidity of sulfur-bound protons. The sulfide complexes and their formation constants, as determined by potentiometric titration by Schwarzenbach, are:  $\text{CH}_3\text{HgS}^-$ ,  $\log K_F = 21.2$ ;  $(\text{CH}_3\text{Hg})_2\text{S}$ ,  $\log K_F = 16.3$ , and  $(\text{CH}_3\text{Hg})_3\text{S}^+$ ,  $\log K_F \sim 7$  (1). These complexes are analogous to the following known oxide complexes,  $\text{CH}_3\text{HgOH}$ ,  $(\text{CH}_3\text{Hg})_2\text{OH}^+$ ,  $(\text{CH}_3\text{Hg})_3\text{O}^+$ , which were discussed in Chapter III of this thesis.

The  $^{199}\text{Hg}$ - $^1\text{H}$  coupling constants of the sulfide complexes were obtained by monitoring the NMR spectra of solutions containing various mole ratios of methylmercury and sulfide. The chemical shift and coupling constant of the complex  $\text{CH}_3\text{HgS}^-$  were obtained from a mole ratio experiment at pH 13.2. Varying the methylmercury to sulfide ratio from 0.2 to 0.7 does not cause any change in the observed chemical shift or coupling constant and therefore does not change the fraction of methylmercury complex. Thus the data obtained from this experiment (Table 15) indicates that essentially all the methylmercury is bound to sulfide in these samples, presumably as  $\text{CH}_3\text{HgS}^-$ . Under the solution conditions of the experiment, there is not enough  $\text{CH}_3\text{Hg}^+$  present to form a dinuclear methylmercury species, nor a sufficient concentration of protons for the formation of  $\text{CH}_3\text{HgSH}$ . Thus the coupling constant for the complex,  $\text{CH}_3\text{HgS}^-$ , is considered to be that measured directly in the above experiment (146.2 Hz). This value

TABLE 15

NMR Data for the Methylmercury-Sulfide System at pH = 13.2

<u>[Methylmercury]<sub>total</sub></u>	<u>[Sulfide]<sub>total</sub></u>	<u><math>\delta_{\text{CH}_3}</math><sup>a</sup></u>	<u><math>J_{\text{CH}_3\text{Hg}}</math><sup>b</sup></u>
<u>M</u>	<u>M</u>		
0.149	0.212	0.519	146.2
0.134	0.224	0.525	145.8
0.118	0.236	0.522	145.9
0.104	0.321	0.521	146.2
0.0932	0.332	0.521	146.1
0.0822	0.343	0.522	146.2
0.706	0.354	0.521	146.2

a) ppm vs. DSS

b) Hz



is considerably smaller than that observed for substituted sulfides. For example, in the cysteinate complex, values around 170 Hz are found (10), which supports the formulation as  $\text{CH}_3\text{HgS}^-$  rather than  $\text{CH}_3\text{HgSH}$ .

In solutions containing more methylmercury than sulfide, for example a three to one methylmercury to sulfide solution, a yellow solid precipitated from solution over the entire pH range. After washing with water and then drying over phosphorous pentoxide, this solid was identified as  $(\text{CH}_3\text{Hg})_2\text{S}$  on the basis of its NMR spectrum in pyridine solution. The spectrum obtained was that of a typical  $\text{CH}_3\text{HgX}$  compound, namely an intense singlet with two small satellite resonances. A spin-spin coupling constant of 156 Hz was obtained from this spectrum, in excellent agreement with the value (156.6 Hz) reported by Scheffold (65), for the coupling constant of  $(\text{CH}_3\text{Hg})_2\text{S}$  in pyridine solution. The magnitude of this coupling constant is also smaller than that of substituted sulfides, for example cysteinate (10). This fact, along with the extreme insolubility of the complex in water, indicates that it is  $(\text{CH}_3\text{Hg})_2\text{S}$  rather than  $(\text{CH}_3\text{Hg})_2\text{SH}^+$ .

To determine the spin-spin coupling constant of the third sulfide complex,  $(\text{CH}_3\text{Hg})_3\text{S}^+$ , the NMR spectrum of methylmercury in a five to one methylmercury to sodium sulfide solution was monitored as a function of pH. The coupling constant of the methylmercury in this

solution is presented as a function of pH in Figure 16. Because of exchange broadening of the satellite resonances, the uncertainty of the measurements is large ( $\pm 0.5$  Hz) in the pH region 5.3 to 6.3. Above 6.3 a solid precipitated from solution, presumably the  $(\text{CH}_3\text{Hg})_2\text{S}$  complex, whose importance is expected to be lessened at lower pH where the methylmercury exists primarily as  $\text{CH}_3\text{Hg}^+$ . The coupling constant of the complex  $(\text{CH}_3\text{Hg})_3\text{S}^+$  was determined from the data in the coupling constant titration curve, Figure 16. The calculations are based on the assumption that all the sulfide in the solution exists in the form  $(\text{CH}_3\text{Hg})_3\text{S}^+$ , that is  $[(\text{CH}_3\text{Hg})_2\text{S}] = 0$ . This is a reasonable assumption because of the very small solubility observed for  $(\text{CH}_3\text{Hg})_2\text{S}$  in aqueous solution, and because Schwarzenbach (1) reported a relatively large formation constant for  $(\text{CH}_3\text{Hg})_3\text{S}^+$  ( $\log K_F \sim 7$ ). With this assumption, the concentration of the trimethylmercuric sulfide complex is equal to the total sulfide concentration in the solution. The fractions of free and complexed methylmercury,  $P_C$  and  $P_F$ , were calculated from Equations 37 and 38 where  $[\text{S}^{2-}]_{\text{total}}$  and  $[\text{CH}_3\text{Hg}^+]_{\text{total}}$  represent the

$$P_C = \frac{[(\text{CH}_3\text{Hg})_3\text{S}^+]}{[\text{CH}_3\text{Hg}^+]_{\text{total}}} = \frac{[\text{S}^{2-}]_{\text{total}}}{[\text{CH}_3\text{Hg}^+]_{\text{total}}} \quad (37)$$

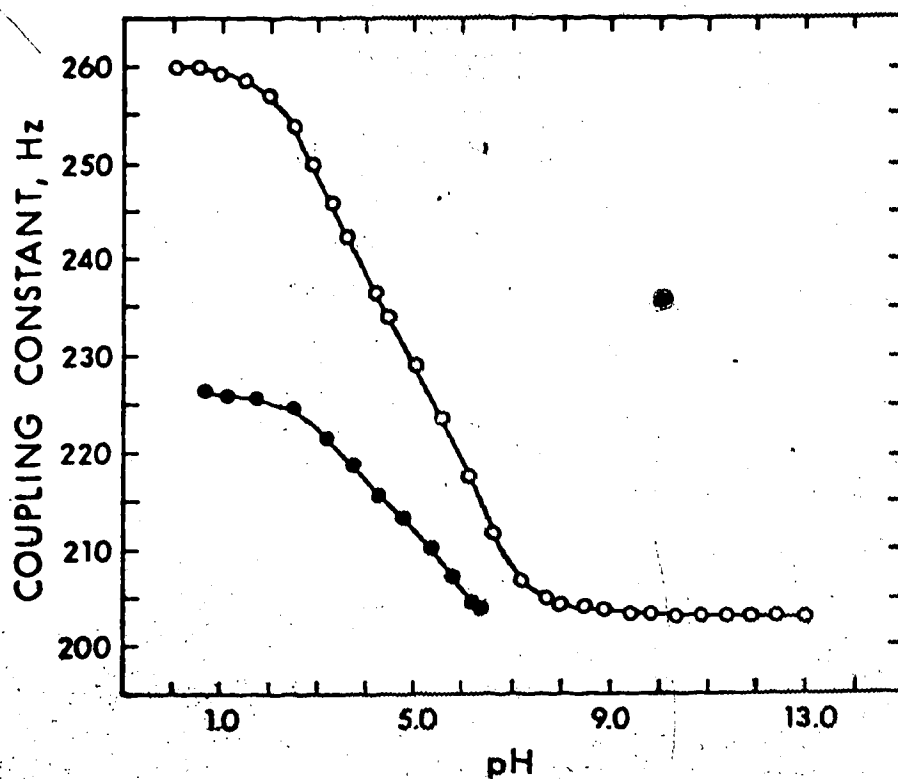


Figure 16. pH dependence of the mercury-proton spin-spin coupling constant of methylmercury in an aqueous solution containing 0.100 M methylmercury (open points) and in an aqueous solution containing 0.108 M methylmercury and 0.0215 M sodium sulfide (solid points).

$$\begin{aligned}
 P_f &= [\text{CH}_3\text{Hg}^+]_{\text{total}} - 3[(\text{CH}_3\text{Hg})_3\text{S}^+] \\
 &= [\text{CH}_3\text{Hg}^+]_{\text{total}} - 3[\text{S}^{2-}]_{\text{total}} \quad (38)
 \end{aligned}$$

total ligand and the total methylmercury concentrations. The concentration of each free methylmercury species and thus  $J_F$ , the coupling constant of the free methylmercury, were calculated at each pH, by the method described for the calculation of the formation constant of the methylmercury-sulfate complex. Thus, the equation describing the observed coupling constant of the methylmercury,  $J_{\text{obs}}$ , can be expressed in terms of the concentrations and coupling constants of the free and complexed methylmercury by Equation 39, in which only  $J_F$ , the coupling

$$J_{\text{obs}} = P_F J_F + P (\text{CH}_3\text{Hg})_3\text{S}^+ J (\text{CH}_3\text{Hg})_3\text{S}^+ \quad (39)$$

constant of the free methylmercury, is pH dependent. Equation 39 was then solved for  $J (\text{CH}_3\text{Hg})_3\text{S}^+$ , the coupling constant of the complex. The coupling constant of the complex obtained in this manner for each data point in the coupling constant titration curve is shown in Table 16. The trend towards increasing  $J (\text{CH}_3\text{Hg})_3\text{S}^+$  as the pH is decreased could be an indication of the presence of

TABLE 16

Calculated Mercury-Proton Coupling Constants for the  
Trimethylmercurisulphonium Ion

---

<u>pH</u>	<u><math>J_{\text{CH}_3\text{Hg}}^{\text{a}}</math></u>
6.33	199.5
6.18	199.7
5.77	200.5
5.32	201.1
4.78	201.8
4.27	201.4
3.72	202.2
3.19	202.2
2.48	203.4
1.72	203.3
1.10	203.4
0.65	204.2

a) Hz

some  $(\text{CH}_3\text{Hg})_2\text{S}$ , the amount of which would be pH dependent.

To eliminate interference from  $(\text{CH}_3\text{Hg})_2\text{S}$  as much as possible, the coupling constant of the trimethylmercuric sulfide complex was also calculated from the NMR coupling constant data of a mole ratio experiment at pH 1, in which the methylmercury to sulfide ratio was varied from five to eight. This data, along with the coupling constants calculated by the procedure described above, are shown in Table 17. The calculated coupling constant remains constant in this experiment, giving a value of 202 Hz for the coupling constant of the  $(\text{CH}_3\text{Hg})_3\text{S}^+$  complex. This value is large for a sulfur-bonded methylmercury complex, although it is comparable to the surprisingly large value observed for the  $\text{CH}_3\text{HgSCN}$  complex. The large formation constant of this complex apparently reflects the relatively small formation constant (1), which was reported by Schwarzenbach to be  $\log K_F \sim 7$ .

The Raman spectrum of  $\text{CH}_3\text{HgS}^-$  was studied. A solution of methylmercuric sulfide showed five bands in the Raman. The position of these bands and their assignments are given in Table 7. The  $\text{CH}_3$  deformation ( $1188 \text{ cm}^{-1}$ ), the Hg-C stretch ( $537 \text{ cm}^{-1}$ ) and the Hg-S stretch ( $353 \text{ cm}^{-1}$ ) are in accord with the values listed in Table 7 for other sulfur-bonded methylmercury species. A band at  $2574 \text{ cm}^{-1}$ , in the range for S-H stretching vibrations, was observed only under very high instrument

TABLE 17

NMR Data for the Methylmercury-Sulfide System at pH = 1.0

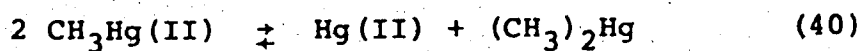
<u>[Methylmercury] total</u>	<u>[Sulfide] total</u>	<u>J<sub>CH<sub>3</sub>Hg</sub><sup>a</sup></u>	<u>J<sub>(CH<sub>3</sub>Hg)<sub>3</sub>S<sup>+</sup>a,b</sub></u>
<u>M</u>	<u>M</u>		
0.106	0.0211	225.5	202.5
0.120	0.0200	231.0	201.8
0.134	0.0189	235.4	201.9
0.147	0.0180	238.7	202.0

a) Hz

b) Calculated from observed J<sub>CH<sub>3</sub>Hg</sub> for the given total methylmercury and total sulfide concentrations.

gain and is assigned to a small amount of  $\text{HS}^-$ .

After exposure to the laser beam or, more slowly on standing, the solution of  $\text{CH}_3\text{HgS}^-$  yielded a gas and a black precipitate, presumably mercuric sulfide. The Raman spectrum of the supernatant has a band at  $349\text{ cm}^{-1}$  but no bands from methyl groups or mercury-carbon vibrations. These observations are accountable in terms of the equilibrium represented by Equation 40, being



moved to the right by the formation of insoluble mercuric sulfide and gaseous dimethylmercury, as discussed by Fagerstrom and Jernelov (66). The formation of  $\text{HgS}_2^{2-}$  from  $\text{HgS}$  and excess sulfide is shown by the Raman band at  $349\text{ cm}^{-1}$  from the symmetric mercury-sulfur stretching vibration, in agreement with authentic samples and solid cinnabar (67).

The Raman spectrum of  $(\text{CH}_3\text{Hg})_3\text{S}^+$  was reported by Clarke and Woodward (56) and that of the  $(\text{CH}_3\text{Hg})_2\text{S}^-$  species by Green (20). The Raman bands of interest in the spectra of these complexes are listed in Table 7 for comparison with the spectrum of  $\text{CH}_3\text{HgS}^-$  which is reported above.

The methylmercury-selenide complexes were studied by experiments similar to those used to study the methylmercury-sulfide system. A mole ratio experiment at



pH 13.5 was performed to evaluate the spin-spin coupling constant of the  $\text{CH}_3\text{HgSe}^-$  complex. NMR spectra were obtained for five samples containing methylmercury and sodium selenide in ratios ranging from 0.2 to 0.4. At higher ratios of methylmercury to ligand, a solid precipitated from solution, presumably  $(\text{CH}_3\text{Hg})_2\text{Se}$ . The data obtained from this experiment is presented in Table 18. As for the analogous methylmercury-sulfide experiment, the methylmercury chemical shift and coupling constant remained constant over the entire mole ratio range studied, indicating that the methylmercury existed entirely as  $\text{CH}_3\text{HgSe}^-$ . This species has a coupling constant of 143.1 Hz, which is only slightly smaller than that determined above for  $\text{CH}_3\text{HgS}^-$  (146 Hz), suggesting that the strength of the two complexes is also similar. Breitingger and Morell (30) determined a value of 146 Hz for the coupling constant of  $(\text{CH}_3\text{Hg})_2\text{Se}$  in carbon disulfide solution and a value of 196 Hz for the coupling constant of  $[(\text{CH}_3\text{Hg})_3\text{Se}]\text{NO}_3$  in  $\text{CD}_3\text{CN}$ . These values are again very similar to those determined above for the corresponding sulfide complexes, suggesting that the strengths of these selenide complexes are also similar to those of the corresponding sulfide complexes.

Attempts to obtain the Raman spectrum of  $\text{CH}_3\text{HgSe}^-$  were unsuccessful because of decomposition of the sample in the laser beam. Breitingger and Morell (30) have

TABLE 18

NMR Data for the Methylmercury-Selenide System at pH = 13.51

<u>[Methylmercury]<sub>total</sub></u>	<u>[Selenide]<sub>total</sub></u>	<u><math>\delta_{\text{CH}_3}</math><sup>a</sup></u>	<u><math>J_{\text{CH}_3\text{Hg}}</math><sup>b</sup></u>
<u>M</u>	<u>M</u>		
0.106	0.518	0.554	143.0
0.121	0.493	0.558	143.5
0.136	0.469	0.558	143.0
0.149	0.448	0.556	143.2
0.162	0.427	0.555	143.0

a) ppm vs. DSS  
b) Hz

reported the vibrational spectra of  $(\text{CH}_3\text{Hg})_2\text{Se}$  and solid  $[(\text{CH}_3\text{Hg})_3\text{Se}]\text{NO}_3$ , concluding that the similarity between these spectra and those of  $(\text{CH}_3\text{Hg})_2\text{S}$ , and  $(\text{CH}_3\text{Hg})_3\text{Se}^+$  implies similarity of the corresponding S- and Se-containing complexes.

#### 6. The Interaction of Phosphite with Methylmercury

To study the complexation of methylmercury by the phosphite anion  $\text{HPO}_3^{2-}$ , a solution containing 0.225 M methylmercury and 0.450 M phosphorous acid was prepared and samples were withdrawn over the pH range 1 to 7. At pH ~7, metallic mercury precipitated and a colorless gas escaped from the solution. On standing, metallic mercury also precipitated from the low pH samples. A possible explanation of this is that  $\text{HPO}_3^-$  catalyzes the reduction of  $\text{CH}_3\text{Hg}^+$  to  $\text{Hg}^0$  and presumably methane.

The NMR spectrum of phosphite solutions is of interest because the proton in the  $\text{HPO}_3^{2-}$  species does not exchange with water protons on the NMR time scale, and therefore results in a resonance in the NMR spectrum. This proton is apparently bonded directly to the phosphorous atom, since its resonance appears as a doublet, due to spin-spin coupling with  $^{31}\text{P}$  (natural abundance 100%, nuclear spin 1/2). The magnitude of this coupling constant is large (> 700 Hz) and pH dependent, indicating that the coupling is through only one bond.

## C. Discussion

### 1. The Complexation of Methylmercury by Inorganic Anions

The results presented in this chapter demonstrate that sulfur, selenium and oxygen-binding anions are all potential ligands for coordination to methylmercury in aqueous solution. Of the complexes studied, methylmercuric selenide has the smallest coupling constant, closely followed by methylmercuric sulfide. From a consideration of the relationship observed by Scheffold (49) between the magnitude of the coupling constant and the formation constant of a methylmercury complex, these results suggest that the selenide complex is a stronger complex than the sulfide complex. The coupling constants and the formation constants of all the complexes studied are summarized in Table 19. For every pair of sulfur-selenium complexes studied, the spin-spin coupling constant of the methylmercury complex of the selenium-containing ligand is smaller than that of the corresponding sulfur-containing ligand. The exception to this is the sulfite-selenite pair, which form different types of complexes with methylmercury. In addition, for those cases in which it was possible to measure formation constants, it was observed that the selenium-containing ligand binds methylmercury more strongly than the sulfur-

TABLE 19

Summary of Formation Constants and Coupling Constants  
of Methylmercury Complexes with Selected Inorganic  
Ligands

Complex	$\log K_F$	$J_{CH_3Hg}^a$
$CH_3HgOSO_3^-$	0.94	251.4
$CH_3HgOSeO_3^-$	1.12	248.5
$CH_3HgSO_3^-$	7.96	172.4
$CH_3HgOSeO_2^-$	6.46	223.5
$CH_3HgOSeO_2H$	2.68	234.6
$CH_3HgS^-$	21.2 <sup>b</sup>	146.2
$(CH_3Hg)_2S$	16.3 <sup>b</sup>	156.0 <sup>c</sup>
$(CH_3Hg)_3S^+$	7 <sup>b</sup>	202.0
$CH_3HgSe^-$	-d	143.1
$(CH_3Hg)_2Se$	-d	146 <sup>e</sup>
$(CH_3Hg)_3Se^+$	-d	196 <sup>f</sup>
$CH_3HgSCN$	6.05	203.0
$CH_3HgSeCN$	6.79	200.4

a) Hz

b) Reference 1

c) Measured in pyridine solution

d) Not determined

e) Measured in  $CS_2$  solution, Reference 30f) Measured in  $CD_3CN$  solution, Reference 30

containing ligand, with selenite and sulfite again being the exceptions. These results suggest that selenium-containing methylmercury complexes are more stable than the corresponding sulfur-containing complexes. This observation has implications in the search for an effective antidote for methylmercury poisoning, although the question of why selenite, itself a toxic compound, can function as a protecting agent against methylmercury remains unanswered. Methylmercury is known to poison the body by inactivating important sulfhydryl sites in proteins and enzymes (12). It is therefore possible that the presence of selenohydryl analogues of sulfhydryl-containing amino acids might prevent this poisoning of the proteins and enzymes. This is suggested by the results reported in this thesis, from which selenohydryl amino acids are expected to bind methylmercury more strongly than the corresponding sulfhydryl-containing amino acids. With this in mind, Sugiura and coworkers (68) have investigated the binding of the selenohydryl group by methylmercury using proton NMR. The coupling constant of the selenocysteamine complex of methylmercury,  $\text{CH}_3\text{HgSeCH}_2\text{CH}_2\text{NH}_3^+$ , was measured as 162.0 Hz compared to 185.7 Hz for the methylmercury cysteamine complex,  $\text{CH}_3\text{HgSCH}_2\text{CH}_2\text{NH}_3^+$  (10). These workers interpret this difference as an indication of the high affinity of the selenohydryl group for methylmercury in comparison with

that of the sulfhydryl group. Thus, there is promise that selenium compounds may be able to function effectively against methylmercury poisoning.

## 2. Significance of the Mercury-Proton Coupling Constant of Methylmercury Compounds

The dependence of the mercury proton coupling constant in  $\text{CH}_3\text{HgX}$  compounds on the nature of X was first reported by Hattón et al. in 1963 (23). These workers noticed that the magnitude of the coupling constant decreases as X is made more electronegative. The dependence of the coupling constant on the nature of X is further illustrated by the results of a study of the binding of methylmercury by selected carboxylic acids in aqueous solution (46). It was found that the magnitude of the coupling constant decreases approximately linearly as both the  $\text{pK}_A$  of the ligand and the  $\log K_F$  of the complex increase. More recently, a linear relationship was observed between the magnitude of the coupling constant and the logarithm of the formation constants for thioether, hydroxyl, sulfhydryl, and amino complexes of methylmercury (42). The results of this study of the methylmercury complexes of inorganic anions, summarized in Table 19, indicate that the observed relationship of the magnitude of the coupling constant and the  $\log K_F$  of the complex can be extended to the methylmercury complexes

of inorganic anions, with the magnitude of the coupling constant being very dependent on the donor atom of the ligand.

This finding suggests that the form in which methylmercury is present in natural systems might be identifiable by the coupling constant of the methylmercury. Unfortunately, on closer examination, this does not seem practical, since one would expect the methylmercury to exist as one of its most stable complexes, i.e. complexed to either a sulfur or a selenium atom. The data in Table 19 shows that the corresponding sulfur and selenium ligands form very similar complexes with methylmercury. Therefore it does not seem possible to identify the methylmercury species solely on the basis of its coupling constant, because the species most likely to be found have coupling constants which differ by only a few Hz.



## BIBLIOGRAPHY

1. G. Schwarzenbach and M. Schellenberg, *Helv. Chim. Acta*, 48, 28 (1965).
2. For a general discussion of this see R.G. Pearson, *J. Chem. Educ.*, 45, 585, 645 (1968).
3. S. Mansy and R.S. Tobias, *J. Amer. Chem. Soc.*, 96, 6874 (1974).
4. W.L. Hughes, Jr., *Cold Spring Harbor Symposia*, XIV, 79 (1950).
5. R.B. Simpson, *J. Amer. Chem. Soc.*, 83, 4711 (1961).
6. R.B. Simpson, *J. Amer. Chem. Soc.*, 86, 2059 (1964).
7. D.L. Rabenstein, R. Ozubko, S. Libich, C.A. Evans, M.T. Fairhurst, and C. Suvanprakorn, *J. Coord. Chem.*, 3, 263 (1974).
8. M.T. Fairhurst and D.L. Rabenstein, *Inorg. Chem.*, 14, 1413 (1975).
9. P.G. Simpson, T.E. Hopkins, and R. Hague, *J. Phys. Chem.*, 77, 2282 (1973).
10. D.L. Rabenstein and M.T. Fairhurst, *J. Amer. Chem. Soc.*, 97, 2086 (1975).
11. T. Takeuchi, *Pathology of Minamata Disease, Study Group of Minamata Disease, Kumamoto University, Japan, August 1968*, p. 141-252.
12. L.T. Kurland, S.N. Faro and H. Siedler, *World Neurol.*, 1, 370 (1960).

13. J.M. Wood, F.S. Kennedy, and C.G. Rosen, *Nature*, 220, 173 (1968).
14. S. Jensen and A. Jernelov, *Nature*, 223, 753 (1969).
15. H. Tokuomi, *Minamata Disease, Study Group of Minamata Disease, Kumamoto University, Japan, 1968*, p. 68.
16. H.E. Ganther, C. Goudie, M.L. Sunde, M.J. Kopecky, P. Wagner, S. Oh, and W.G. Hoekoha, *Science*, 175, 1122 (1972).
17. H. Iwata, H. Okamoto, and Y. Ohsawa, *Res. Commun. Chem. Path. and Pharmacol.*, 5, 673 (1973).
18. T.D. Waugh, H.F. Walton, and J.A. Laswick, *J. Phys. Chem.*, 59, 395 (1955).
19. D. Grdenic and F. Zado, *J. Chem. Soc.*, 521 (1962).
20. J.H.S. Green, *Spectrochim. Acta*, 24A, 863 (1968).
21. S. Mansy, T.E. Wood, J.C. Sprowles, and R.S. Tobias, *J. Amer. Chem. Soc.*, 96, 1762 (1974).
22. R.B. Simpson, *J. Chem. Phys.*, 46, 4775 (1967).
23. J.V. Hatton, W.G. Schneider, and W. Siebrand, *J. Chem. Phys.*, 39, 1330 (1963).
24. D.N. Ford, P.R. Wells, and P.C. Lauterbur, *Chem. Commun.*, 616 (1967).
25. P.L. Goggin and L.A. Woodward, *Trans. Faraday Soc.*, 58, 1495 (1962).
26. D.L. Rabenstein, C.A. Evans, M.C. Tourangeau, and M.T. Fairhurst, *Anal. Chem.*, 47, 338 (1975).

27. D. Grdenic and B. Markusic, *J. Chem. Soc.*, 2434 (1958).
28. V.W. Thiel, F. Weller, J. Lorbeth, and K. Dehnicke, *Z. Anorg. Allgem. Chem.*, 381, 57 (1971).
29. D. Breitinger, K. Geske, and W. Beitelschmidt, *Angew. Chem. internat. Edit.*, 10, 555 (1971).
30. D. Breitinger and W. Morell, *Inorg. Nucl. Chem. Lett.*, 10, 409 (1974).
31. D. Breitinger and G.P. Arnold, *Inorg. Nucl. Chem. Lett.*, 10, 517 (1974).
32. F.A. Cotton and G. Wilkinson, "Advanced Inorganic Chemistry", Interscience, New York, 1966, p. 620.
33. G. Plazzogna, P. Zanella, and L. Doretta, *J. Organomet. Chem.*, 29, 169 (1973).
34. A.J. Carty and A. Marker, *Inorg. Chem.*, 15, 425 (1976).
35. P.L. Goggin and L.A. Woodward, *Trans. Faraday Soc.*, 62, 1423 (1966).
36. L.F. Sytsma and R.J. Kline, *J. Organometal. Chem.*, 54, 15 (1973).
37. R. Barbieri and J. Bjerrum, *Acta. Chem. Scan.*, 19, 469 (1965).
38. J. Relf, P. Cooney, and H.F. Henneke, *J. Organometal. Chem.*, 39, 75 (1972).
39. Y.S. Wong, P.C. Cheih, and A.J. Carty, *Can. J. Chem.*, 51, 2597 (1973).

40. Y.S. Wong, N.J. Taylor, P.C. Cheih, and A.J. Carty, Chem. Commun., 625 (1974).
41. M. Eigen, Pure Appl. Chem., 6, 9 (1963).
42. M.T. Fairhurst, Ph.D. Thesis, University of Alberta, 1975.
43. J.H.R. Clarke and L.A. Woodward, Trans. Faraday Soc., 62, 3022 (1966).
44. J.H.R. Clarke and L.A. Woodward, Trans. Faraday Soc., 64, 1041 (1968).
45. S. Mansy, T.E. Wood, J.C. Sprowles, and R.S. Tobias, J. Amer. Chem. Soc., 96, 1762 (1974).
46. S. Libich and D.L. Rabenstein, Anal. Chem., 45, 118 (1973).
47. D.F. Evans, P.M. Ridout, and I. Wharf, J. Chem. Soc. (A), 2127 (1968).
48. P.L. Goggin, R.J. Goodfellow, S.R. Haddock and J.G. Cary, J. Chem. Soc. Dalton, 647 (1972).
49. R. Scheffold, Helv. Chim. Acta, 52, 56 (1969).
50. W.J. Blaedel and V.W. Meloche, "Elementary Quantitative Analysis", Harper and Row, New York, 1963, p. 290.
51. R.B. Fischer and D.G. Peters, "Quantitative Chemical Analysis", W.B. Saunders Co., Philadelphia, Penn., 1968, p. 397.
52. Reference 50, p. 794.

53. L. Meites, "Handbook of Analytical Chemistry", McGraw-Hill, New York, N.Y., 1963, pp. 1-8.
54. P.L. Goggin and L.A. Woodward, Trans. Faraday Soc., 56, 1591 (1960).
55. J. Lorbeth and F. Weller, J. Organomet. Chem., 32, 145 (1971).
56. J.H.R. Clarke and L.A. Woodward, Spectrochim. Acta, 23A, 2077 (1967).
57. D.L. Rabenstein, M.C. Tourangeau, and C.A. Evans, Can. J. Chem., in press.
58. G.E. Walrafen, J. Chem. Phys., 39, 1479 (1963).
59. K. Broderson, Chem. Ber., 57, 2703 (1957).
60. G.P. Syrtsova, Y.Y. Kharitonov, and T.S. Bolgar, Russ. J. Inorg. Chem., 17, 1425 (1972).
61. B. Nyberg and R. Larson, Acta Chem. Scand., 27, 63 (1973).
62. J.L. Dye and V.A. Nicely, J. Chem. Educ., 48, 443 (1971).
63. R.J.P. Cooney and J.R. Hall, Aust. J. Chem., 22, 2117 (1969).
64. E.E. Aynsley, N.N. Greenwood, and M.J. Sprague, J. Chem. Soc., 2395 (1965).
65. R. Scheffold, Helv. Chim. Acta., 50, 1419 (1967).
66. T. Fagerström and A. Hernelov, Water. Res., 6, 1193 (1972).

67. D.M. Adams, in "Metal-Ligand and Related Vibrations", Edward Arnold, London, 1967, p. 324.
68. Y. Suguira, Y. Hojo, Y. Tamai, H. Tanaka, J. Amer. Chem. Soc., 98, 2339 (1976).

Part II

AQUEOUS LANTHANIDE SHIFT REAGENTS

## CHAPTER V

### INTRODUCTION

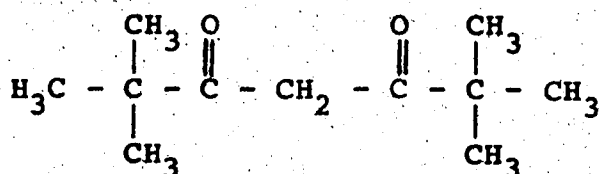
In 1969, Hinckley reported that the dipyridine adduct of the europium complex of dipivalomethane,  $[\text{Eu}(\text{dpm})_3 \cdot 2\text{py}]$ , induced stereospecific changes in the chemical shifts of the protons of cholesterol (1). Complexation between the coordinately unsaturated chelate (a Lewis acid) and the nucleophile (a Lewis base) results in large changes in the NMR spectrum of the nucleophile due to magnetic interactions with the paramagnetic lanthanide ion. Since the discovery by Hinckley of the effect of such complexes, which he termed shift reagents, their use has increased rapidly, especially in the areas of spectral clarification and the determination of molecular structures and conformations in solution.

While several other systems, including nickel(II) and cobalt(II) complexes (2-8), radical anions (9), and iron(II) phthalocyanins (10) have been used as shift reagents, it now seems that some of the lanthanide chelates are far superior since they produce substantial shifts with little accompanying broadening for atoms as far removed as 20 Å from the site of coordination to the shift reagent (11).

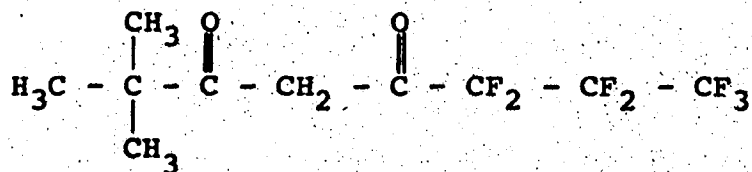
The most frequently used lanthanide shift reagents in organic solvents have been the tris( $\beta$ -diketonate)



complexes of europium(III) and praseodymium(III),  $\text{Ln}(\text{dpm})_3$  and  $\text{Ln}(\text{fod})_3$ , where Ln represents the lanthanide cation, dpm is the conjugate base of dipivalomethane(I), and fod is the conjugate base of 6,6,7,7,8,8,8,-heptafluoro-2,2-dimethyl-3,5-octanedione(II). These shift reagents are capable of inducing large isotropic shifts



I



II

in the NMR spectra of a large variety of molecules including alcohols, amines, ketones, aldehydes, sulfoxides, and esters (11,12).

However, these widely used shift reagents cannot be used in aqueous solution because they are decomposed by water (13). In aqueous solution, the nitrate and perchlorate salts of the trivalent lanthanides have been

used as shift reagents, but their applications are limited due to their precipitation as lanthanide hydroxides above pH *ca.* 6.5 (11,13). By complexing the lanthanide cations with aminopolycarboxylic acids, they can be kept in solution at high pH. In addition, if all the coordination sites of the lanthanide ion are not occupied by the chelating ligand, the lanthanide ion can complex to other ligands to form mixed complexes and act as a shift reagent, even at high pH.

In Part II of this thesis, the results of an investigation of the aqueous solution shift reagent properties of selected lanthanide ions and lanthanide chelates of aminopolycarboxylic acids are reported.

#### A. Theory of Paramagnetic Shift Reagents

The NMR spectra of paramagnetic systems are characterized by large chemical shifts and, often, spectral line broadening (14). Nuclei in paramagnetic complexes are subject to influences from the unpaired electrons. The isotropic chemical shift arising from this electron spin-nuclear spin interaction can be expressed as the sum of two distinct effects, a contact shift and a dipolar, or pseudocontact, shift (14).

The Fermi contact interaction takes place only if there is a finite probability of finding some unpaired electron spin density at the nucleus in question. This

implies that there is unpaired spin density in an s-type orbital of the atom, since p, d, etc. orbitals all have nodes at the nucleus. Unpaired spin density can be transferred to the nucleus by direct delocalization and via spin polarization. In principle, this type of interaction should lead to a splitting of the nuclear resonance (15), but in practice, the electron relaxation time,  $T_{1e}$ , is usually short enough on the NMR time scale to cause an effective decoupling of the splitting ( $T_{1e} \ll$  the reciprocal of the hyperfine coupling constant) (15). An electron relaxation time which is not quite short enough to meet this criterion results in broadening of the nuclear resonance, analogous to an intermediate exchange rate in chemical exchange studies (16). Although the nucleus senses only the average magnetic field produced by the unpaired electrons, this magnetic field is not equal to zero since, in the presence of an applied magnetic field, there are slightly more unpaired electrons oriented with the field than against it. A contribution from the paramagnetic metal ion to the total chemical shift is then observed. The paramagnetic contribution is weighted according to the populations of the Zeeman levels of the electron spin. The population of these levels, and thus the induced chemical shift, are temperature dependent (15).

The fundamental equation for the contact shift (17)

is presented in Equation 1. The induced chemical shift,

$$\frac{\Delta H^{\text{contact}}}{H} = - \frac{(A/h) 2\pi g_J \beta (g_J - 1) S(S+1)}{\gamma_N 3kT} \quad (1)$$

$\Delta H^{\text{contact}}$ , in a magnetic field  $H$ , is given in terms of  $(A/h)$ , the electron-nuclear hyperfine coupling constant in Hz,  $S$ , the total angular momentum quantum number of the unpaired electrons,  $\gamma_N$ , the nuclear magnetogyric ratio,  $\beta$ , the Bohr magneton, and  $g_J$ , the electronic g-factor. The hyperfine coupling constant is dependent on the number and the type of bonds separating the paramagnetic ion from the nucleus in question, and thus, it can vary in both sign and magnitude for nuclei in the same molecule. The dependence of the contact shift on the hyperfine coupling constant results in different contact shifts for different nuclei in the same molecule (11). The relative magnitudes of contact shifts for various magnetically-active nuclei were calculated by Goodman and Raynor (18). For example, they calculated that, for the same fractional spin occupancy, an  $^{17}\text{O}$  nucleus will experience twenty-four times the contact shift experienced by a proton in the same molecule, while a  $^{13}\text{C}$  nucleus will experience almost nine times the contact shift of the proton.

The second type of effect observed in paramagnetic

systems results from through-space dipole-dipole interaction between the magnetic dipoles of the unpaired electrons and those of the nuclear spins. The strength of this field, and thus its effect on the nuclei of the ligand system, varies with the location of the nuclei with respect to the magnetic axis of the complex. Thus, the magnitude of the dipolar shift provides information about the geometry of the ligand system. The dipolar electron-nuclear interaction in complexes with isotropic g-tensors is effectively averaged to zero (14). If an ion is magnetically isotropic, or has a symmetrical electron cloud, the generated magnetic field is independent of the orientation of the paramagnetic ion with respect to the direction of  $H_0$ , the applied magnetic field. Therefore, due to rapid tumbling of the molecule in solution, the net field induced at any nucleus by the unpaired electrons is zero. For the case of a magnetically anisotropic ion, the generated magnetic field is dependent on the orientation of the paramagnetic ion with respect to the applied field,  $H_0$ , and is not averaged to zero by tumbling (14). Each nucleus in the molecule experiences a net shielding or deshielding, and therefore a change in its chemical shift, due to the presence of the unpaired electrons.

Equation 2 describes the dipolar shift of a nucleus of spherical polar coordinates  $r$ ,  $\theta$ , and  $\phi$  in

$$\frac{\Delta H^{\text{dipolar}}}{H} = D \left[ \frac{3\cos^2\theta - 1}{r^3} \right] - D' \left[ \frac{\sin^2\theta \cos 2\phi}{r^3} \right] \quad (2)$$

the coordinate system of the principal magnetic axis of the complex (14).  $D$  and  $D'$  are constants which depend on the principal molar magnetic susceptibilities of the complex. With the assumptions that there is axial symmetry in the complex or axial symmetry approximated by rapid tumbling in solution (19), and that the principal axis is colinear with the lanthanide-ligand bond (20,21) or is defined by the ligand (22,23), Equation 2 simplifies to Equation 3. In Equation 3,  $\theta_i$  is defined as the angle between the principal axis of the paramagnetic molecule and a vector  $r_i$ , joining the metal to the

$$\frac{\Delta H^{\text{dipolar}}}{H} \propto \frac{3(\cos^2\theta - 1)}{r^3} \quad (3)$$

nucleus in question. Equations 2 and 3 predict that the dipolar interaction is independent of the nucleus being observed, but strongly dependent on the location of the nucleus with respect to the paramagnetic ion and the principal axis of symmetry of the molecule. The angular dependence predicts that, within the same molecule, there may be dipolar shifts of different signs, since

$(3\cos^2\theta-1)$  changes sign at  $\theta = 54^\circ 44'$ . The third power distance dependence of the dipolar interaction implies that its effect will attenuate rapidly with distance from the lanthanide ion, so that a large range of magnetic fields will be experienced by the different nuclei. Thus spectral simplification will result, the overlapping resonances will be spread out and resolved spectra observed. In the presence of lanthanide shift reagents, second order splitting patterns are often changed to first order spectra without any effect on the spin-spin coupling constants.

The amount of broadening of the NMR resonances due to dipolar interactions is dependent on the electron spin relaxation time of the paramagnetic ion. Qualitatively, the situation can be explained by a simple chemical exchange formalism (16). If the electron spin relaxation time,  $T_{1e}$ , is short on the NMR time scale, the neighboring nuclei experience an average of the possible spin states, weighted according to the net population of each state. This is the fast exchange region in which one sharp resonance is observed for each nucleus, the position of the resonance shifted from its diamagnetic position according to the relative populations of the electronic spin states. If the electron spin relaxation time is long, the unpaired electron spends a long time in a given spin state, permitting each nucleus to

experience exclusively the magnetic field generated by that state. Separate resonances would be observed for the nuclei which experience the different magnetic fields. The intensities of the resonances would not be the same since the populations of the electronic states are not the same, but are temperature dependent. This is the slow exchange region. Because most lanthanide ions have short electron spin relaxation times, on the order of  $10^{-13}$  -  $10^{-12}$  sec. (24), exchange averaged resonances are observed in lanthanide shift reagent systems. Some paramagnetic transition metal ions and lanthanide ions, [Eu(II), Gd(III)] have  $T_{1e}$ 's which are intermediate between the fast and slow cases (11). In this intermediate region, there is a large spread in the distribution of local magnetic fields within the sample, resulting in an uncertainty of the resonance position, that is a broadening of the resonance.

Quantitatively, the resonance broadening associated with the dipolar interaction is proportional to  $r^{-6}$ , where  $r$  is the distance from the paramagnetic ion to the nucleus in question (11,25). Thus, in systems in which the  $T_{1e}$  is long enough to broaden the NMR resonances, the line width of each nuclear resonance depends on the location of the particular nucleus in the molecule. This dependence of the resonance line widths on the geometry of the system offers a second method of



obtaining structural information from paramagnetic systems. Paramagnetic ions which have  $T_{1e}$  values of suitable magnitude ( $10^{-8}$  -  $10^{-9}$  seconds), for example Gd(III), are often referred to as broadening reagents, and are now used regularly in conjunction with shift reagents for molecular structure studies (26).

The unpaired electrons of the lanthanide ions are in highly shielded 4f orbitals, so that transfer of spin density from the lanthanide ions, either by direct delocalization or spin polarization, is unlikely since it would have to occur via the higher energy 6s orbital (27). Chemical shifts induced by lanthanide ions or lanthanide ion chelates are therefore usually attributed to the dipolar mechanism (11) and are then dependent only on the magnetic anisotropy of the complex, and the geometric factor  $(3\cos^2\theta-1)/r^3$ . The relative shifting abilities and the direction of the chemical shift induced by the lanthanide ions has been correlated with magnetic susceptibility anisotropy and/or g-tensor anisotropy of the complex (11). In several series of iso-structural lanthanide salts, it has been shown (28,29) that, for a given structure, dipolar shifts are proportional to the susceptibility tensor anisotropy. In each series of salts, the induced shifts change direction at the same places in the lanthanide series, corresponding to sign changes in the susceptibility

tensors. This observation is reasonable since, in an isostructural series, the magnetic anisotropy will be determined by the particular  $f^n$  configuration of the lanthanide ion and therefore the relative magnitude and sign of the anisotropy tensor will be the same as in any other isostructural series. The importance of the geometric factor in determining the direction of lanthanide induced shifts is illustrated by the report of Tanswell et al. (30) that Eu(III) induces downfield shifts in the  $^1\text{H}$  resonances of the nucleotide, ATP while upfield shifts are observed for other nucleotides in the presence of Eu(III).

#### B. Lanthanide Shift Reagents

The first reported application of lanthanide shift reagents was the simplification of the NMR spectrum of cholesterol by the addition of the dipyridine adduct of  $\text{Eu}(\text{dpm})_3$  (1), but it was soon realized that "plain"  $\text{Eu}(\text{dpm})_3$  was a more effective shift reagent (31), due to the elimination of the competition between pyridine and cholesterol for coordination sites on Eu(III). The analogous praseodymium chelate,  $\text{Pr}(\text{dpm})_3$  was shown to induce chemical shifts in the opposite direction to those induced by the europium chelate (32), thus they can be used in a complimentary manner. Soon thereafter, Rondeau and Sievers reported that the Eu(III) and Pr(III)

chelates of the partially fluorinated  $\beta$ -diketone ligand, fod (Structure II, page 128) are even more effective shift reagents (33).  $\text{Pr}(\text{fod})_3$  and  $\text{Eu}(\text{fod})_3$  are more soluble than the dpm chelates, are better Lewis acids, and thus are able to coordinate to a wider range of substituent molecules.

One of the early observations with these shift reagent systems was that the induced shifts increase with increasing shift reagent to substituent molar ratio (12). This indicates that the exchange of substituent between its shift reagent-complexed form and its free form is fast on the NMR time scale. Thus shift reagent data can be explained in terms of complex formation equilibria. The induced shift is quantitatively related to the formation constant of the shift reagent-substituent complex, and the chemical shift of the substituent in the complex (34-39). A second early observation with paramagnetic lanthanide systems was that the chemical shift induced in the various protons of the substituent molecule is dependent on the distance of the proton from the site of complexation to the shift reagent (12). This distance dependence of the isotropic shift is indicative of a dominant dipolar interaction between the lanthanide ion and the substituent. The distance dependence of the dipolar shift can be analyzed to determine the conformation and structure of molecules in solution (40-43).

Although most of the research and applications of lanthanide shift reagents have been with the dpm and fod chelates in organic solvents, aqueous solution lanthanide shift reagents have also been studied. Reuben and Fiat studied the interaction of various anions with the trivalent lanthanide cations in aqueous solution (44). By monitoring the  $^{17}\text{O}$  and  $^1\text{H}$  chemical shifts as a function of the concentration of added anions, they determined that nitrate, sulfate, acetate, and to a lesser extent, chloride, form complexes with the lanthanides while perchlorate does not. The hydrated lanthanide ions have been shown to induce shifts in the proton resonances of carboxylic, aminocarboxylic, and hydroxycarboxylic acids in aqueous solution (45,46). The results of Hart et al. (46) suggest that the deprotonated carboxyl group binds to the lanthanide ions, whereas the amino and hydroxyl groups do not.

Barry and coworkers (40) used lanthanide salts as shift reagents in studies of mononucleotide conformations in aqueous solution. From a combination of chemical shift and resonance broadening data, they determined that the phosphate group of the nucleotide binds to the lanthanide ion and results in selective shifts and/or broadenings in the nucleotide resonances.

Praseodymium and europium chlorides and nitrates were reported to cause differential shifts in the NMR

spectra of aqueous carbohydrate solutions, provided the carbohydrate possesses a steric arrangement of hydroxyl groups suitable for complexation (47-49). Spoormaker and coworkers (47) report that tridentate complexation by three consecutive hydroxyl groups of the carbohydrate is likely. Angyal and coworkers (49) used lanthanide induced shifts to determine the conformations of several carbohydrate molecules in aqueous solution.

To assess the relative importance of contact and dipolar shifts on the proton NMR spectra of lanthanide complexes in aqueous solution, Donato and Martin investigated the lanthanide-2,6 dipicoline (dpa) system (50). The trivalent lanthanide ions induced large shifts in the proton NMR spectra of dpa in basic solution, until the dpa to lanthanide ratio exceeded three, when peaks characteristic of the excess ligand also appeared. This was taken to indicate the formation of a strong  $\text{Ln}(\text{dpa})_3^{3-}$  complex. Analysis of the observed shifts indicated a dominant dipolar mechanism for this interaction in aqueous solution.

Birnbaum and coworkers (51,52) studied the interaction of the shift reagent,  $\text{Nd}(\text{III})$ , with a variety of carboxylic acids, amino acids, and histidine in aqueous solution. They reported that only the deprotonated carboxylate group of aminocarboxylic acids complexes  $\text{Nd}(\text{III})$  at low pH, but that between pH 6.0 and 7.0,  $\text{Nd}(\text{III})$  will

bind to histidine in a bidentate manner via the carboxyl group and the imidazole nitrogen. They used a combination of iteration and least squares fitting techniques to simultaneously determine the conditional formation constants of these complexes at selected pH values, and the chemical shifts of the ligand protons in the complexed form from the chemical shift data. The results of studies of this type are of importance in view of the criterion which must be met to obtain conformational information from lanthanide induced shift studies. Birdsall et al. (26) have pointed out that if a molecule binds a single lanthanide ion at a unique binding site, the analysis of the observed dipolar shifts can define the geometry of the substituent molecule.

Anteunis and coworkers (53,54) have used lanthanide salts to simplify the NMR spectra of small (penta to hepta) peptides in  $D_2O$  solution. They observed the interaction of the shift reagent at the deprotonated carboxylate sites and also at the amino sites at a pH greater than the isoelectric point. They observed no interaction of shift reagent at the peptide functional site (53). They suggested that the formation of ion pair clusters could account for some of the interaction observed at the amino site, and that at low pH, the  $NH_3^+$  moieties could also form complexes with the shift reagent via ion pair formation with the counterion of the

lanthanide cation.

Lanthanide ion complexes of ethylenediaminetetraacetic acid have been used as NMR shift and broadening probes to study the conformations of nucleotides in aqueous solution (55). The use of the lanthanide-EDTA complex as the shift reagent prevents the precipitation of the lanthanide hydroxides, which usually occurs before pH 7, and thus expands the pH range over which shift reagent effects can be studied. The lanthanide-EDTA complexes have also been shown to induce chemical shifts in the NMR spectra of salicylaldehyde and *o*-nitrophenol at high pH where the hydroxyl groups are deprotonated (56). It is suggested that chelation plays an important role in the complexation of these molecules by the shift reagent complex.

### C. Overview of Part II

In view of the abundance of information about the conformation and structures of molecules in solution and the assistance in spectral interpretation which can be obtained from lanthanide induced shifts, and the lack of a comprehensive study of the interaction of possible aqueous shift reagents with a variety of donor groups, it was decided to evaluate several lanthanide systems as possible aqueous shift reagents. It was mentioned earlier in this chapter that such information is essential if

conformational information is to be extracted from lanthanide induced shift studies. In Chapter VII of this thesis, the shift reagent properties of Eu(III) and Pr(III) are compared. A method is described for determining both the chemical shift of the complexed substituent molecule and the formation constant of the lanthanide-substituent complex. The dependence of the paramagnetic shift on the counterion of the lanthanide salt, and the interaction of the lanthanide cations with a variety of functional groups are also investigated. In Chapter VIII, several polyaminopolycarboxylic acid chelates of Pr(III) are considered as possible aqueous shift reagents.



## CHAPTER VI

### EXPERIMENTAL

#### A. Chemicals

$\text{Pr}(\text{NO}_3)_3$  and  $\text{Eu}(\text{NO}_3)_3$  were obtained from Research Organic/Inorganic Chemicals.  $\text{PrCl}_3 \cdot 6\text{H}_2\text{O}$  and  $\text{Pr}(\text{ClO}_4)_3 \cdot 6\text{H}_2\text{O}$  were obtained from Alfa Inorganics. Solutions prepared from these salts were first filtered and then standardized as described below. Ethylenediaminetetraacetic acid (Fisher Chemicals), N-(2-hydroxyethyl)-ethylenediaminetriacetic acid (Aldrich Chemicals), and cyclohexanediaminetetraacetic acid (K + K Laboratories) were used without further purification. All other chemicals were reagent grade and were used without further purification.

#### B. Preparation of Solutions

In general, all solutions were prepared as described in Chapter II, Section C.

#### C. Preparation and Standardization of Lanthanide Salt and Ligand Solutions

Stock solutions of approximately 0.4 M lanthanide salt in triply-distilled water were filtered to remove the insoluble impurities, which looked like paper fibers. An aliquot of this stock solution was diluted fifty-fold for standardization. The standardization procedure

involved adding a known excess of EDTA to a 25 ml aliquot of the diluted solution, buffering the solution at pH 10 with triethanolamine, and then titrating the excess EDTA with standard zinc nitrate to an Eriochrome black T endpoint. The moles of lanthanide ion in the 25 ml aliquot was taken to be equal to the total moles of EDTA minus the moles of  $Zn^{2+}$  required to reach the endpoint.

Acetic acid and methanesulfonic acid solutions were standardized by titration with standard sodium hydroxide to a phenolphthalein endpoint. Methylamine and N-methylimidazole solutions were standardized by titration with standard nitric acid to a methyl red endpoint.

Stock solutions containing approximately 0.4 M N-(2-hydroxyethyl)-ethylenediaminetriacetic acid in triply-distilled water or 0.4 M cyclohexanediaminetetraacetic acid in triply-distilled water were standardized by titrating aliquots, buffered with triethanolamine, with standard zinc nitrate to an Eriochrome black T endpoint.

#### D. pH Measurements

pH measurements were carried out as described in Chapter II, Section D, with the exception that a Fisher Accumet 520 pH meter was also used. In some experiments, the third figure after the decimal in the pH reading was

recorded. Although this digit has no significance in the actual meaning of the pH value, the change in pH between successive data points is expected to be significant at this decimal place and there was less scatter in the calculated formation constant values when this digit was used.

#### E. NMR Measurements and Reference Compounds

NMR measurements were carried out as described in Chapter II, Section F, with the exception that the chemical shifts are reported relative to t-butanol rather than sodium 2,2-dimethyl-2-silapentane-5-sulfonic acid (DSS).

To determine the effect of aqueous lanthanide shift reagents on possible NMR reference compounds, increments of  $\text{Pr}(\text{NO}_3)_3$  were added to a solution 0.2 M in each of t-butanol, dioxane, DSS, tetramethylammonium nitrate (TMA), and acetone up to a  $\text{Pr}(\text{NO}_3)_3$  concentration of 0.2 M. The chemical shift of the resonance of each solute molecule was measured relative to all the other resonances after each increment of  $\text{Pr}(\text{NO}_3)_3$  was added. The data indicated that the relative positions of the resonances did not change, except for DSS which appeared to be shifting downfield with the addition of the shift reagent. In a solution containing approximately equimolar concentrations of DSS and  $\text{Pr}(\text{NO}_3)_3$ , the DSS singlet appeared 0.05 ppm.

downfield from its position when no  $\text{Pr}(\text{NO}_3)_3$  was present. This change in chemical shift was taken to indicate a  $\text{Pr}(\text{III})$ -DSS interaction and therefore DSS was not used as a reference compound in this work. Dioxane, t-butanol, and TMA were used as references.

An interaction between the PrHEDTA shift reagent and the reference compound TMA was also observed. The TMA resonance in a solution containing approximately 0.2 M TMA and 0.1 M PrHEDTA was shifted 0.083 ppm downfield from its position when no PrHEDTA was present. This interaction will be discussed further in Chapter VIII, but it should be noted that TMA is not a suitable reference compound for this type of shift reagent system, and therefore only dioxane and t-butanol were used.

## CHAPTER VII

### THE HYDRATED Pr(III) AND Eu(III) CATIONS AS AQUEOUS SHIFT REAGENTS

#### A. Introduction

In this chapter, the hydrated Pr(III) and Eu(III) ions are investigated as aqueous solution shift reagents.

As mentioned in Chapter V, the rate of exchange of the substituent molecule between its lanthanide complex and its free forms is generally fast on the NMR time scale, and thus the observed chemical shift is a weighted average of the shifts of the free and complexed forms. Consequently, the lanthanide induced shift depends on both the shift of the complexed form and the fraction of the molecule in the complexed form; the fraction of the molecule in the complexed form depends on the formation constant of the shift reagent-substituent complex. Thus, to characterize the properties of similar shift reagents, both the chemical shift of the complexed form and the formation constant of the complex are important parameters.

First the shift reagent properties of the hydrated Eu(III) and Pr(III) ions are compared by studying the shifts they induce in the proton NMR spectrum of acetic acid. A method is described for determining both the chemical shift of the complexed substituent and the

formation constant of the complex from the lanthanide induced chemical shifts and applied to the Eu(III)-acetic acid and Pr(III)-acetic acid systems. Based on the results obtained from this study, the Pr(III) system was selected for further study. Next, the effect of the counterion of the lanthanide salt was examined by comparing the effect of  $\text{Pr}(\text{ClO}_4)_3$ ,  $\text{Pr}(\text{NO}_3)_3$  and  $\text{PrCl}_3$  on the NMR spectrum of the acetic acid ligand. The formation constant and chemical shift of the Pr(III)-acetate complex were determined in the presence of each counterion. The results of this study indicated that  $\text{Pr}(\text{ClO}_4)_3$  would induce the largest chemical shifts. Therefore, the effect of  $\text{Pr}(\text{ClO}_4)_3$  on various functional groups was investigated. The carboxylate, amino, sulfonate, sulfhydryl, and imidazole-nitrogen functional groups were selected as the potential complexation sites of organic molecules, such as amino acids and peptides, which are of interest in aqueous solution.

## B. Results

### 1. A Comparison of the Shift Reagent Properties of $\text{Eu}(\text{NO}_3)_3$ and $\text{Pr}(\text{NO}_3)_3$

To compare the shift reagent properties of the europium(III) and praseodymium(III) cations in aqueous solution, their effect on the NMR spectrum of acetic acid was investigated. The hydrated lanthanide ions are known

to interact with deprotonated carboxylate groups but not with the protonated carboxylic acid groups (51). Therefore, changing the pH of a Pr(III)-acetic acid solution effectively changes the amount of ligand available for complexation, that is, it effectively changes the Pr(III)-substituent ratio. Thus, the magnitude of the induced shift of the acetate resonance of a Pr(III)-acetic acid solution is dependent on the solution pH. The lanthanide salt-acetic acid interactions were studied by monitoring the chemical shift of the acetate resonance as a function of pH for solutions containing approximately equal concentrations of acetic acid and the appropriate lanthanide salt. The chemical shift data is presented as a function of pH in Table 20 for a solution containing 0.0995 M acetic acid and 0.0766 M  $\text{Eu}(\text{NO}_3)_3$  and a solution containing 0.0973 M acetic acid and 0.0749 M  $\text{Eu}(\text{NO}_3)_3$ . Similar data is presented in Table 21 for a solution containing 0.0980 M acetic acid and 0.0890 M  $\text{Pr}(\text{NO}_3)_3$  and a solution containing 0.0932 M acetic acid and 0.0885 M  $\text{Pr}(\text{NO}_3)_3$ . The data presented in these two tables demonstrates the major difference between praseodymium and europium shift reagents; namely that they induce chemical shifts in opposite directions. In solutions of acetic acid titrated to high pH, the acetate resonance occurs 0.67 ppm downfield from t-butanol. In the presence of an approximately equivalent amount of Eu(III), the acetate

TABLE 20

The Chemical Shift of the Methyl Protons of Acetic Acid as a Function of pH, in  
 $\text{Eu}(\text{NO}_3)_3$ -Acetic Acid Solutions

A. 0.0766 M $\text{Eu}(\text{NO}_3)_3$ , 0.0955 M HOAc				B. 0.0749 M $\text{Eu}(\text{NO}_3)_3$ , 0.0973 M HOAc			
pH	$\delta^a$	$\Delta\delta^b$		pH	$\delta^a$	$\Delta\delta^b$	
2.980	0.364	-0.483		4.212	-1.117	-1.909	
3.129	0.234	-0.610		4.279	-1.178	-1.961	
3.235	0.131	-0.711		4.328	-1.219	-2.001	
3.286	0.075	-0.766		4.383	-1.277	-2.054	
3.327	0.029	-0.812		4.471	-1.351	-2.126	
3.389	-0.041	-0.880		4.571	-1.420	-2.182	
3.479	-0.152	-0.990		4.696	-1.508	-2.254	
3.543	-0.235	-1.070		4.836	-1.584	-2.315	
3.628	-0.347	-1.178		4.973	-1.637	-2.360	
3.719	-0.464	-1.291		5.150	-1.693	-2.403	
3.817	-0.594	-1.416		5.330	-1.738	-2.436	
3.917	-0.725	-1.543		5.460	-1.765	-2.458	
4.011	-0.846	-1.656		5.621	-1.773	-2.461	
4.121	-0.974	-1.778		5.864	-1.765	-2.467	

<sup>a</sup> ppm in t-butanol.

<sup>b</sup>  $\Delta\delta$  is the difference in ppm between the observed acetate chemical shift and that of a solution containing only acetic acid at the same pH.



TABLE 21

The Chemical Shift of the Methyl Protons of Acetic Acid as a Function of pH in  $\text{Pr}(\text{NO}_3)_3$ -Acetic Acid Solutions

A. 0.0800 M $\text{Pr}(\text{NO}_3)_3$ , 0.0980 M HOAc				B. 0.0885 M $\text{Pr}(\text{NO}_3)_3$ , 0.0932 M HOAc			
pH	$\delta^a$	$\Delta\delta^b$		pH	$\delta^a$	$\Delta\delta^b$	
2.750	1.341	0.494		3.979	4.071	3.257	
2.890	1.496	0.652		4.093	4.339	3.533	
3.015	1.664	0.818		4.222	4.633	3.842	
3.103	1.800	0.956		4.329	4.839	4.058	
3.215	1.993	1.151		4.392	4.958	4.181	
3.315	2.186	1.345		4.511	5.168	4.397	
3.412	2.388	1.549		4.601	5.276	4.516	
3.516	2.619	1.783		4.744	5.448	4.706	
3.632	2.887	2.056		4.868	5.578	4.849	
3.725	3.111	2.284		4.960	5.642	4.918	
3.827	3.353	2.531		5.041	5.696	4.977	
4.026	3.822	3.013		5.200	5.778	5.073	
4.137	4.068	3.266		5.296	5.812	5.111	
4.235	4.273	3.483		5.517	5.874	5.183	
4.335	4.458	3.677		5.847	5.911	5.229	
				5.995	5.928	5.247	

<sup>a</sup> ppm vs.  $\beta$ -butanol.

<sup>b</sup>  $\Delta\delta$  is the difference in ppm between the observed acetate chemical shift and that of a solution containing only acetic acid at the same pH.

resonance appears 1.6 ppm upfield from t-butanol. In a solution containing approximately equal concentrations of Pr(III) and acetate, the acetate resonance appears 5.7 ppm downfield from t-butanol. This suggests that Pr(III) would be a more suitable shift reagent because it induces downfield shifts. Resonances of protons nearest the possible coordination sites of ligand molecules are generally further downfield than those of other protons in the ligand. Upon addition of Pr(III), the resonances of nuclei close to the binding site move further downfield resulting in spectral clarification. In the presence of Eu(III), these resonances would move upfield and likely cross over the resonances of other nuclei of the ligand molecule, and spectral clarification would not necessarily be achieved. For the same reason,  $\text{Eu}(\text{fod})_3$  and  $\text{Eu}(\text{dpm})_3$  are generally used in preference to  $\text{Pr}(\text{fod})_3$  and  $\text{Pr}(\text{dpm})_3$  in organic solution studies, since these europium chelates induce downfield shifts while the analogous praseodymium chelates induce upfield shifts (11).

To quantitatively compare the shift reagent properties of the Eu(III) and Pr(III) cations, the formation constants and chemical shifts of the Eu(III)-acetate and Pr(III)-acetate complexes were evaluated by a combination of linear and nonlinear least squares fitting techniques. In Eu(III)-acetic acid and Pr(III)-acetic

acid systems, the exchange of the acetate ions between the free and lanthanide-complexed forms is fast on the NMR time scale, as indicated by the presence of only one acetate resonance in the NMR spectra of lanthanide ion-acetate solutions. The chemical shift of the acetate resonance is dependent on the lanthanide ion to acetate ratio. The observed chemical shift,  $\delta_{\text{obs}}$ , is a weighted average of the chemical shifts of each acetate species in solution, according to Equation 4.  $\delta$  represents the

$$\delta_{\text{obs}} = P_f \delta_f + P_{1:1} \delta_{1:1} + P_{1:2} \delta_{1:2} + P_{1:3} \delta_{1:3} \quad (4)$$

Chemical shift of the acetate protons in the indicated species;  $\delta_f$  is determined by the relative concentration of acetic acid, HOAc, and acetate,  $\text{OAc}^-$ , which depends only on  $\text{pH}$ , and their chemical shifts.  $P$  represents the fraction of acetate in the free and the 1:1, 1:2, and 1:3 complexed forms, as indicated.  $P_{1:1}$ ,  $P_{1:2}$ , and  $P_{1:3}$  are defined by Equations 5-7, where  $[\text{HOAc}]_{\text{total}}$  is the

$$P_{1:1} = \frac{[\text{Ln}(\text{OAc})_2^{2+}]}{[\text{HOAc}]_{\text{total}}} \quad (5)$$

$$P_{1:2} = \frac{2[\text{Ln}(\text{OAc})_3^{+}]}{[\text{HOAc}]_{\text{total}}} \quad (6)$$

$$P_{1:3} = \frac{3[\text{Ln}(\text{OAc})_3]}{[\text{HOAc}]_{\text{total}}} \quad (7)$$

total acetate concentration in the solution and Ln the appropriate lanthanide cation. The sum of all the fractions,  $P_f + P_{1:1} + P_{1:2} + P_{1:3}$ , is unity. The formation constant and chemical shift of the acetate protons in the 1:1 lanthanide-acetate complexes have been determined from the chemical shift data of solutions in which the lanthanide ion concentration,  $[\text{Ln}^{3+}]$ , was somewhat greater than the acetate ion concentration,  $[\text{OAc}^-]$ . Under these conditions it can be assumed that the 1:2 complex,  $\text{Ln}(\text{OAc})_2^+$ , and complexes of higher acetate content, can be neglected. It will be shown that the relative magnitudes of the formation constants of the 1:1 complex,  $K_{f1}$  and of the 1:2 complex,  $K_{f2}$ , justify this assumption in both the Eu(III)-acetate and Pr(III)-acetate systems. The formation constant and the chemical shift of the acetate protons of  $\text{Pr}(\text{OAc})_2^+$  were determined from the  $\text{pH} < 4$  data of Table 21 by the linear curvefitting method described below. This data meets the criterion that  $[\text{Pr}^{3+}] \gg [\text{OAc}^-]$ , since at  $\text{pH} < 4$  most of the acetate is present as HOAc. At  $\text{pH} > 4$ , a deviation from linearity was taken to indicate that the  $\text{Pr}(\text{OAc})_2^+$  complex was also important. The formation constant and chemical shift of

the methyl protons of  $\text{Pr}(\text{OAc})_2^+$  were determined from the pH 4 data of Table 21 by the nonlinear least squares method also described below. Calculations using the value of 9.80 for the  $\text{pK}_a$  of  $\text{PrOH}_2^{3+}$  (57) indicate that at a pH less than 6, the concentration of  $\text{PrOH}^{2+}$  is negligible.

With the assumption that only the 1:1 lanthanide-acetate complex is important, Equation 4 simplifies to Equation 8. The formation constant of the  $\text{Pr}(\text{OAc})_2^+$

$$\delta_{\text{obs}} = P_f \delta_f + P_{1:1} \delta_{1:1} \quad (8)$$

complex is defined by Equation 9 in which  $[\text{Pr}^{+3}]$  is the

$$K_{f1} = \frac{[\text{Pr}(\text{OAc})_2^+]}{[\text{Pr}^{+3}][\text{OAc}^-]} = \frac{P_{1:1} [\text{HOAc}]_{\text{total}}}{[\text{Pr}^{+3}] \alpha P_f [\text{HOAc}]_{\text{total}}} \quad (9)$$

concentration of uncomplexed praseodymium ion,  $[\text{HOAc}]_{\text{total}}$  is the total concentration of acetate in all forms, and  $[\text{OAc}^-]$ , is the concentration of free ligand in the deprotonated form, equal to  $\alpha P_f [\text{HOAc}]_{\text{total}}$ .  $\alpha$  is the fraction of free ligand which is in the deprotonated form and is dependent only on pH. Using the relationship  $P_f + P_{1:1} = 1$ , Equation 10 is obtained by substituting Equation 9 into 8. When  $(\delta_f - \delta_{\text{obs}})/\alpha[\text{Pr}^{+3}]$  is the y-axis variable and  $\delta_{\text{obs}}$  the x-axis variable, Equation 10 is then the equation

$$\frac{\delta_f - \delta_{\text{obs}}}{\alpha[\text{Pr}^{+3}]} = \delta_{\text{obs}} K_{f1} - \delta_c K_{f1} \quad (10)$$

of a straight line with slope  $K_{f1}$  and intercept  $-\delta_c K_{f1}$ . The concentration of free Pr(III) is unknown and is dependent on the formation constant. Therefore, for each data point,  $[\text{Pr}^{+3}]$  was obtained by an iteration procedure. Initially, it was assumed that  $[\text{Pr}^{+3}]$  for each data point was equal to the total concentration of Pr(III) in the solution, and the straight line defined by Equation 10 was determined. The slope of this line gives a value for  $K_{f1}$ ; this value of  $K_{f1}$  was used to calculate a better  $[\text{Pr}^{+3}]$  for each data point, and thus a better estimate of  $K_{f1}$  was obtained from the new straight line. This procedure was repeated until the calculated values of  $[\text{Pr}^{+3}]$  converged at each data point, usually within ten iterations. The formation constant and chemical shift of the  $\text{Pr}(\text{OAc})^{2+}$  were obtained from the slope and y-axis intercept of the straight line in the last iteration step. Figure 17 shows the straight line obtained in the last iteration of the procedure for the  $\text{pH} < 4$  data of Table 21, including the nonlinear data points at  $\text{pH}$  values greater than 4. From the slope and intercept of this graph, values of  $53.2 \pm 0.4$  and  $9.095 \pm 0.01$  ppm were obtained for the formation constant and chemical

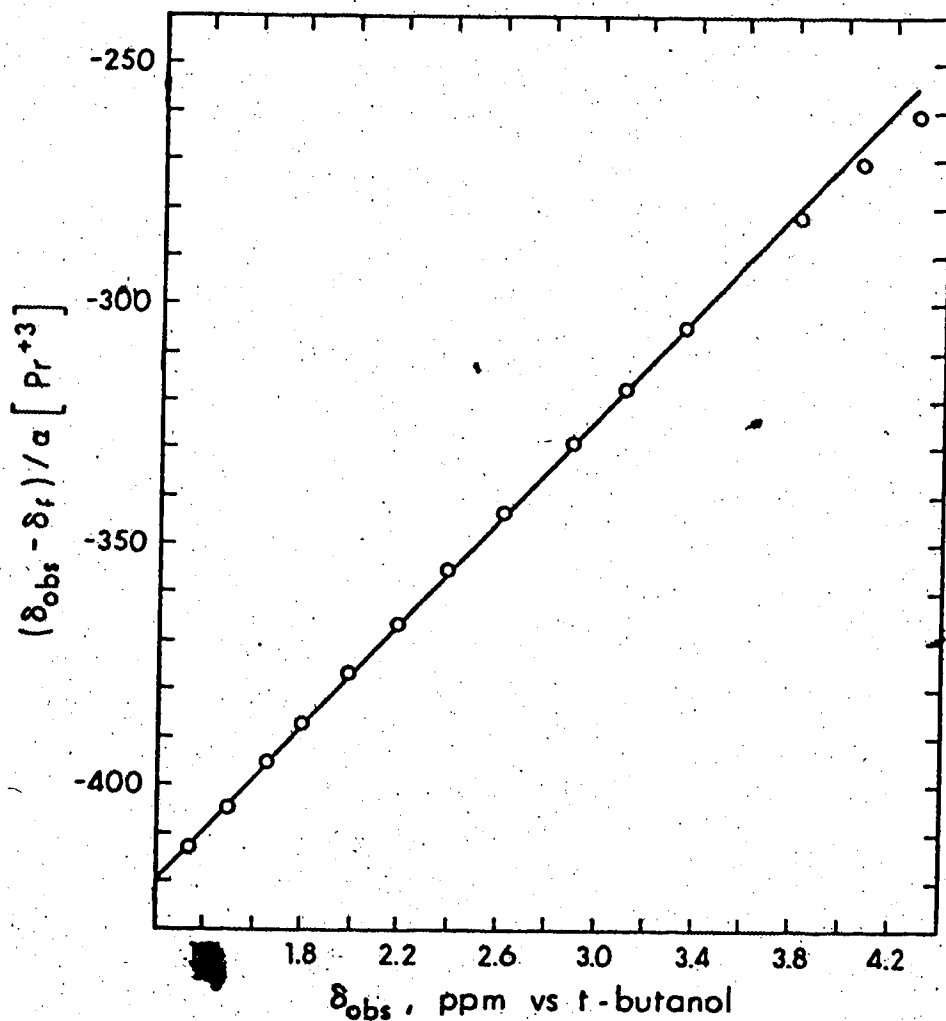


Figure 17. Plot of  $(\delta_{\text{obs}} - \delta_f) / \alpha [\text{Pr}^{+3}]$  versus the observed chemical shift of the methyl protons of acetic acid in an aqueous solution containing 0.0980 M acetic acid and 0.0800 M  $\text{Pr}(\text{NO}_3)_3$  at pH values ranging from 3.01 to 4.33. The straight line joining the points was determined by a linear least squares analysis of the "linear" points, that is, all the points shown except the three corresponding to the largest  $\delta_{\text{obs}}$  values. See text for discussion.

shift of the  $\text{Pr}(\text{OAc})^{2+}$  complex. This formation constant is in good agreement with the value 65 obtained by Sonesson (58) from potentiometric titration data for solutions of higher ionic strength ( $I = 2.0$ ).

The formation constant of the 1:2 Pr(III)-acetate complex,  $\text{Pr}(\text{OAc})_2^+$ , is defined by Equation 11. When this

$$K_{f2} = \frac{[\text{Pr}(\text{OAc})_2^+]}{[\text{Pr}(\text{OAc})^{2+}][\text{OAc}^-]} \quad (11)$$

complex is present, the observed chemical shift of the acetate resonance is given by Equation 12 in which  $P_{1:1}$

$$\delta_{\text{obs}} = P_f \delta_f + P_{1:1} \delta_{1:1} + P_{1:2} \delta_{1:2} \quad (12)$$

and  $P_{1:2}$  are the fractions of ligand in the  $\text{Pr}(\text{OAc})^{2+}$  and  $\text{Pr}(\text{OAc})_2^+$  complexes (defined by Equations 5 and 6) and  $\delta_{1:1}$  and  $\delta_{1:2}$  are the chemical shifts of the acetate protons in these complexes. The formation constant and chemical shift of the acetate protons of the  $\text{Pr}(\text{OAc})_2^+$  complex were calculated from the  $\text{pH} > 4$  data of Table 21. The nonlinear least squares fitting program, KINFIT (59) was used to fit the observed chemical shift for each data point to a calculated value to determine  $K_{f2}$  and  $\delta_{1:2}$ , using in the calculation the values for  $K_{f1}$  and  $\delta_{1:1}$  obtained above. The program KINFIT varies the unknowns  $K_{f2}$  and  $\delta_{1:2}$  until the best



fit is obtained between the observed chemical shift and that calculated for each data point. The chemical shift at each data point was calculated from a form of Equation 12 in which the fractions of ligand as each species were expressed in terms of pH, the  $K_A$  of the ligand,  $K_{f1}$ , and  $K_{f2}$ . These expressions were obtained by simultaneously solving the mass balance equations for Pr(III) and acetic acid. These calculations resulted in values of  $6.5 \pm 0.6$  and  $5.93 \pm .04$  ppm for the formation constant and the chemical shift of the  $\text{Pr}(\text{OAc})_2^+$  complex. This formation constant is in good agreement with the value of 10 obtained by Sonesson (58) from potentiometric titration data at a higher ionic strength. The small values obtained for  $K_{f1}$  and  $K_{f2}$  as well as the potentiometric titration results of Sonesson (58) indicate that the  $\text{Pr}(\text{OAc})_3$  and  $\text{Pr}(\text{OAc})_4^-$  complexes are not important under the solution conditions of this work.

The formation constant and the chemical shift of the acetate protons of the  $\text{Eu}(\text{OAc})_2^{2+}$  and  $\text{Eu}(\text{OAc})_3^+$  complexes were obtained from similar calculations using the chemical shift data of  $\text{Eu}(\text{NO}_3)_3$ -acetate solutions presented in Table 20. The results of these calculations and of the Pr(III)-acetate system are summarized in Table 22. The results presented in this table show that the formation constants of the  $\text{Pr}(\text{OAc})_2^{2+}$  and  $\text{Eu}(\text{OAc})_2^{2+}$  complexes are similar, but that the chemical shift of

TABLE 22

Formation Constants and Complex Chemical Shifts for  
Pr(III)-Acetate and Eu(III)-Acetate Complexes

<u>Complex</u>	<u>Formation Constant</u>	<u>Chemical Shift<sup>a,b</sup></u>
Pr(OAc) <sup>2+</sup>	53.2	9.095 <sup>c</sup>
Pr(OAc) <sub>2</sub> <sup>+</sup>	6.5	5.93 <sup>c</sup>
Eu(OAc) <sup>2+</sup>	62.6	-3.658 <sup>c</sup>
Eu(OAc) <sub>2</sub> <sup>+</sup>	5.0	-2.00 <sup>c</sup>

a) ppm vs. t-butanol

b) The methyl resonance of acetic acid and of acetate occur 0.850 and 0.676 ppm, respectively, downfield of t-butanol

c) Uncertainty in this value is  $\pm 0.002$  ppm

the praseodymium complex is much larger than that of the europium complex. This indicates that, although Pr(III) and Eu(III) interact to approximately the same extent with the carboxylate group, the induced chemical shifts will be much larger in the presence of Pr(III) than Eu(III) for the same set of solution conditions. Therefore, the direction of Pr(III) induced shifts is not only preferable to that of Eu(III) induced shifts, but their greater magnitude results in better spectral clarification and more precise conformational measurements. Thus, the Pr(III) cation was selected for use in further aqueous shift reagent studies.

## 2. The Counterion Dependence of Pr(III) Induced Chemical Shifts in Aqueous Solution

To determine the effect of the counterion of the lanthanide salt, the Pr(III) induced shifts in the NMR spectrum of acetic acid were investigated, and the effects of  $\text{Pr}(\text{NO}_3)_3$ ,  $\text{PrCl}_3$ , and  $\text{Pr}(\text{ClO}_4)_3$  compared. Birnbaum and Moeller (60) used lanthanide salts as shift reagents for substituted pyridine molecules in acetonitrile solution. They found that, for a given lanthanide cation, the magnitude and the direction of the induced shift depended on the counterion of the lanthanide salt. Therefore, both the direction and magnitudes of the Pr(III) induced shifts in the NMR spectrum of aqueous

acetic acid are of interest for the comparison of the Pr(III) salts.

The acetic acid-praseodymium salt systems were studied by monitoring the chemical shift of the methyl protons of the acetic acid as a function of pH for solutions containing approximately equal concentrations of acetic acid and the appropriate praseodymium salt. The  $\text{Pr}(\text{NO}_3)_3$ -acetate system was discussed in Section 1 above. The chemical shift data is presented as a function of pH in Table 21 for a solution containing 0.0980 M acetic acid and 0.0800 M  $\text{Pr}(\text{NO}_3)_3$  and a solution containing 0.0932 M acetic acid and 0.0885 M  $\text{Pr}(\text{NO}_3)_3$ . Similar chemical shift data is presented in Table 23 for the acetic acid- $\text{PrCl}_3$  system and in Table 24 for the acetic acid- $\text{Pr}(\text{ClO}_4)_3$  system. There are no large differences in the data presented in these three tables, since the magnitudes of the observed chemical shifts are very similar and the direction of the shifts is the same in all three cases. One can conclude, therefore, that the directional dependence of the chemical shift, observed by Birnbaum and Moeller in acetonitrile solution (60), on the anion of the lanthanide salt is not observed in aqueous solution. This presumably is due to the ability of water to compete more effectively than the acetonitrile for the coordination sites of the lanthanide ion, resulting in less lanthanide-counterion interaction.

TABLE 23

The Chemical Shift of the Methyl Protons of Acetic Acid as a Function of pH in  $\text{FeCl}_3$ -Acetic Acid Solutions

A. 0.0789 M $\text{FeCl}_3$ , 0.0985 M HOAc				B. 0.0779 M $\text{FeCl}_3$ , 0.0973 M HOAc			
pH	$\delta^a$	$\Delta\delta^b$		pH	$\delta^a$	$\Delta\delta^b$	
2.460	1.120	0.220		4.001	3.893	3.883	
2.574	1.197	0.348		4.106	4.128	3.322	
2.724	1.325	0.478		4.204	4.342	2.250	
2.788	1.393	0.546		4.283	4.482	3.699	
2.903	1.528	0.681		4.392	4.688	3.915	
3.102	1.820	0.978		4.484	4.834	4.060	
3.191	1.974	1.131		4.584	4.912	4.210	
3.266	2.126	1.284		4.707	5.123	4.377	
3.336	2.266	1.425		4.800	5.222	4.487	
3.410	2.423	1.584		4.914	5.318	4.591	
3.504	2.638	1.803		4.967	5.366	4.641	
3.597	2.870	2.038		5.049	5.413	4.694	
3.657	3.016	2.186		5.167	5.478	4.770	
3.753	3.204	2.418		5.266	5.517	4.814	
3.812	3.389	2.567		5.450	5.579	4.886	
3.908	3.616	2.797		5.721	5.622	4.937	
4.006	3.843	3.033		5.903	5.642	4.961	

a ppm vs. t-butanol.

b  $\Delta\delta$  is the difference in ppm between the observed acetate chemical shift and that of a solution containing only acetic acid at the same pH.

TABLE 24

The Chemical Shift of the Methyl Protons of Acetic Acid as a Function of pH in  
Pr(ClO<sub>4</sub>)<sub>3</sub>-Acetic Acid Solutions

A. 0.0769 M Pr(ClO <sub>4</sub> ) <sub>3</sub> , 0.114 M HOAc			B. 0.0749 M Pr(ClO <sub>4</sub> ) <sub>3</sub> , 0.111 M HOAc		
pH	$\delta^a$	$\Delta\delta^b$	pH	$\delta^a$	$\Delta\delta^b$
2.547	1.391	0.54	4.068	4.386	3.579
2.886	1.780	1.003	4.168	4.227	3.429
3.137	2.320	1.476	4.232	4.662	3.335
3.219	2.494	2.651	4.291	4.735	3.972
3.246	2.549	1.707	4.339	4.833	4.053
3.310	2.697	1.856	4.407	4.935	4.159
3.387	2.876	2.037	4.455	4.995	4.220
3.445	3.009	2.171	4.507	5.059	4.286
3.510	3.207	2.369	4.590	5.148	4.388
3.593	3.357	2.760	4.767	5.305	4.567
3.715	3.633	2.806	4.866	5.426	4.703
3.776	3.773	2.948	5.329	5.558	4.860
3.831	3.903	3.081	6.045	5.622	4.941
3.890	4.029	3.210			
3.954	4.162	3.346			
4.022	4.259	3.490			

<sup>a</sup> ppm vs. t-butanol

<sup>b</sup>  $\Delta\delta$  is the difference in ppm between the observed acetate chemical shift, and that of a solution containing only acetic acid at the same pH.

This suggests, however, that there may be some complexation of the counterions by the lanthanide cations, even in aqueous solution.

To obtain a quantitative evaluation of the differences between the three Pr(III)-acetate systems discussed above, the formation constant for the Pr(III)-acetate complexes and the chemical shift of the acetate protons in these complexes were determined in the presence of the nitrate, the chloride, and the perchlorate anions. The data in Tables 21, 23, and 24 were used to determine these parameters by the method discussed in Section 1 of this chapter. The results of the calculations for each of the systems are presented in Table 25. These results indicate that the Pr(III) interacts less with the perchlorate anion than with the nitrate and chloride anions, since the  $\text{Pr}(\text{OAc})^{2+}$  formation constant is larger in the presence of perchlorate than with either nitrate or chloride. Reuben and Fiat came to a similar conclusion by studying the water  $^{18}\text{O}$  resonances of solutions of the lanthanide salts (44). Thus the praseodymium perchlorate salt would be the best shift reagent both for spectral simplification and for conformational studies, and was used in the remaining aqueous shift reagent studies discussed in this thesis.

TABLE 25

Formation Constants and Complex Chemical Shifts for Pr(III)-Acetate Complexes  
in the Presence of the Nitrate, Chloride, and Perchlorate Counterions

Shift Reagent	$K_{f1}$	$\delta_{\text{Pr(OAC)}_2^{+}}$ a, b	$K_{f2}$	$\delta_{\text{Pr(OAC)}_2^{+}}$ a, b
Pr(NO <sub>3</sub> ) <sub>3</sub>	53.2	9.095	6.5	5.93
PrCl <sub>3</sub>	52.5	9.488	3.8	6.22
Pr(ClO <sub>4</sub> ) <sub>3</sub>	95.5	9.298	4.0	6.42

a) ppm vs. t-butanol.

b) The methyl resonance of acetic acid and of acetate occur 0.850 and 0.676 ppm, respectively, downfield of t-butanol.



### 3. The Interaction of Praseodymium(III) with the Potential Donor Groups of Organic Molecules

#### i) The Carboxylate Group

The interaction of the praseodymium(III) cation with the carboxylate functional group was evaluated by studying the  $\text{Pr}(\text{ClO}_4)_3$ -acetic acid system. The results obtained from this study, discussed above in Section 2, indicate that Pr(III) interacts with the deprotonated carboxylate group over the entire accessible pH range ( $\text{pH} < 6.5$ ). It was also shown that, by the careful choice of solution conditions, the formation of only a 1:1 complex,  $\text{Pr}(\text{OAc})^{2+}$ , was important.

#### ii) The Amino Group

The interaction of the praseodymium(III) cation with the amino functional group was evaluated by studying the Pr(III)-methylamine system. The chemical shift of the methyl protons of methylamine was monitored as a function of pH for a solution containing  $0.0967 \text{ M}$   $\text{Pr}(\text{ClO}_4)_3$  and  $0.18 \text{ M}$  methylamine. The chemical shift of this resonance did not change from the position of uncomplexed  $\text{CH}_3\text{NH}_3^+$  between pH 2.8 and 6.6. At higher pH values, where the ammonium group deprotonates, praseodymium hydroxide precipitates. A second experiment was performed in which the pH was maintained at 6 and the molar ratio of Pr(III) to methylamine was varied.

The chemical shift of the methyl protons of methylamine remained constant for ratios of Pr(III) to methylamine varying from 0 to approximately 3. These results were interpreted as an indication of no interaction of the Pr(III) shift reagent with the amino functional group at pH values less than 6. A similar conclusion was reached by Prados et al. (61) from potentiometric titration studies of lanthanide ion-aminocarboxylic acid solutions and by Birnbaum et al. (62) from NMR and difference absorption spectroscopy studies of neodymium(III)-amino acid systems. However, Katzin and Gulyas (63) report circular dichroism studies which indicate that  $\alpha$ -amino acids can form chelates with Pr(III) in alkaline solution. The ligand coordinates through the amino group and the carboxyl group  $\beta$  to it, to form five-membered rings stable enough to postpone the hydrolysis of Pr(III), which normally occurs before pH 7. Anteunis and coworkers also reported that the free amino function can bind to lanthanide ions in aqueous solution (53,54). This conclusion was based on the results of a study of the effect of added Pr(III) on the NMR spectra of pentapeptides. They observed shifts in the proton resonances of the tail residue when its free amino function was deprotonated by the addition of base. They also suggest that the Pr(III) shift reagent can interact with the  $\beta$ -amino moiety by the formation of an ion pair cluster with the

counterion of the lanthanide salt. This type of interaction will be considered again in Chapter VIII.

### iii) The Sulfonate Group

The interaction of the praseodymium(III) cation with the sulfonic acid functional group was evaluated by studying the Pr(III)-methanesulfonic acid system. Methanesulfonic acid is a strong acid, therefore changing the pH does not change the fraction of ligand available for complexation. However, the chemical shift of the methyl protons was monitored as a function of pH for a solution containing 0.0347 M  $\text{Pr}(\text{ClO}_4)_3$  and 0.110 M  $\text{CH}_3\text{SO}_3\text{H}$  to ensure that no pH dependent interaction was taking place. The chemical shift remained constant for samples ranging in pH values from 1.02 to 6.69. Praseodymium hydroxide precipitated at higher pH. The observed chemical shift of the  $\text{CH}_3\text{SO}_3^-$  in these samples was 1.535 ppm compared to 1.563 ppm for  $\text{CH}_3\text{SO}_3^-$  with no Pr(III) added. This indicates that there is a slight, pH independent interaction of  $\text{CH}_3\text{SO}_3^-$  with Pr(III). To obtain a more quantitative understanding of this system, a mole ratio experiment was performed. The chemical shift of the methyl protons of methanesulfonic acid was monitored as  $\text{Pr}(\text{ClO}_4)_3$  was added and the pH maintained at 4.0. The chemical shift data for solutions of  $\text{Pr}(\text{ClO}_4)_3$  to methanesulfonic acid ratios ranging from 0

3.5 is presented in Table 26. Over this mole ratio range the methanesulfonate resonance shifts 0.06 ppm downfield, indicating only a very weak interaction. This observation is consistent with the finding, discussed in Chapter II, Section E, that the methyl resonance of the NMR reference compound, sodium 2,2-dimethyl-2-silapentane-5-sulfonic acid (DSS), experiences small chemical shift changes in the presence of Pr(III).

iv) The Sulfhydryl Group

The interaction of the praseodymium(III) cation with the sulfhydryl group was investigated by studying the  $\text{Pr}(\text{ClO}_4)_3$ -thioethanol system. The absence of interaction of Pr(III) with the NMR reference compound, t-butanol (see Chapter VI, Section E) indicated that any Pr(III) interaction with thioethanol,  $\text{HOCH}_2\text{CH}_2\text{SH}$ , would be through the sulfhydryl group. In the low pH region (< 6) where praseodymium hydroxide does not precipitate, the sulfhydryl group exists entirely in the protonated form. Therefore the Pr(III)-thioethanol system was studied by monitoring the chemical shift of the ligand resonances as a function of the Pr(III) to thioethanol ratio. No change in the position of the ligand resonances was observed on varying the Pr(III) concentration from 0 to 0.20 M, while maintaining the concentration of thioethanol at 0.11 M and the pH at 4. These results

TABLE 26

The Chemical Shift of the Methyl Protons of Methanesulfonic Acid in Solutions of  $\text{Pr}(\text{ClO}_4)_3$  and Methanesulfonic Acid at pH 4.0

<u><math>[\text{Pr}(\text{ClO}_4)_3]_{\text{total}}</math></u>	<u><math>[\text{CH}_3\text{SO}_3\text{H}]_{\text{total}}</math></u>	<u><math>\delta^a</math></u>
<u>M</u>	<u>M</u>	
0	0.111	1.563
0.0174	0.108	1.544
0.0342	0.105	1.537
0.0507	0.102	1.523
0.0666	0.0994	1.517
0.0822	0.0967	1.511
0.0973	0.0940	1.507
0.1120	0.0915	1.498

a) ppm vs. t-butanol.

indicate that the sulfhydryl functional group cannot coordinate to the praseodymium ion in the pH region where praseodymium hydroxide does not precipitate.

v) The Imidazole Group

The interaction of praseodymium(III) with the imidazole-nitrogen group was investigated by studying the  $\text{Pr}(\text{ClO}_4)_3$ -N-methyl imidazole system. The chemical shifts of the protons of the ligand were monitored as a function of pH for a solution containing 0.110 M  $\text{Pr}(\text{ClO}_4)_3$  and 0.0900 M N-methyl imidazole. The chemical shift titration curves of the ligand protons differed only slightly, if at all, from those obtained for solutions containing N-methylimidazole alone, indicating that no significant interaction of the  $\text{Pr}(\text{III})$  occurs at the imidazole nitrogen site at pH less than 6.0. However, Birnbaum and coworkers (51,52) did conclude from NMR studies and potentiometric titration data that, at pH values greater than 6.0, histidine complexes to neodymium(III) through both the carboxyl group and the imidazole-nitrogen site.

C. Discussion

The results presented in this chapter indicate that, of monofunctional molecules containing the carboxylic acid, amino, sulfhydryl, imidazole, and sulfonic acid groups,  $\text{Pr}(\text{III})$  complexes only with those containing

carboxylic acid and sulfonic acid groups up to pH 6.5.

It was also shown in Chapter VI that Pr(III) does not interact with hydroxyl and ether oxygens in aqueous solution. Thus Pr(III) is an effective shift reagent only

for monocarboxylic acid and monosulfonic acid molecules in aqueous solution, however, the shift induced in the methyl resonance of methanesulfonic acid is quite small.

Although the amino, imidazole, and sulfhydryl groups are protonated in the pH region accessible in this study,

(pH < 7), the possibility of lanthanide complexation by these groups was considered because other metal ions, for example Zn(II), are capable of displacing the protons and complexing these functional groups in the pH region

(64). In aqueous solution, the conditions are less favorable for lanthanide-induced shifts than in organic solution, where interaction with these functional groups has been observed (11), since the functional group must compete with water molecules for the coordination sites

on the lanthanide cation. This is analogous to the observation that  $\text{Eu}(\text{dpm})_3 \cdot 2\text{pyridine}$  induces smaller shifts than  $\text{Eu}(\text{dpm})_3$  in the spectrum of cholesterol (1,30) because of competition between pyridine and cholesterol for the  $\text{Eu}(\text{dpm})_3$ .

The results of other workers suggest, however, that the situation may be different for polyfunctional molecules in which chelation can occur. For example,

Katzin and Gulyas (63) concluded from circular dichroism studies that  $\alpha$ -amino acids can form chelates with Pr(III) via the carboxylate and the amino groups, to form stable 5-membered rings. Birnbaum and coworkers (51,52) concluded that histidine forms a bidentate complex with Nd(III), at pH greater than 6.0, by complexation through both the carboxyl group and the imidazole nitrogen site. Therefore, although the results presented in this chapter indicate that in monofunctional molecules, the amino, imidazole, and sulfhydryl groups do not interact with Pr(III), if the molecule also contains a carboxylic acid group located such that chelation can occur, then interaction at these functional groups might also be important. It will be important in future studies to determine with which pairs of functional groups and under what solution conditions chelation becomes important. These results are of interest in view of the structural and conformational information which can be obtained from lanthanide induced shifts if a single lanthanide ion interacts at a unique binding site of the molecule of interest (26). It should be noted however, that in many peptides and proteins, the potential coordination sites are separated and the molecular structure is such that it is unlikely that more than one functional group would, or even could, simultaneously coordinate to the same metal ion. In such



cases, the present results indicate that the lanthanide cations would complex only the carboxylate group of the peptide or protein molecule.

## CHAPTER VIII

### AMINOPOLYCARBOXYLIC ACID CHELATES OF Pr(III) AS

#### AQUEOUS SHIFT REAGENTS

##### A. Introduction

In this chapter, the ethylenediaminetetraacetic acid, (EDTA), the N-(2-hydroxyethyl)ethylenediaminetriacetic acid, (HEDTA), and the cyclohexanediaminetetraacetic acid, (CDTA) chelates of Pr(III) are investigated as aqueous solution shift reagents.

The results presented in Chapter VII indicate that the use of the hydrated lanthanide cations as shift reagents in aqueous solution is limited due to their precipitation as lanthanide hydroxides above ca. 6.5. By complexing the lanthanide cations with aminopolycarboxylic acids, they remain in solution at high pH. In addition, the lanthanide cations are known to exhibit large coordination numbers (65) and some 8-, 9-, and 10-coordinate species have been characterized (66). Therefore the praseodymium chelates are expected to be capable of complexing substituent molecules, and thus functioning as shift reagents, over a large pH range. The interactions of several praseodymium chelate shift reagents with the carboxylate, amino, sulfhydryl, sulfonate and imidazole functional groups are considered in this chapter

(67).

## B. Results

### 1. The Pr(III) Complex of EDTA as an Aqueous Shift Reagent

The ethylenediaminetetraacetic acid complex of praseodymium(III) was investigated as a possible shift reagent for use in aqueous solution. The formation constant of this complex,  $3.6 \times 10^{16}$  (68) is large, suggesting that praseodymium hydroxide would not precipitate in the presence of an equivalent amount of EDTA until very high pH. However, the  $\text{PrEDTA}^-$  complex itself precipitated from aqueous solution after a few minutes, except at very high pH ( $> 12.5$ ).  $\text{PrEDTA}^-$ -acetate and  $\text{PrEDTA}^-$ -methylamine solutions also formed a precipitate shortly after preparation. Dobson and coworkers (55) showed that EDTA complexes of the lanthanides would act as shift reagents for nucleotides in aqueous solution. Presumably complexation to the nucleotide solubilizes the  $\text{PrEDTA}^-$  complex. While this thesis was being written, Reuben (56) reported that EDTA complexes of the lanthanide cations induce shifts in the NMR spectra of salicylaldehyde and *o*-nitrophenol by complexation to the deprotonated hydroxyl group. However, they used the lithium salt of EDTA and LiOH to adjust the pH. Presumably the lanthanide-EDTA complexes are soluble in the presence of the lithium cation, whereas the results of this research

indicated that PrEDTA is insoluble in the presence of both  $\text{Na}^+$  and  $\text{K}^+$ . For this reason it is unlikely that the  $\text{PrEDTA}^-$  complex would be a suitable shift reagent for general use in aqueous solution.

2. The Pr(III) Complex of HEDTA as an Aqueous Shift Reagent

The N-(2-hydroxyethyl)-ethylenediaminetriacetic acid complex of Pr(III) was investigated as a possible shift reagent for use in aqueous solution.  $\text{PrHEDTA}$  is soluble over the pH range from less than 1 to greater than 12. It has a large formation constant,  $4.1 \times 10^{14}$  (69), and therefore prevents the precipitation of praseodymium hydroxide at pH less than 12. The HEDTA resonances of the  $\text{PrHEDTA}$  complex do not interfere with the resonances of the substituent molecule being studied. Indeed, the proton NMR spectrum of the  $\text{PrHEDTA}$  complex was never observed, although a 3500 Hz region of the spectrum was searched at temperatures ranging from 25°C to 95°C. The NMR spectrum of the  $\text{PrEDTA}^-$  complex has been observed at 80°C (70). Presumably at the high temperature the rate of any intramolecular exchange of the ligand is fast on the NMR time scale, resulting in sharp resonances in the NMR spectrum. At lower temperatures, and probably over the entire temperature range examined in the  $\text{PrHEDTA}$  system, the rate of this exchange seems to be intermediate

on the NMR time scale, and broadening of the spectral resonances makes them unobservable. In the PrHEDTA complex, and in other such praseodymium chelates, the praseodymium ion is not coordinately saturated by the chelating ligand. For example, in the PrHEDTA complex it is expected that five, or possibly six, of the possible coordination sites are occupied by HEDTA. Presumably, the remaining coordination sites are occupied by water molecules, which can be displaced by substituent molecules. In this manner, the praseodymium chelate can coordinate other molecules in the solution, and Pr(III) induced chemical shifts will be observed in their NMR spectra.

i) The Carboxylate Group

The interaction of the PrHEDTA shift reagent with the carboxylate group was investigated by studying the PrHEDTA-acetic acid system. The chemical shift of the acetate resonances was monitored as a function of pH for a solution containing 0.111 M  $\text{Pr}(\text{ClO}_4)_3$ , 0.111 M HEDTA, and 0.100 M acetic acid. This chemical shift data is presented in Figure 18, along with the chemical shift titration curve of the acetate protons in a solution containing only acetic acid for comparison. The shape of the titration curve indicates that, at pH less than 6, the observed chemical shift, and therefore the amount

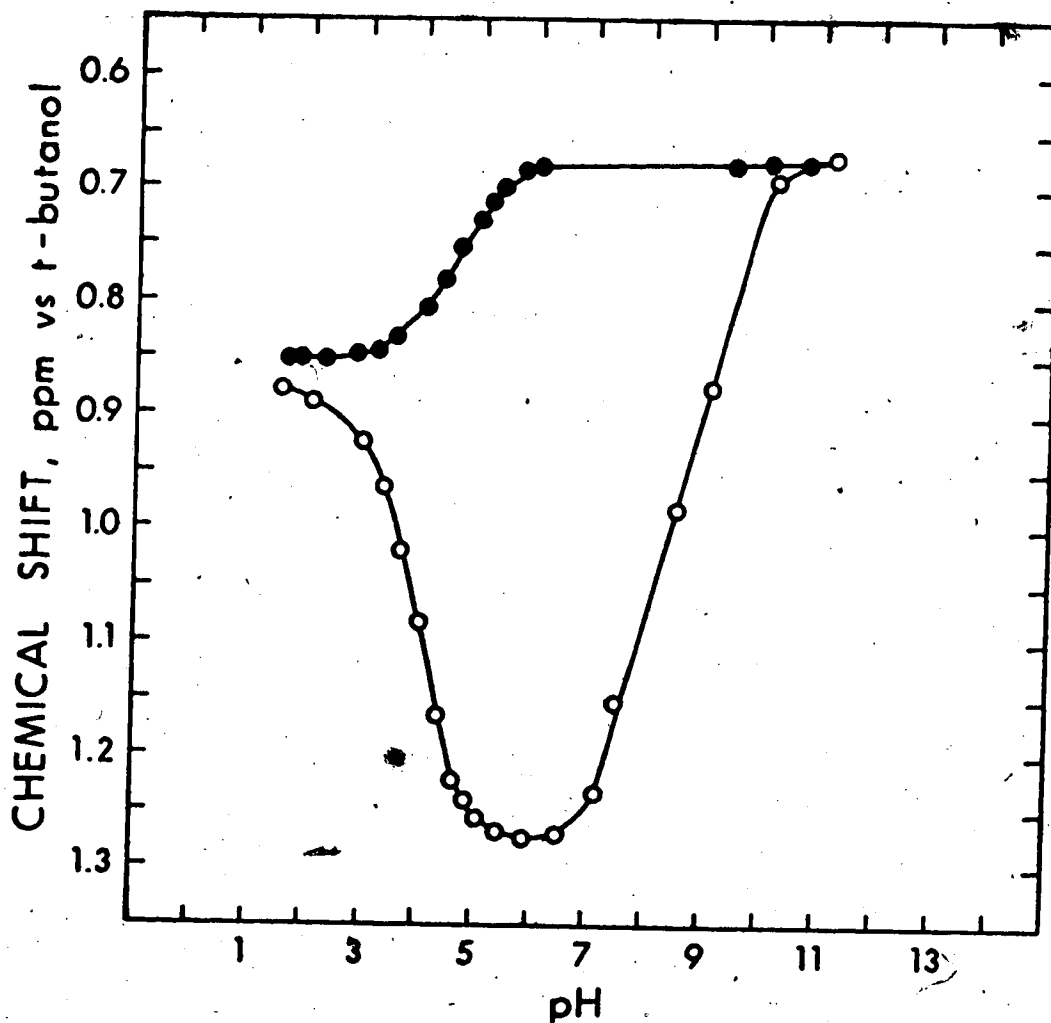


Figure 18. pH dependence of the chemical shift of the methyl protons of acetic acid in an aqueous solution containing 0.0305 M acetic acid (solid points) and in an aqueous solution containing 0.100 M acetic acid, 0.111 M  $\text{Pr}(\text{ClO}_4)_3$ , and 0.111 M HEDTA (open points).

of shift reagent-acetate complex increases at the same rate as the acetic acid deprotonates, but at pH greater than 6, the concentration of shift reagent-acetate complex apparently decreases with increasing pH. The shape of the graph indicates that, although there is some shift reagent-acetate complex present over the entire pH range 1 to 11, only a small fraction of the acetate exists in that form at pH values greater than 9.5. Gupta and Powell have reported a value of 3.69 for the logarithm of the formation constant of the PrHEDTA(OH)<sup>-</sup> complex (71). The magnitude of this formation constant indicates that at a pH of 10.31 only half the PrHEDTA in the solution is complexed to hydroxide. The chemical shift titration curve of the PrHEDTA-acetic acid solution (Figure 18), suggests that at this pH, only a small amount of the PrHEDTA is still available for complexation to acetate. In an attempt to resolve this ambiguity, potentiometric titrations of a  $1.27 \times 10^{-3}$  M solution of HEDTA and of a  $1.27 \times 10^{-3}$  M solution of PrHEDTA with 0.0536 M NaOH were obtained. These two titration curves, presented in Figure 19, are consistent with the value of the formation constant of PrHEDTA(OH)<sup>-</sup> reported by Gupta and Powell (71). A comparison of the two titration curves indicates that at pH 9.5, the PrHEDTA solution has consumed only three equivalents of hydroxide corresponding to the

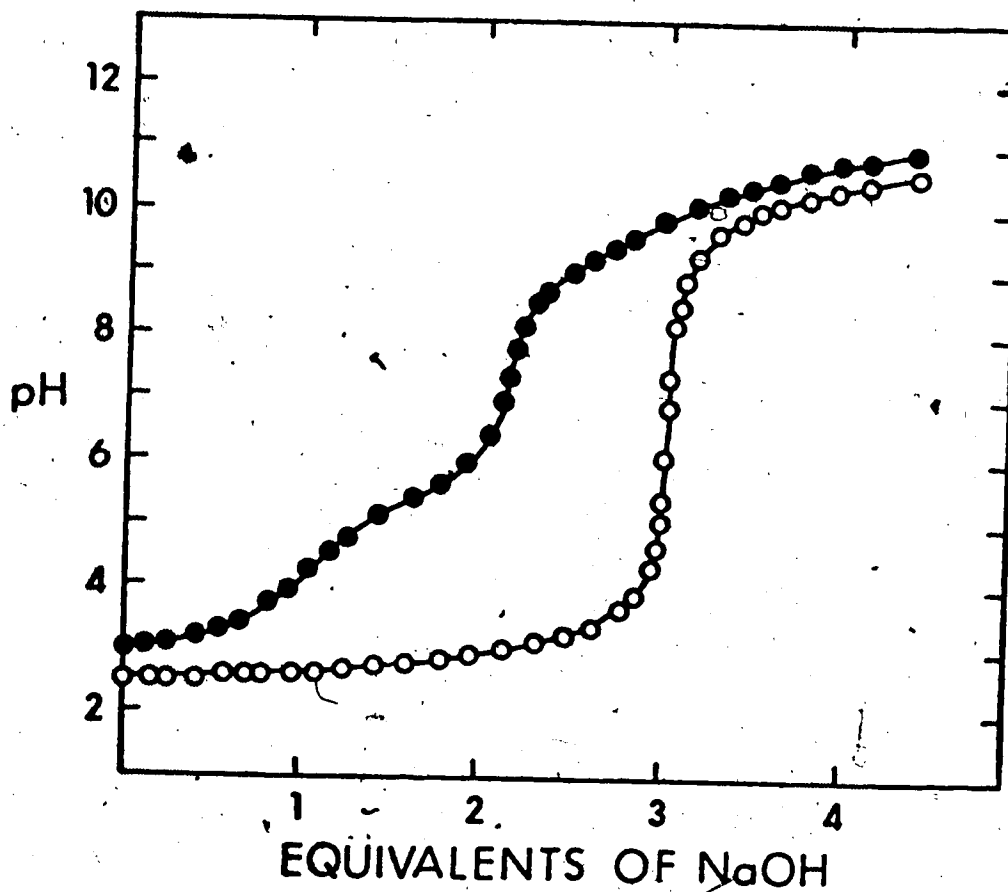


Figure 19. Potentiometric titration curves for the titration of 250 ml of an aqueous solution containing  $1.27 \times 10^{-3}$  M HEDTA with 0.05356 M NaOH (upper curve) and for the titration of 250 ml of an aqueous solution containing  $1.27 \times 10^{-3}$  M Pr(ClO<sub>4</sub>)<sub>3</sub> and  $1.27 \times 10^{-3}$  M HEDTA with 0.05356 M NaOH (lower curve). Each solution titrated also contained 0.3 M NaClO<sub>4</sub> to maintain a constant pH throughout the titration.



titration of the three acidic hydrogens of HEDTA. The chemical shift titration curve indicates that, by pH 9.5, a large fraction of the PrHEDTA is apparently no longer available to the acetate, suggesting that it might exist in a hydroxide-complexed form. However, this would show up in the pH titration data as the consumption of four rather than three equivalents of base to reach pH 9.5.

Part of the inconsistency between the potentiometric titration and chemical shift titration curves could be attributed to a contribution to the observed chemical shift from shifts induced by unchelated Pr(III) in solution. Calculations using the formation constant of the PrHEDTA complex (69) and the chemical shift of the Pr(OAc)<sup>2+</sup> complex, determined in Chapter VI, indicate that a  $3.0 \times 10^{-4}$  M concentration of free Pr(III) in solution would contribute 0.03 ppm to the observed chemical shift. Such an uncertainty reduces the precision of any calculations. However, when a 10% excess of HEDTA was present, the acetate chemical shift titration curve showed the same behavior as that of Figure 18, with a small decrease in the magnitude of the PrHEDTA induced shift. This decrease in the Pr(III) induced shift is probably due to competition of the excess HEDTA with the acetate for the free coordination sites. The presence of Pr(III) induced shifts even in the presence of excess HEDTA indicates that PrHEDTA and not Pr(III) is

responsible for the chemical shift of the acetate protons observed in the data of Figure 18.

ii) The Amino Group

The interaction of the amino functional group with the shift reagent PrHEDTA was investigated by studying the PrHEDTA-methylamine system. The chemical shift of the methyl proton resonance was monitored as a function of pH for a solution containing 0.102 M Pr(ClO<sub>4</sub>)<sub>3</sub>, 0.102 M HEDTA, and 0.118 M CH<sub>3</sub>NH<sub>2</sub>. This chemical shift data is presented in Figure 20, along with the chemical shift titration curve of a solution containing only methylamine. This data indicates that there is an interaction between the methylamine and the PrHEDTA over the entire pH range 1-12. The two titration curves of Figure 20 differ most between pH 3 and 8, suggesting that the interaction is greatest in this region. As the pH increases beyond 8, the two titration curves begin to approach each other and are coincident by pH 12. These observations suggest that it is the protonated amine, CH<sub>3</sub>NH<sub>3</sub><sup>+</sup> rather than CH<sub>3</sub>NH<sub>2</sub> which interacts with the shift reagent. Such an interaction would explain the chemical shift titration curve over the entire pH range. The conditional formation constants calculated for the PrHEDTA complex indicate that it is not completely formed until pH 3. At pH 1, about 90% of the PrHEDTA complex is

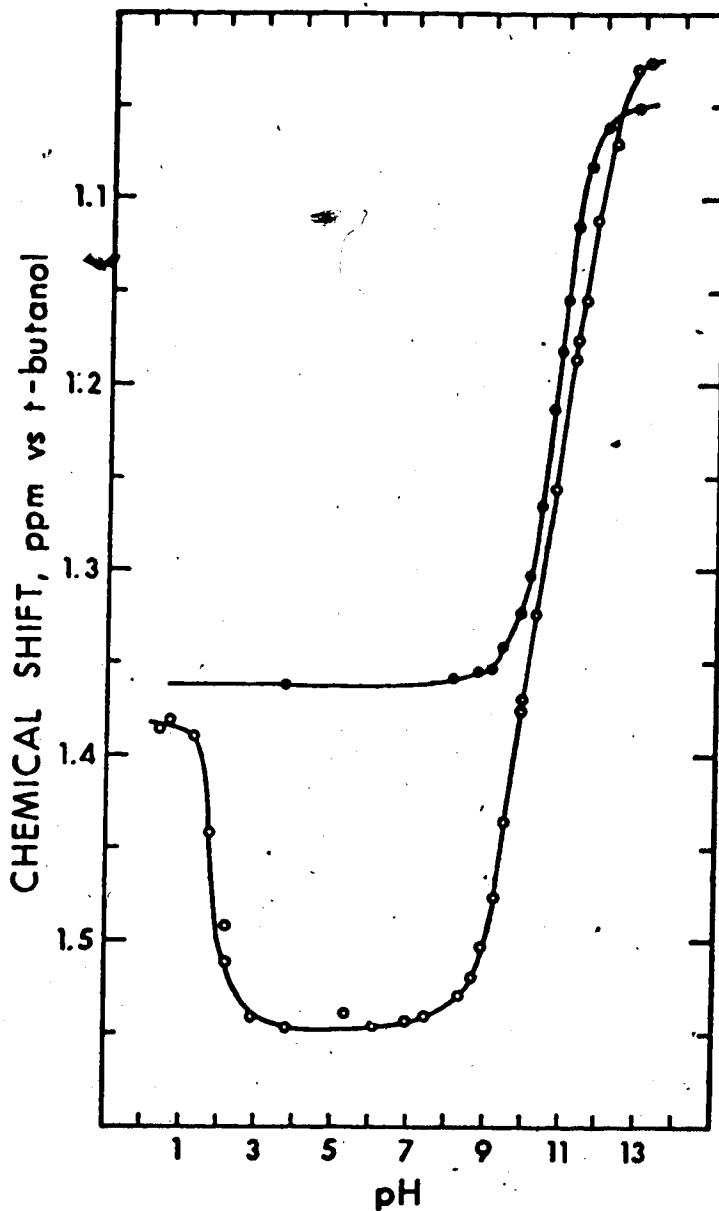


Figure 20. pH dependence of the chemical shift of the methyl protons of methylamine in an aqueous solution containing 0.10 M methylamine (solid points) and in an aqueous solution containing 0.118 M methylamine, 0.102 M  $\text{Pr}(\text{ClO}_4)_3$ , and 0.102 M HEDTA (open points).

dissociated. At pH 2, only 10% of the PrHEDTA complex is dissociated. In Chapter VII it was shown that Pr(III) does not interact with methylamine at pH values less than ca. 6.5. Therefore the section of the titration curve at pH less than 3 can be explained by the increasing concentration of PrHEDTA with increasing pH, resulting in an increasing fraction of PrHEDTA-associated  $\text{CH}_3\text{NH}_3^+$ . In the pH region 3 to 7, the concentrations of shift reagent and  $\text{CH}_3\text{NH}_3^+$  remain constant, and the fraction of PrHEDTA-associated  $\text{CH}_3\text{NH}_3^+$ , and therefore the observed chemical shift, are also constant. At a pH of approximately 7,  $\text{CH}_3\text{NH}_3^+$  begins to deprotonate, resulting in less interaction between  $\text{CH}_3\text{NH}_3^+$  and the shift reagent. This is indicated by the methylamine resonance moving towards its uncomplexed position. That the deprotonation of  $\text{CH}_3\text{NH}_3^+$  is responsible for the high pH region behavior of the titration curve is supported by the fact that the midpoint of that curve is located at the  $\text{pK}_a$  of methylamine (~ 10.7).

### iii) The Imidazole Group

The interaction of the shift reagent, PrHEDTA with N-methylimidazole was studied. The chemical shifts of the ligand protons were monitored as a function of pH for a solution containing 0.0900 M N-methyl imidazole, 0.110 M  $\text{Pr}(\text{ClO}_4)_3$ , and 0.110 M HEDTA. The chemical

shift data for the methyl protons of the ligand is presented in Figure 21 along with the chemical shift curve for the same protons in a solution containing only N-methyl imidazole. This data is similar to that presented in Figure 20 for the PrHEDTA-methylamine system. Interaction of the protonated and not the deprotonated imidazole site is suggested by the shape of the titration curve, which indicates that the greatest interaction occurs between pH 3 and 5, and decreases as the imidazole-nitrogen site deprotonates. The midpoint of this titration curve is also located at the  $pK_a$  of the ligand ( $\approx 7$ ), supporting the theory that the high pH region behavior of the titration curve is due to deprotonation of the nitrogen site.

#### iv) The Sulfhydryl Group

The interaction of the shift reagent PrHEDTA with the sulfhydryl group was investigated by studying the PrHEDTA-thioethanol system. The chemical shifts of the thioethanol resonances were measured as a function of pH for a solution containing 0.102 M  $\text{Pr}(\text{ClO}_4)_3$ , 0.102 M HEDTA, and 0.11 M thioethanol. These chemical shift titration curves were found to be identical to those of the same resonances in a solution containing only thioethanol. Thus the sulfhydryl group does not interact with the lanthanide chelate, even at pH 13 where

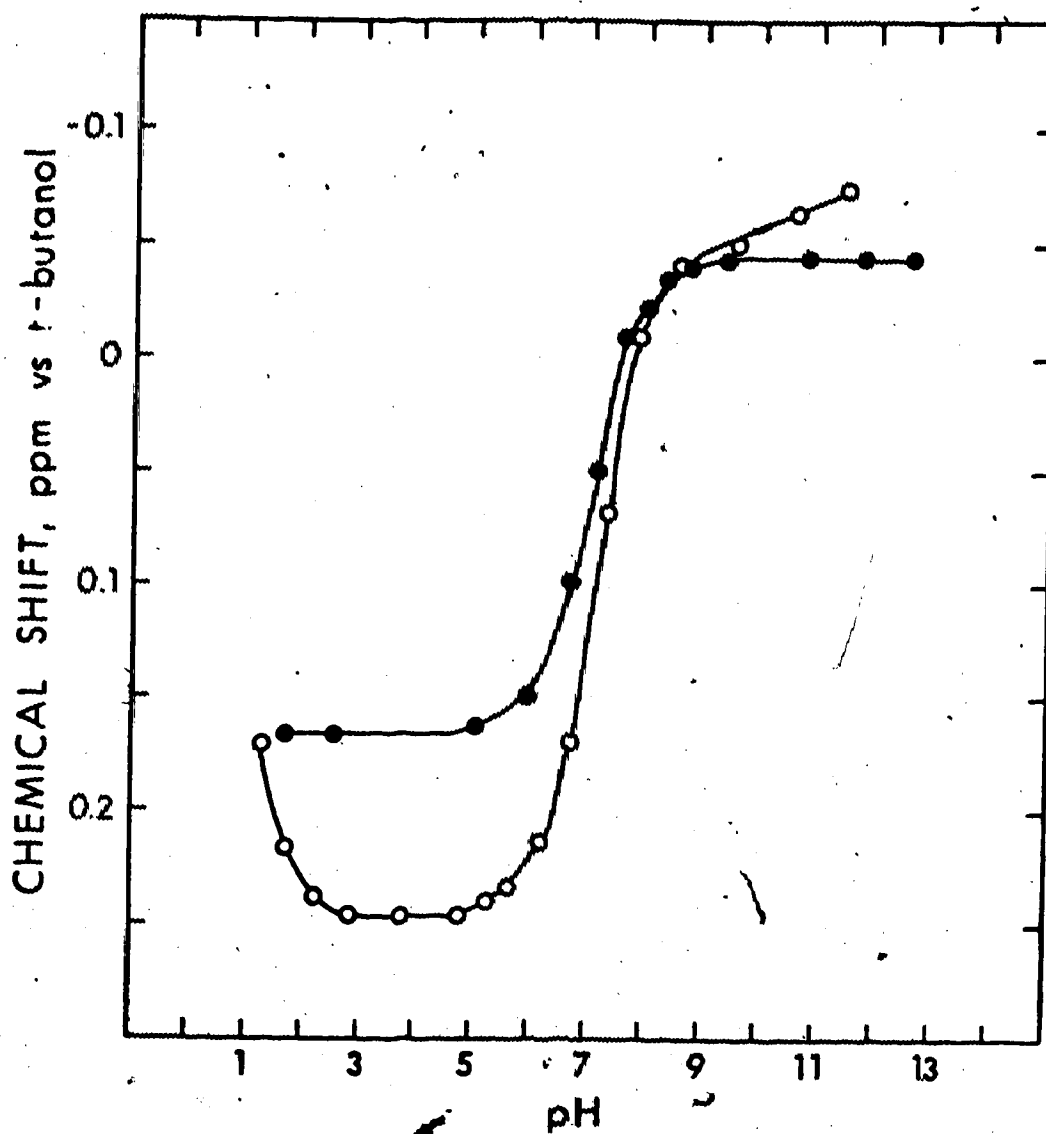


Figure 21. pH dependence of the chemical shift of the methyl protons of N-methyl imidazole in an aqueous solution containing 0.140 M N-methyl imidazole (solid points) and in an aqueous solution containing 0.0900 M N-methyl imidazole, 0.110 M  $\text{Pr}(\text{ClO}_4)_3$ , and 0.110 M HEDTA (open points).

the sulfhydryl is deprotonated.

### 3. The Pr(III) Complex of CDTA as an Aqueous Shift Reagent

The cyclohexanediaminetetraacetic acid complex of Pr(III) was investigated as a possible shift reagent for use in aqueous solution. This complex differs from the PrHEDTA complex in that  $\text{PrCDTA}^-$  is negatively charged, which may result in different behavior with the various functional groups, and possibly in the number of Pr(III) coordination sites occupied by the chelate. The  $\text{PrCDTA}^-$  complex also appears to have the characteristics required of an aqueous shift reagent. It is soluble over the pH range 2 to 12, has a large formation constant,  $2.0 \times 10^{17}$  (72), thereby preventing the precipitation of praseodymium hydroxide. The CDTA resonances of the  $\text{PrCDTA}$  complex are not observed, and therefore do not interfere with the resonances of the substituent molecule being studied.

#### i) The Carboxylate Group

The interaction of the shift reagent,  $\text{PrCDTA}^-$  with the carboxylate group was investigated by studying the  $\text{PrCDTA}$ -acetic acid system. The chemical shift of the acetate resonances was monitored as a function of pH for a solution containing  $0.100 \text{ M Pr}(\text{ClO}_4)_3$ ,  $0.100 \text{ M CDTA}$ , and  $0.0912 \text{ M}$  acetic acid. This chemical shift data,

presented in Figure 22, indicates that the  $\text{PrCDTA}^-$ -acetate complex is stable up to a higher pH (8.5) than the corresponding PrHEDTA complex. A comparison of Figures 18 and 22 also suggests that  $\text{PrCDTA}^-$  would be a better shift reagent than PrHEDTA for molecules containing the carboxylate functional group, because  $\text{PrCDTA}^-$  induces larger chemical shifts in the substituent as well as functioning efficiently over a wider pH range.

ii) The Amino-Group

The interaction of the shift reagent,  $\text{PrCDTA}^-$  with the amino functional group was investigated by studying the  $\text{PrCDTA}^-$ -methylamine system. The chemical shift of the methyl protons of methylamine was monitored as a function of pH for a solution containing 0.101 M  $\text{Pr}(\text{ClO}_4)_3$ , 0.101 M CDTA, and 0.117 M  $\text{CH}_3\text{NH}_2$ . This chemical shift data, presented in Table 27, shows the same behavior as was observed for the PrHEDTA-methylamine system (Figure 20), with the maximum Pr(III) induced shift occurring in the pH region from 3 to 8. The  $\text{PrCDTA}^-$ -methylamine chemical shift titration data can be explained by the same reactions as those postulated for the PrHEDTA-methylamine system. At low pH (< 3), the chemical shift changes with the formation of the  $\text{PrCDTA}^-$  complex. From pH 3 to approximately 8, the fraction of shift reagent-associated  $\text{CH}_3\text{NH}_3^+$ , and therefore the observed chemical



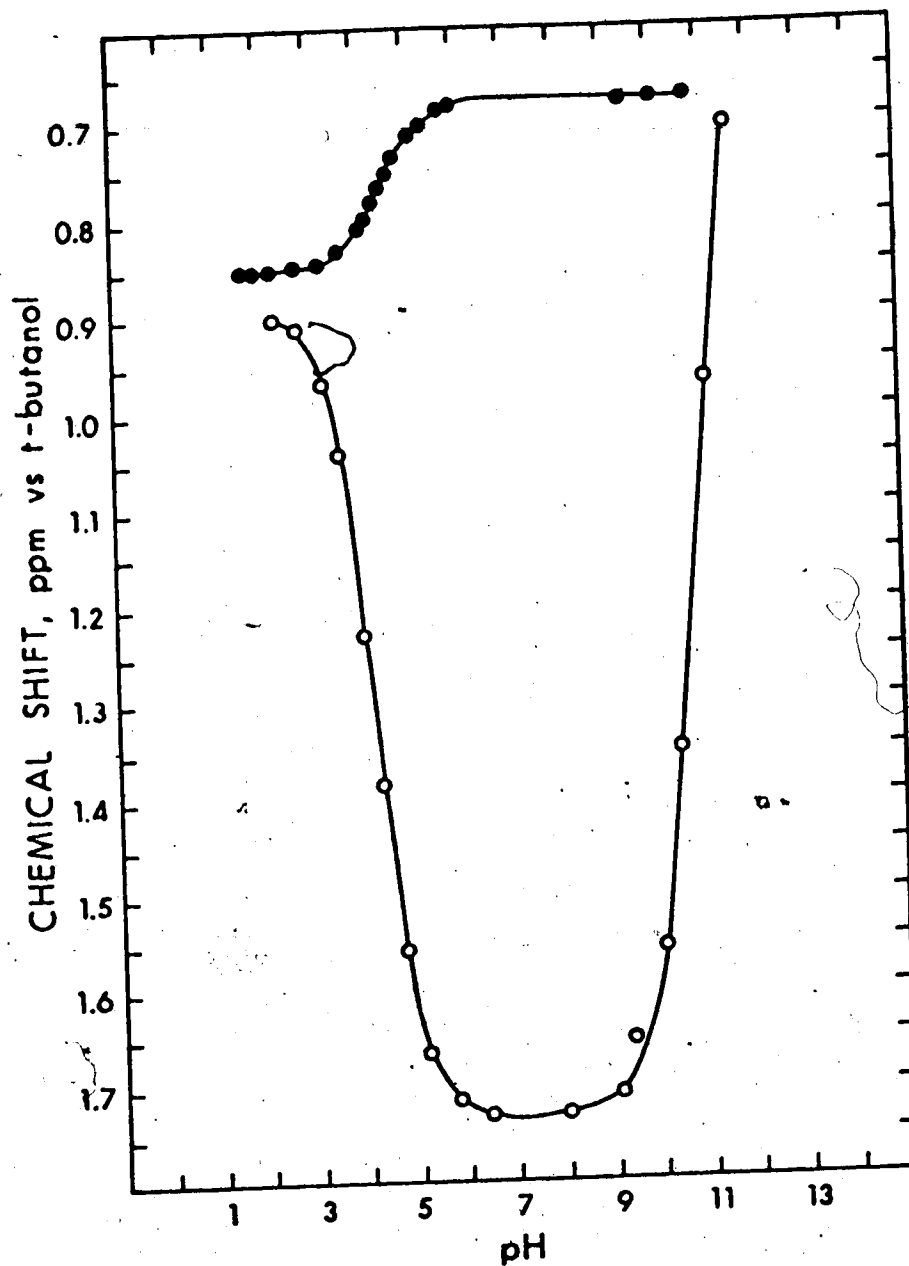


Figure 22. pH dependence of the chemical shift of the methyl protons of acetic acid in an aqueous solution containing 0.0305 M acetic acid (solid points) and in an aqueous solution containing 0.0912 M acetic acid, 0.100 M  $\text{Pr}(\text{ClO}_4)_3$ , and 0.100 M CDTA (open points).

TABLE 27

The Chemical Shift of the Methyl Protons of Methylamine as a Function of pH in a Solution Containing 0.101 M PrCDTA<sup>-</sup> and 0.117 M Methylamine.

<u>pH</u>	<u><math>\delta^a</math></u>	<u><math>\Delta\delta^b</math></u>
12.97	1.032	-0.018
12.35	1.018	-0.044
11.98	1.013	-0.048
11.51	1.029	-0.064
11.21	1.057	-0.076
10.85	1.145	-0.033
10.31	1.318	0.055
9.86	1.417	0.099
9.40	1.447	0.102
8.68	1.465	0.110
8.13	1.470	0.112
6.75	1.470	0.112
5.08	1.472	0.114
3.55	1.474	0.116
3.17	1.469	0.109
2.68	1.461	0.101
2.29	1.447	0.089

a) ppm vs. t-butanol.

b)  $\Delta\delta$  is the difference in ppm between the observed methylamine chemical shift and that of a solution containing only methylamine at the same pH.

shift remain constant. At pH greater than 8, the ammonium group of  $\text{CH}_3\text{NH}_3^+$  deprotonates, resulting in less interaction between  $\text{CH}_3\text{NH}_3^+$  and the  $\text{PrCDTA}^-$  shift reagent. This is indicated by the methylamine resonance moving towards its uncomplexed position. As in the  $\text{PrHEDTA}-\text{CH}_3\text{NH}_2$  system, the midpoint of the high pH region titration curve coincides with the  $\text{pK}_a$  of methylamine.

### iii) The Sulfonate Group

The interaction of the shift reagent  $\text{PrCDTA}^-$  with the sulfonic acid group was investigated by studying the  $\text{PrCDTA}^-$ -methanesulfonic acid system. The methyl resonance of methanesulfonic acid was monitored as a function of pH for a solution containing 0.107 M  $\text{CH}_3\text{SO}_3\text{H}$ , 0.113 M  $\text{Pr}(\text{ClO}_4)_3$  and 0.113 M CDTA. The position of this resonance remained constant over the pH range 2.09 to 12.34, and its chemical shift was equal to that of a solution containing only methanesulfonic acid. It can therefore be concluded that there is no interaction between the sulfonate functional group and the lanthanide chelate.

## C. Discussion

The results presented in this chapter indicate that the praseodymium chelates interact significantly with the carboxylate, amino, and imidazole-nitrogen functional groups in aqueous solution. This suggests

that they would be useful shift reagents for spectral clarification and for identification of resonances in complicated NMR spectra. However, the Pr(III) chelates would not be as suitable as the hydrated Pr(III) cation for the determination of the structure or conformation of polyfunctional molecules in aqueous solution, since the chelates do not coordinate to a unique functional group of the molecule (26).

The chemical shifts induced by the shift reagents PrHEDTA and PrCDTA<sup>-</sup> in carboxylate-containing molecules are much smaller than those induced by the Pr(III) shift reagent. The PrHEDTA and PrCDTA<sup>-</sup> induced chemical shifts measured in this research are also much smaller than those induced in carboxylate-containing molecules in CDCl<sub>3</sub> solution by the shift reagent Eu(fod)<sub>3</sub> (73). This can be explained by the fact that water is a coordinating solvent and therefore the carboxylate-containing substituent molecules must compete with the water molecules for the Pr(III) coordination sites not occupied by the chelating ligand of the shift reagent.

The observation, discussed above in Section B, that the protonated amino group and the protonated imidazole-nitrogen group interact with the lanthanide chelate shift reagents, suggests that an ion pair formation rather than a complexation reaction, is taking place. Because PrHEDTA is a neutral species, interaction of the

lanthanide counterion with the PrHEDTA must be postulated to account for its interaction with positively charged species, such as  $\text{NH}_3^+$ . Anteunis and Callens (54) postulate the formation of ion pair clusters to explain the effect of added Pr(III) on the NMR spectrum of aqueous pentapeptide solutions at various pH values. They suggest that the  $\text{NH}_3^+$  moieties of the peptides can form complexes with Pr(III) via ion pair formation with the counterion of the lanthanide salt. Graves and Rose (74) observed the formation of ion pairs between the shift reagent  $\text{Eu}(\text{fod})_3$ , organic cations such as quaternary ammonium ions, and their counterions. Their study was done in  $\text{CDCl}_3$  solution, in which the low dielectric constant of the solvent facilitates ion pairing. However, ion pairing of quaternary ammonium salts with the hexacyanoferrate(III) ion,  $\text{Fe}(\text{CN})_6^{3-}$  has been observed in aqueous solution (75) by proton NMR studies. But this is not surprising considering the large charge on the  $\text{Fe}(\text{CN})_6^{3-}$  species. Because the  $\text{PrCDTA}^-$  complex is already charged, the complexation of the lanthanide counterion is not required for ion pairing between the shift reagent and the  $\text{NH}_3^+$  or protonated imidazole groups.

The proposed ion pair formation between the protonated amino and imidazole sites and PrHEDTA, is supported by the observation that PrHEDTA induces shifts in the NMR resonance of the tetramethylammonium ion, TMA,

(see Chapter VI, Section E). In this species, the nitrogen atom is coordinately saturated and cannot form complexes. Thus the formation of an ion pair must be responsible for the PrHEDTA-TMA interaction.

These observations have several implications for the use of shift reagents in aqueous solution (67). First, TMA is not a suitable NMR reference compound because of the possibility of its interaction with the shift reagent. Second, the geometry of the ion pair cluster must be rigid or must have definite preferred orientations or the praseodymium(III) induced shifts would average to zero. The formation of one or several species of definite orientation facilitate the extraction of structural information from lanthanide induced chemical shifts (26). Third, the counterion of the lanthanide salt must be interacting with PrHEDTA to a certain extent, resulting in a negatively charged species. This interaction is not observed in Pr(III) shift reagent systems since four perchlorate anions would need to be associated with a Pr(III) ion to provide a negatively charged species. In addition, the geometry of an ion associated with a hydrated Pr(III) ion would be much less rigid than that of the PrHEDTA system.

The results reported in this chapter suggest that, although the PrHEDTA and PrCDTA<sup>-</sup> species do not interact

with polyfunctional molecules at a unique coordination site, it should be possible to design other lanthanide chelate shift reagents which would interact selectively at positively charged centres via an ion pair formation.

The diethylenetriaminepentaacetic acid complex of Pr(III),  $\text{PrDTPA}^{2-}$ , which is 8-coordinate and has a negative two charge, and the nine-coordinate 2,6-dipicoline complex of Pr(III),  $\text{Pr(dpa)}^{3-}$ , studied by Donato and Martin (49) are possible selective shift reagents for positive centres.

BIBLIOGRAPHY

1. C.C. Hinckley, J. Amer. Chem. Soc., 91, 5160 (1969).
2. D.R. Eaton, A.D. Josey, W.D. Phillips and R.E. Benson, J. Chem. Phys., 39, 3513 (1963).
3. R.W. Kluber and W. DeW. Horrocks, Jr., J. Amer. Chem. Soc., 88, 1399 (1966).
4. E.E. Zaev, V.K. Voronov, M.S. Shvartsberg, S.F. Vasilevsky, Y.N. Molin, and I.L. Kotljarevsky, Tetrahedron Lett., 617 (1968).
5. H.A.O. Hill, A.J. Macfarlane, B.E. Mann, and R.J.P. Williams, Chem. Commun., 123 (1968).
6. W.A. Szarek, E. Dent, T.B. Grindley, and M.C. Baird, Chem. Commun., 953 (1969).
7. W.A. Szarek and M.C. Baird, Tetrahedron Lett., 2079 (1970).
8. E. Gilles, W.A. Szarek, and M.C. Baird, Can. J. Chem., 49, 211 (1971).
9. A.M. Grotens, J. Smid, and E. deBoer, J. Mag. Resonance, 6, 612 (1972) and references therein.
10. J.E. Maskasky, J.R. Mooney, and M.E. Kenney, J. Amer. Chem. Soc., 94, 2132 (1972) and references therein.
11. J. Reuben, "Prog. in NMR Spectroscopy", J.W. Emsley, J. Feeney, and L.H. Sutcliffe, Eds., 9, 1 (1973), and references therein.



12. W. DeW. Horrocks, Jr. and J.P. Sipe(III), J. Amer. Chem. Soc., 93, 6800 (1971), and references therein.
13. J.K.M. Sanders, S.W. Hanson, and D.H. Williams, J. Amer. Chem. Soc., 94, 5325 (1972).
14. W. DeW. Horrocks, Jr., in "NMR of Paramagnetic Molecules", G.N. LaMar, W. DeW. Horrocks, Jr., and R.H. Holm, Eds., Academic Press, New York, 1973, pp. 127-177.
15. J.P. Jesson, in "NMR of Paramagnetic Molecules", G.N. LaMar, W. DeW. Horrocks, Jr., and R.H. Holm, Eds., Academic Press, New York, 1973, pp. 1-52.
16. T.J. Swift, in "NMR of Paramagnetic Molecules", G.N. LaMar, W. DeW. Horrocks, Jr., and R.H. Holm, Eds., Academic Press, New York, 1973, pp. 53-83.
17. W. DeW. Horrocks, Jr., J.P. Sipe(III), and D. Sudnick, in "Nuclear Magnetic Resonance Shift Reagents", R.E. Sievers, Ed., Academic Press, New York, 1973, pp. 53-86.
18. B.A. Goodman and J.B. Raynor, Adv. Inorg. Chem. Radiochem., 13, 135 (1970).
19. J.M. Briggs, G.P. Moss, E.W. Randall, and K.D. Sales, Chem. Commun., 1180 (1972).
20. J.M. Briggs, F.A. Hart, and G.P. Moss, Chem. Commun., 1506 (1970).
21. M.R. Wilcott, R.F. Leninski, and R.E. Davis, J. Amer. Chem. Soc., 94, 1742 (1972).

22. C.D. Barry, A.C.T. North, J.A. Glasel, R.J.P. Williams, and A.V. Xavier, *Nature*, 232, 236 (1971).
23. C.D. Barry, J.A. Glasel, A.C.T. North, R.J.P. Williams, and A.V. Xavier, *Biochem. Biophys. Res. Commun.*, 47, 166 (1972).
24. J. Reuben and D. Fiat, *J. Chem. Phys.*, 51, 4918 (1968).
25. H. Sternlicht, *J. Chem. Phys.*, 42, 2250 (1965).
26. For an example see B. Birdsall, N.J.M. Birdsall, J. Feeney, and J. Thornton, *J. Amer. Chem. Soc.*, 97, 2845 (1975).
27. W.B. Lewis, J.A. Jackson, J.F. Lemons, and H. Taube, *J. Chem. Phys.*, 36, 694 (1962).
28. R.J. Kurland and B.R. McGarvey, *J. Magn. Resonance*, 2, 286 (1970).
29. B.R. McGarvey, *J. Chem. Phys.*, 53, 86 (1970).
30. P. Tanswell, J.M. Thornton, A.V. Korda, and R.J.P. Williams, *Eur. J. Biochem.*, 57, 135 (1975).
31. J.K.M. Saunders and D.H. Williams, *Chem. Commun.*, 4227 (1970).
32. J. Briggs, G.H. Frost, F.A. Hart, G.P. Moss, and M.L. Staniforth, *Chem. Commun.*, 749 (1970).
33. R.E. Rondeau and R.E. Sievers, *J. Amer. Chem. Soc.*, 93, 1522 (1971).
34. B.L. Shapiro and M.D. Johnston, Jr., *J. Amer. Chem. Soc.*, 94, 8185 (1972).

35. I. Armitage, G. Dunsmore, L.D. Hall, and A.G. Marshall, *Can. J. Chem.*, 50, 2119 (1972).
36. J. Reuben, *J. Amer. Chem. Soc.*, 95, 3534 (1973).
37. B.L. Shapiro, M.D. Johnston, Jr., and M.J. Shapiro, *Org. Mag. Res.*, 5, 21 (1973).
38. A.D. Sherry, C. Yoshida, E.R. Birnbaum, and D.W. Darnall, *J. Amer. Chem. Soc.*, 95, 3011 (1973).
39. J. Reuben, in "Nuclear Magnetic Resonance Shift Reagents", R.E. Sievers, Ed., Academic Press, New York, 1973, pp. 341-352.
40. C.D. Barry, A.C.T. North, J.A. Glasel, R.J.P. Williams, and A.V. Xavier, *Nature*, 232, 236 (1971).
41. M.R. Wilcott(III) and R.E. Davis, in "Nuclear Magnetic Resonance Shift Reagents", R.E. Sievers, Ed., Academic Press, New York, 1973, pp. 141-171.
42. I.M. Armitage, L.D. Hall, A.G. Marshall, and L.G. Werbelow, in "Nuclear Magnetic Shift Reagents", R.E. Siever, Ed., Academic Press, New York, 1973, pp. 313-339.
43. J.D. Roberts, G.E. Hawkes, J. Husar, A.W. Roberts, and D.W. Roberts, *Tetrahedron*, 30, 1833 (1974) and references therein.
44. J. Reuben and D. Fiat, *J. Chem. Phys.*, 51, 4909 (1969).
45. C. Reyes-Zamora and C.S. Tsai, *Chem. Commun.*, 1047 (1971).

46. F.A. Hart, G.P. Moss, and M.L. Staniforth, *Tetrahedron Lett.*, 3389 (1971).
47. T. Spoormaker, A.P.G. Kieboom, A. Sinnema, J.M. van der Toorn, and H. van Bekkum, *Tetrahedron Lett.*, 3713 (1974).
48. S.J. Angyal, *Carbohydr. Res.*, 26, 271 (1973).
49. S.J. Angyal, D. Greeves, and J.A. Mills, *Aust. J. Chem.*, 27, 1447 (1974).
50. H. Donato, Jr., and R.B. Martin, *J. Amer. Chem. Soc.*, 94, 4129 (1972).
51. A.D. Sherry, C. Yoshida, E.R. Birnbaum, and D.W. Darnall, *J. Amer. Chem. Soc.*, 95, 3011 (1973).
52. A.D. Sherry, E.R. Birnbaum, and D.W. Darnall, *J. Biol. Chem.*, 247, 3489 (1972).
53. M. Anteunis and J. Gelan, *J. Amer. Chem. Soc.*, 95, 6502 (1973).
54. M. Anteunis and R. Callens, *J. Mag. Resonance*, 15, 317 (1974).
55. C.M. Dobson, R.J.P. Williams, and A.V. Xavier, *J. Chem. Soc., Dalton*, 1762 (1974).
56. J. Reuben, *J. Amer. Chem. Soc.*, 98, 3726 (1976).
57. L.G. Sillen and A.E. Martell, "Stability Constants of Metal Ion Complexes", The Chemical Society, London, 1964, p. 44.
58. A. Sonesson, *Acta. Chem. Scan.*, 12, 1937 (1958).

59. J.L. Dye and V.A. Nicely, *J. Chem. Educ.*, 48, 443 (1971).
60. E.R. Birnbaum and T. Moeller, *J. Amer. Chem. Soc.*, 91, 7274 (1969).
61. R. Prados, L.G. Stadherr, H. Donato, Jr., and R.B. Martin, *J. Inorg. Nucl. Chem.*, 36, 689 (1973).
62. E.R. Birnbaum, C. Yoshida, J.E. Gomez, and D.W. Darnall, *Proc. Ninth Rare Earth Res. Conf.*, 1970, pp. 264-267.
63. L.I. Katzin and E. Gulyas, *Inorg. Chem.*, 7, 2442 (1968).
64. B.J. Fuhr and D.L. Rabenstein, *J. Amer. Chem. Soc.*, 95, 6944 (1973).
65. F.A. Cotton and G. Wilkinson, "Advanced Inorganic Chemistry", John Wiley and Sons, New York, 1966, p. 1063.
66. M.D. Lind, B. Lee, and J.L. Hoard, *J. Amer. Chem. Soc.*, 87, 1611 (1965).
67. D.L. Rabenstein and M.C. Tourangeau, submitted for publication.
68. L.G. Sillen and A.E. Martell, "Stability Constants of Metal Ion Complexes", The Chemical Society, London, 1964, p. 639.

69. L.G. Sillen and A.E. Martell, "Stability Constants of Metal Ion Complexes", The Chemical Society, London, 1964, p. 643.
70. T.H. Siddall<sup>o</sup> (III) and W.E. Stewart, Inorg. Nucl. Chem. Lett., 5, 421 (1969).
71. A.K. Gupta and J.E. Powell, Inorg. Chem., 1, 955 (1962).
72. L.G. Sillen and A.E. Martell, "Stability Constants of Metal Ion Complexes", The Chemical Society, London, 1964, p. 692.
73. J.P. Shoffner, J. Amer. Chem. Soc., 96, 1599 (1974).
74. R.E. Graves and P.I. Rose, Chem. Commun., 630 (1973).
75. D.W. Larsen and A.C. Wahl, Inorg. Chem., 4, 1281 (1965).